Institut für Geowissenschaften
Mathematisch-Naturwissenschaftliche Fakultät
Universität Potsdam

Late Quaternary Climate Changes and Landscape Evolution in the Northwest Himalaya

Geomorphologic Processes in the Indian Summer Monsoon Domain

Bodo Bookhagen

Dissertation
zur Erlangung des akademischen Grades
Doktor der Naturwissenschaften (Dr. rer. nat.)
in der Wissenschaftsdisziplin Geologie

eingereicht an der Mathematisch-Naturwissenschaftlichen Fakultät
der Universität Potsdam

Potsdam, im November 2004

Wenn man einen Stein ins Wasser wirft, so eilt er auf dem schnellsten Weg zum Grunde des Wassers. So ist es, wenn Siddhartha ein Ziel, einen Vorsatz hat. Siddhartha tut nichts, er wartet, er denkt, er fastet, aber er geht durch die Dinge der Welt hindurch wie der Stein durchs Wasser, ohne etwas zu tun, ohne sich zu rühren: er wird gezogen, er läßt sich fallen. Sein Ziel zieht ihn an sich, denn er läßt nichts in seine Seele ein, was dem Ziel widerstreben könnte. Das ist es, was Siddhartha bei den Samanas gelernt hat. Es ist das, was die Toren Zauber nennen und wovon sie meinen, es werde durch die Dämonen bewirkt. Nichts wird von den Dämonen bewirkt, es gibt keine Dämonen. Jeder kann zaubern, jeder kann seine Ziele erreichen, wenn er denken kann, wenn er fasten kann.

–Hermann Hesse, Siddhartha

ABSTRACT

The India-Eurasia continental collision zone provides a spectacular example of active mountain building, plateau development and climatic forcing. Tectonic deformation and climatic influences exerted by mountain building in the region extend well beyond the Himalaya; for example, the elevated Tibetan plateau initiates, controls and forces the Asian monsoon. While the Tibetan plateau today remains arid, the southern Himalayan front receives several meters of rainfall during the Indian summer monsoon season between June and September. A recently proposed hypothesis concerning orogenic evolution suggests that regional variations in climate strongly influence spatial variations of deformation across an actively deforming orogen. Thus, the southern Himalayan mountain front represents an ideal location to study monsoonal oscillations, their influence on geomorphic processes leading to localized mass removal, and potential feedback mechanisms between denudation and exhumation.

In order to quantify the critically important process of mass removal, I analyzed spatial and temporal precipitation patterns of the oscillating monsoon system and their geomorphic imprints. Along the humid southern Himalayan mountain front, the interplay between topography and Indian summer monsoon circulation profoundly controls precipitation distribution, erosion, sediment transport, and river discharge. I processed passive microwave satellite data to derive high-resolution rainfall estimates for the last decade and identified an abnormal monsoon year in 2002. During this year, precipitation migrated far into the Sutlej Valley in the northwestern part of the Himalaya and reached regions behind orographic barriers that are normally arid. There, sediment flux, mean basin denudation rates, and channel-forming processes such as erosion by debris-flows increased significantly. Similarly, during the late Pleistocene and early Holocene, solar forcing increased the strength of the Indian summer monsoon for several millennia and presumably lead to analogous precipitation distribution as were observed during 2002. However, the persistent humid conditions in the steep, high-elevation parts of the Sutlej River resulted in different erosional landscape responses, such as deep-seated landsliding. Landslides were exceptionally large, mainly due to two processes that I infer for this time: At the onset of the intensified monsoon at 9.7 ka BP heavy rainfall and high river discharge removed aggragated the alluviated material, and lowered the baselevel. At this point, rivers were able to erode into bedrock again. During the intensified monsoon phase, enhanced discharge, sediment flux, and increased pore-water pressures along the hillslopes eventually lead to exceptionally large landslides that have not been observed in other periods.

The excess sediments that were removed from the upstream parts of the Sutlej Valley were rapidly deposited in the low-gradient sectors of the lower Sutlej River. There, a 120m thick and more than 70km long fluvial infill has been incised episodically during the Holocene. Timing of downcutting correlates with centennial-long weaker monsoon periods that were characterized by lower rainfall. I explain this relationship by taking sediment flux and rainfall dynamics into account: High sediment flux derived from the upstream parts of the Sutlej River during strong monsoon phases prevents fluvial incision due to oversaturation the fluvial sediment-transport capacity. In contrast, weaker monsoons result in a lower sediment flux that allows incision in the low-elevation parts of the Sutlej River.

These results demonstrate that mass evacuation as the driving force of erosional unloading occurs episodically and is strongly nonlinear. Thus, potential feedback mechanisms, if they exist, are most likely controlled by climatic oscillations rather than by a generally wetter climate.

ZUSAMMENFASSUNG

Die Indisch-Eurasische Kontinentalkollision ist ein beeindruckendes Beispiel für aktive Prozesse der Gebirgs- und Hochebenenbildung, aber auch für weitreichenden, tektonisch kontrollierten klimatischen Einfluss. Während das Tibetplateau heute die meiste Zeit trocken ist, fallen an der südlichen Himalajafront jedes Jahr mehrere Meter Regen in der Monsunsaison von Juni bis September. Eine kürzlich aufgestellte und umstrittene Hypothese besagt, dass die Gebirgsbildung durch klimatische Prozesse mitgesteuert wird. Dabei geht man davon aus, dass fokussierter Niederschlag, wie er entlang des südlichen Himalajas beobachtet wird, möglicherweise Deformationen in der Erdkruste nach sich zieht.

Um den Einfluss von klimatisch bedingter Erosion auf die Orogenese zu testen, habe ich erosive Oberflächenprozesse, Monsunvariationen und fluviatilen Massentransfer auf verschiedenen Zeitscheiben analysiert. Entlang der feuchten südlichen Himalajafront wird die Regenverteilung durch die Stärke des Monsuns und durch die Topographie kontrolliert. Um genaue Niederschläge auf einem grossen Raum zu quantifizieren, habe ich durch Wettersatelliten aufgezeichnete passive Mikrowellendaten für die letzten zehn Jahre untersucht. Erstaunlicherweise variiert der Niederschlag nur wenig von Jahr zu Jahr und ein Großteil des Regens wird durch orographische Effekte gesteuert. Im Jahre 2002 allerdings, habe ich ein abnormal starkes Monsunjahr feststellen können. Zu dieser Zeit ist der Monsunniederschlag weiter in das Gebirge vorgedrungen und hat viele Massenbewegungen wie z.B. Schuttströme und Muren ausgelöst. Dabei verdoppelten sich die Erosionsraten im Einzugsgebiet. Ich zeige anhand von Satellitenbildern, aufgenommen vor und nach dem Monsun, dass sich hierbei vor allen Dingen kleine, neue Flussläufe entwickeln.

In höher gelegenen, normalerweise trockenen Gebieten findet man auch Überreste von enormen Bergstürzen und dahinter aufgestauten Seen. Datierungen dieser geomorphologischen Phänomene zeigen, dass sie nur in zwei Phasen während der letzten 30.000 Jahre auftreten: Im späten Pleistozän vor rund 27.000 Jahren und im frühen Holozän vor 8000 Jahre. Diese Zeiten sind durch einen starken Monsun, der durch die Insolation kontrolliert wird, gekennzeichnet. Analog zur Niederschlagsverteilung im Jahre 2002 ist der Monsun aber nicht nur für ein Jahr, sondern mehrere hundert oder tausend Jahre lang kontinuierlich in die heute ariden Gebiete vorgedrungen. Der erhöhte Porenwasserdruck und die erstarkten Flüsse lösten dann durch laterale Unterschneidung große Bergstürze aus, die zu keiner anderen Zeit beobachtet wurden. Interessant ist auch die Beobachtung, dass man keine Überreste von Bergstürzen in dem immerfeuchten Gürtel entlang des südlichen Himalajas findet. Die temporären Becken in den Hochlagen, die durch Bergstürze entstanden sind, entstehen in Feuchtphasen und werden in schwächeren Monsunphasen von Flüssen abgetragen und verdeutlicht die komplexe Beziehung zwischen Klima und Massentransfer verdeutlicht.

Im flachen Bereich des unteren Sutlej Tals sind 120 Meter mächtige Flussschotter vorzufinden, die ich mit Hilfe von kosmogenen Nukliden datiert habe. Die oberste und somit älteste Terrasse ist zeitglich entstanden mit dem Beginn der verstärkten Monsunphase vor 9.700 Jahren. Lithologie und Größe der Komponenten dieser Schüttung legen die Vermutung nahe, dass dieser Flussschotter ein Produkt des fluviatilen Auswaschens von glazialem Material ist, das sich während der letzten Eiszeit entlang der Flussläufe akkumuliert hat. Die Bildung von darunter eingeschnit-

tenen Terrassen fällt zeitlich mit drei schwächeren, jeweils einige hundert Jahre langen Monsunphasen zusammen. Der oszillierende Monsun und damit die wechselnde Niederschlagsverteilung erreichen je nach Monsunstärke unterschiedliche Bereiche des Tals und der Sutlej führt so mehr oder weniger Sediment mit sich. Beim Erreichen des flachen Vorlandes wird das überschüssige Sediment abgelagert, das aufgrund der geringen Fließgeschwindigkeit und daher verminderter Transportkraft nicht mehr im Fluss transportiert werden kann. Ähnlich verhält es sich während jahrhundertelanger, schwächerer Monsunphasen, wenn der geringe Sedimentanteil im Fluss Einschneidung in den Flussschotter erlaubt.

Zusammenfassend läßt sich sagen, dass Erosion und vollständige Auswaschung von Sediment aus dem Gebirge nur während eines kompletten Klimazyklus mit Feucht- und Trockenphasen stattfindet. Interessant dabei ist, dass diese Zyklen und der Einfluss auf den Massentransfer in verschiedenen Zeiträumen – von Jahren über Jahrhunderte bis zu Jahrtausenden – abläuft. Somit ist eine mögliche Kopplung von Klima und tektonischer Deformation nur mit stark oszillierenden Randbedingungen, wie während des Pleistozäns, möglich.

ALLGEMEINE ZUSAMMENFASSUNG

Das Himalaja ist mit seinen acht höchsten Bergen mit Gipfeln über 8 Kilometern das spektakulärste Gebirge der Erde. Nicht nur landschaftlich, auch klimatisch beeinflusst es Kulturen, beschäftigt und fasziniert Geologen weit über seine Grenzen hinaus. Im Norden schließt das Tibet Plateau an, eine Hochfläche mit einer Durchschnittshöhe von 5000 Metern und einer Ausdehnung von etwa 500 x 1500 Kilometern. Diese Hochfläche bildet das größte Hochplateau der Erde und hat maßgeblich Einfluß auf die klimatischen Bedingungen in Asien, da es wie eine Heizfläche in die Atmosphäre hineinragt und durch starke Erhitzung im Sommer sowie Abkühlung im Winter die Luftdruckverhältnisse des asiatischen Monsunsystem bestimmt. So wird die Hochebene bereits im April stark durch die Sonne erhitzt und die schnell aufsteigenden, trockenen Luftmassen ziehen wie ein großer Wirbel feuchte Meeresluft von den umliegenden Ozeanen an, die sich an der Gebirgsfront des Himalaya abregnet. Besonders Feuchtigkeit aus der Bucht von Bengalen fällt als Niederschlag mit mehreren Metern pro Jahr entlang der Südseite des Himalajas (im Vergleich: In Berlin regnet es ca. 0.5 Meter pro Jahr).

Der monsunale Starkregen – man spricht auch vom tropischen Konvektionsregen – wird durch die Höhenverteilung der Täler und Bergrücken im Himalaja kontrolliert: Niederschlag zieht weit in Nord-Süd gerichtete Flusstäler hinein und erreicht so interne, höhere Bereiche des Gebirges. Im Gegensatz dazu gibt es 4000 bis 5000 m hohe Gebirgsfronten, die einen Großteil der Feuchtigkeit abregnen lassen und auf diese Weise trockene Gebiete im Innern des Himalajas formen. Es existiert also ein Gürtel mit hohen Niederschlägen, der sich südlich entlang von hohen Bergmassiven zieht. In diesem Bereich kommt es während der Monsunsaison zwischen Juni und September zu hohen Abtragungsraten durch Muren, kleine bis mittlere Bergstürze und große, reißende Flüsse.

Der Schwerpunkt dieser Dissertation liegt im Erkennen, Beschreiben und Quantifizierung der Oberflächenprozesse, die die erhöhten Abtragungen repräsentieren. Dazu wurden Satellitendaten verarbeitet, um die genaue Niederschlagsverteilung im Himalaja bestimmen zu können. Während der Niederschlag in der letzten Dekade homogen verteilt war, stellt das Jahr 2002 eine abnormal starke Monsunsaison dar. Dabei ist der Niederschlag im Nordwesten des Himalajas weit in das Gebirge vorgedrungen und hat sogar die internen, normalerweise trockenen Bereiche erreicht. In diesen Gebieten kam es verstärkt zu Muren und Schlammströmen, die weite Teile der wüstenähnlichen Landschaft geformt und beeinflusst haben. Ein wichtiges Merkmal dieses abnormalen Monsunjahres ist daher die verstärkte Abtragung in einer Region, die keine schützende Vegetationsdecke besitzt.

Während des späten Pleistozäns und im frühen Holozän vor 27.000 bzw. 8000 Jahren zeigen klimatische Archive, dass der Monsun nicht nur für ein Jahr, sondern mehrere Jahrtausende lang verstärkt war. Es kann davon ausgegangen werden, dass diese langfristig wirksamen Anomalien eine ähnliche Verteilung der Niederschläge nach sich gezogen haben, wie die derzeitigen Anomalien während verstärkter Monsunjahre. Zu diesen Zeiten ist der Niederschlag kontinuierlich in die sonst trockenen Gebiete vorgedrungen. Dort hat die Zunahme an Regen die Flüsse anschwellen lassen und die Bergrücken durch Dauernässe instabil gemacht, da durch eindringendes Wasser die Porendrucke ansteigen und die Kohäsion des Gesteins herabgesetzt wird. Die steilen und destabilisierten Hänge reagierten mit enormen Bergstürzen auf die zusätzlichen Belastungen.

Diese Massenbewegungen hatten Volumina von über 0.5 km^3 und bildeten Staudämme für Flüsse und schufen Seen mit bis zu 14 km Länge, die z.T. mehrere tausend Jahre existieren. Interessant ist die Beobachtung, dass nur während der verstärkten Monsunphasen und nur im internen Bereich des Himalaja diese enormen Bergstürze auftraten. Die Abtragung dieser großen mit Wasser und Sediment gefüllten Becken geschieht allerdings in Jahren mit schwächerem Monsun. Diese Beobachtung deutet darauf hin, dass die Beziehung zwischen Abtragung und möglicher tektonischer Reaktion äußert komplex und vielseitig ist.

CONTENTS

LIST OF FIGURES

LIST OF TABLES

Acknowledgements

So many have contributed to the successful completion of my PhD at Potsdam University that it is impossible to thank everyone, and I apologize for any oversights here.

First, I would like to thank my advisor, Manfred Strecker, for guiding and supporting my field research, and for allowing me the freedom to pursue my interests in satellite-data processing, landscape evolution, and cosmogenic dating. Thanks also to Samuel Niedermann for serving as a very valuable guide to cosmogenic nuclides. I also would like to thank Bill Dietrich and Roland Bürgmann for guidance and the possibility to study at Berkeley as a visiting scholar. Bill served as an unofficial advisor, folding me in with the rest of the geomorphology group at UC Berkeley. The same goes for Kunihiko Nishiizumi and Kees Welten from the Space Science Lab. Both of them provided many insights of chemical separation procedures for cosmogenic nuclides sample processing. I also would like to acknowledge Bernhard Grasemann from the University of Vienna and J.-C. Vannay from Lausanne for introducing us to the Himalaya. I'd like to express my thanks to the other faculty I've interacted with over the years, particularly Peter Blisniuk, Anke Friedrich, Kirk Haselton, George Hilley, Ed Sobel, Lindsay Schoehnbohm, Andreas Bergner, Martin Trauth, and Antje Müller from Potsdam University, and Dominik Fleitmann and Michael McWilliams from Stanford University, as well as Ramon Arrowsmith from Arizone State Univ. Also, I owe a large debt to our colleagues A.K Jain and S. Singh from IIT Roorkee, India who supported us during several months of field work in northwest India.

At Potsdam University, fellow students have been very important to my success and to my general happiness. I especially would like to thank my friend and colleague Rasmus Thiede. Both of us spend several months in northwestern India conducting field work, and we mutually motivated us while being back in the office in Golm. I also would like to thank the students Angela Landgraf, Jörn Hauer, Nadja Insel, Miriam Dühnforth, Silvana Möllerhenn, and Henry Wichura who provided valuable help in digitizing maps and hardrock-sample processing. I also appreciate the patience and help from Michael Singer, John Stock, Taylor Perron, Ken Ferrier, Elywin Yager and many other graduate students from the geomorphology group at Berkeley.

Finally, I wish to thank my family for being supportive throughout my whole education. They made all this possible through their encouragement and comfort. Most important of all, my love and thank goes to Linda who makes San Francisco the most worthy and fascinating city to live in.

1. INTRODUCTION

> Everyone has their little faults. Mine is in California.
>
> – Lex Luther

The fields of tectonics and geomorphology have undergone a revitalization in the past several years due to the increased availability of new dating techniques, including the use of cosmogenic nuclides, digital topography, high-resolution satellite-geodetic and remote sensing data, as well as quantification of surface processes. In the realm of tectonics and surface geomorphology, I have studied the response of landscapes to spatial and temporal variations in climate and deformation, rates of tectonic and surface processes (river incision, river aggradation, sedimentation, landsliding), and mass-balance considerations in rapidly eroding mountain belts.

One of the most provocative – yet largely untested – recent hypotheses concerning orogenic evolution posit that regional variations in climate strongly influence spatial variations in the style and magnitude of deformation across an actively deforming orogen [e.g., *England and Molnar*, 1990; *Molnar and England*, 1992; *Raymo and Ruddiman*, 1992; *Molnar et al.*, 1993; *Whipple et al.*, 1999; *Willett*, 1999; *Montgomery et al.*, 2001; *Montgomery and Brandon*, 2002; *Koons et al.*, 2002; *Reiners et al.*, 2003]. For example, rock uplift generates topographic relief, thereby enhancing orographic precipitation, which focuses erosion. Both aspects may in turn influence rates and spatial patterns of further rock uplift. Although theoretical links between climate, erosion and uplift have received much attention [e.g., *Tucker and Slingerland*, 1994; *Willett et al.*, 2001], few studies have shown convincing correlations between observable indicators of these processes on the scale of mountain ranges [e.g., *Brozovic et al.*, 1997; *Sobel et al.*, 2003]. The critical factors for potential feedback mechanisms are thus localized mass removal and relief-forming processes. For example, mass-transfer estimations need to take into account the different climatic regions in an orogen and their significantly varying denudation rates in time and space. In addition, identifying and quantifying erosional processes producing relief in the landscape are necessary to decipher the role of tectonic-climatic interactions. Recent progress in quantifying both geomorphic and tectonic rates as well as in modeling surface processes [e.g., *Dietrich et al.*, 1992; *Anderson*, 1994; *Montgomery and Dietrich*, 1994; *Tucker and Slingerland*, 1997; *Hovius et al.*, 2000; *Sklar and Dietrich*, 2001; *Burbank*, 2002; *Dadson et al.*, 2003], allow integrated,

quantitative, field- and laboratory-based investigation of the interactions and possible feedbacks between geomorphic, climatic, and tectonic processes. Thus, I use these methods to analyze landscape-shaping processes in response to climate forcing and synthesize varying timescales and processes.

In order to test the hypothesis of feedback between erosion and tectonic uplift, my thesis focuses on factors controlling relief formation, climate-dependent surface erosion, and periods of enhanced mass transport. I describe relief formation, channel-network evolution, and erosive hillslope processes as functions of climate. While wetter climates potentially increase hillslope erosion on annual timescales, the fluvial system responsible for material transport from the orogen to the foreland imposes a significant time lag on mass evacuation from the orogen. Similarly, relief-forming processes such as river incision and landsliding are primarily dominated by climatic oscillations and not – as previously argued – on the intensity or longevity of humid periods. Importantly, the steep mountainous landscapes of the study region have self-organized features, which limit erosion through massive landsliding barriers that create sediment traps. Thus, the apparent nonlinear response of the landscape to climatic forcing depends strongly on the observer's timescale.

This thesis focuses on monsoonal variations on short (1 year) to medium (10^3 years) timescales and their implications for landscape shaping processes. These interactions were studied in the Sutlej River valley in northwest India. The Sutlej River valley is well suited to assess climatically controlled geomorphic processes because it is situated at the northwestern end of the monsoonal conveyer belt and only receives high amounts of rainfall during abnormal monsoon years or long-lasting intensified monsoon phases, e.g. in the early Holocene. Thus, the preservation potential of geomorphic relicts to infer complex surface processes in the past is high.

In order to document the nature of recent monsoonal precipitation distribution and orographic effects in high mountains with strong rainshadows and annual inundation, I have processed passive microwave satellite data from 1992 to 2002 (Chapter 3) and identified an abnormally strong monsoon year in 2002. During this year, enhanced precipitation controls sediment transport and geomorphic processes that relate to fluvial network evolution. Thus, on annual to centennial timescales extreme climatic events impose a strong control on landscape-shaping processes, and sediment evacuation from the orogen toward the foreland might be limited to these years.

During the late Pleistocene and early Holocene, there existed millennial-long, intensified monsoon phases inferred to be analogous in their precipitation distribution to the abnormally strong monsoon year in 2002 (Chapter 4). At these times, rainfall was enhanced and migrated far into the orogen to reach orographically shielded regions that are arid under present conditions. Eventually, increased pore-pressure and intensified fluvial incision lead to massive landsliding that only occurred during these millennial-long, wet periods. These extensive mass movements

temporarily counteract relief formation by damming rivers and trapping sediments.

Despite an overall stronger monsoon phase during the early Holocene, high-resolution records show centennial-long, weaker phases. In order to decipher the influence of monsoonal dynamics on sediment flux and river aggradation, I analyzed fill-and-cut terraces in the low-gradient reaches of the lower Sutlej Valley and used cosmogenic nuclides to derive an absolute chronology for these landforms (Chapter 5). These features represent the fluvial response to monsoonal forcing and integrated catchment-wide effects. My analyses show that incision or terrace downcutting is controlled by sediment flux and hence varying precipitation distributions during weaker monsoon phases, and not by the absolute strength of the monsoon. Thus, similar to millennial-scale effects, relief formation is a function of oscillating climate.

With the exception of this chapter and Chapter 6 (Conclusions), each of the chapters of this thesis have been submitted to peer-reviewed journals. Chapter 3 ("Abnormal monsoon years and their control on erosion and sediment flux in the high, arid northwest Himalaya" by Bodo Bookhagen, Rasmus C. Thiede and Manfred R. Strecker) is in press in *Earth and Planetary Science Letters*, Chapter 4 ("Late Quaternary intensified monsoon phases control landscape evolution in the northwest Himalaya" by Bodo Bookhagen, Rasmus C. Thiede and Manfred R. Strecker) is in press in *Geology*, and Chapter 5 ("Holocene monsoonal dynamics and fluvial terrace formation in the northwest Himalaya" by Bodo Bookhagen, Dominik Fleitmann, Kuni Nishiizumi, Manfred R. Strecker, Rasmus C. Thiede) has been submitted to the journal *Geophysical Research Letters*.

2. CLIMATIC AND TECTONIC SETTING

The India-Eurasia continental collision is the most spectacular example of active mountain building, orogenic plateau development and climatic forcing on Earth (Fig. 2.1, 2.2) [e.g., *Gansser*, 1964, 1980; *Allegre et al.*, 1984; *Molnar*, 1997; *Hodges*, 2000; *Zheng et al.*, 2000; *Zhisheng et al.*, 2001]. Related tectonic deformation and climatic influences extend well beyond the Himalaya and Indian subcontinent. For example, the elevated Tibetan plateau initiates, controls, and forces the Asian monsoon [e.g., *Riehl*, 1954; *Flohn*, 1969; *Hahn and Manabe*, 1976; *Hahn and Shukla*, 1976; *Webster*, 1987; *Prell and Kutzbach*, 1992]. While the Tibetan Plateau largely remain arid, the southern Himalayan mountain front receives several meters of rainfall during the Indian summer monsoon season between June and September [e.g., *Barros et al.*, 2000; *Bookhagen et al.*, 2005b; *Parthasarathy et al.*, 1992]. This intense precipitation gradient across the orogen arguably influences the deformation field through enhanced hillslope and fluvial erosion processes, eventually leading to massive crustal unloading [e.g., *Zeitler et al.*, 2001; *Finlayson et al.*, 2002; *Reiners et al.*, 2003]. For example, persistent humid conditions associated with sustained mass removal along the southern Himalayan mountain front might lead to higher uplift rates in response to isostatic unloading [e.g., *Wobus et al.*, 2003; *Hodges et al.*, 2004; *Thiede et al.*, 2004]. This relationship is probably a long-lived feature, because for at least the past 10 Ma the tectonic evolution of Himalaya has been under the influence of the Asian monsoon, thereby providing a site to examine the interactions and feedbacks between tectonics and climate [e.g., *Zhisheng et al.*, 2001; *Dettman et al.*, 2003]. However, these feedback processes are still a matter of ongoing debate and long-term erosional effects are difficult to decipher [e.g., *Burbank et al.*, 1993, 2003; *Willett*, 1999; *Reiners et al.*, 2003].

2.1 Tectonic Structures and Geology

The Himalayan kinematic evolution is associated with major faults, bounding the various terrane and rock complexes that are linked to collision processes at the southern margin of Eurasia [e.g., *Gansser*, 1964; *Vannay and Steck*, 1995; *Hodges*, 2000; *Tapponnier*, 2002; *Steck*, 2003]. The Himalaya can thus be subdivided into several contrasting tectono-stratigraphic units separated by major tectonic contacts (Fig. 2.3). From north to south, that is, from the internal to the

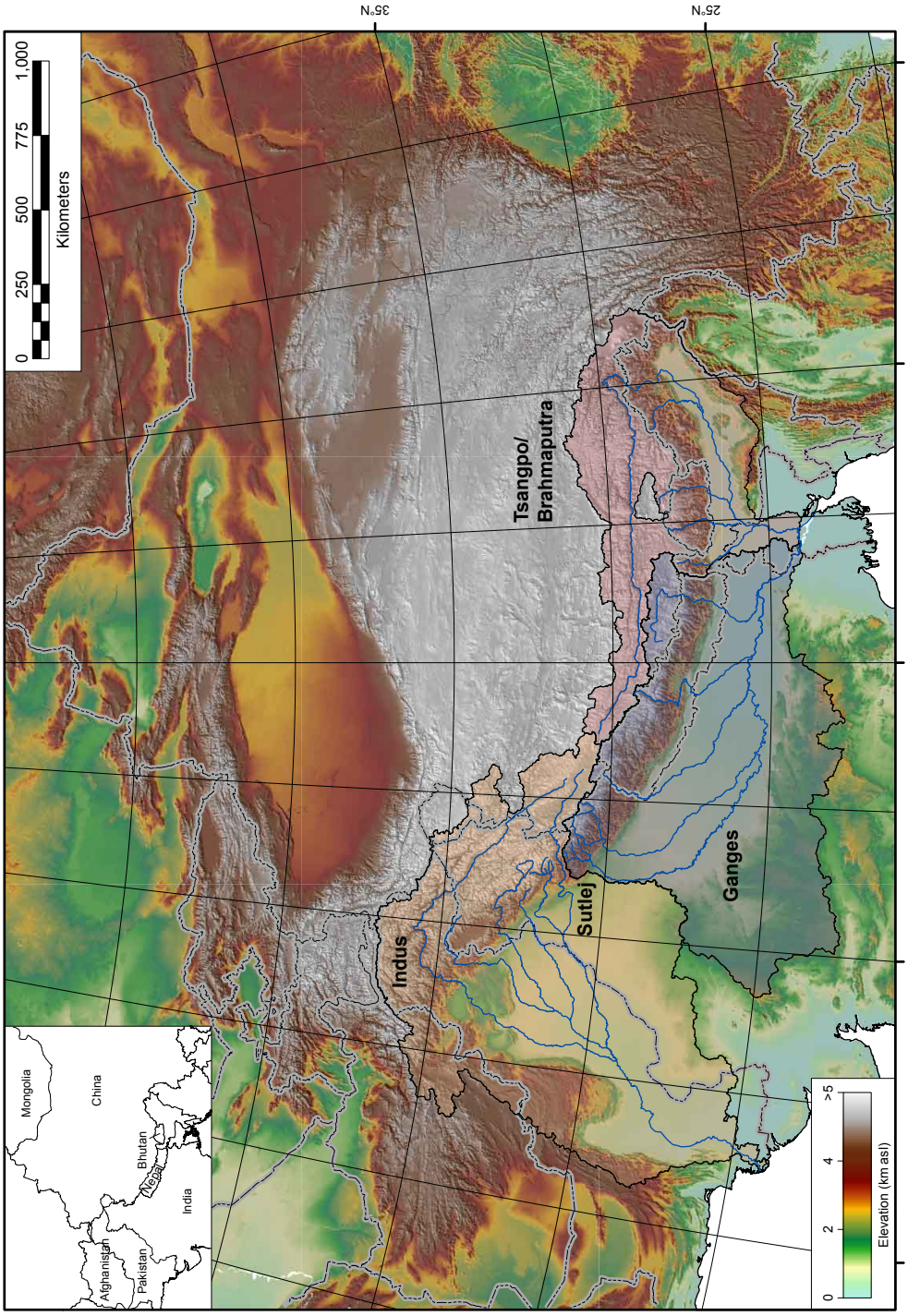

Figure 2.1: Topography (HYDRO1K) for the Himalaya and adjacent regions. Rivers are shown in blue and drainage areas are colored as follows: Indus drainage area in yellow, Ganges in blue and Tsangpo/Brahmaputra in light red. Drainage basins were determined using flow-routing algorithms.

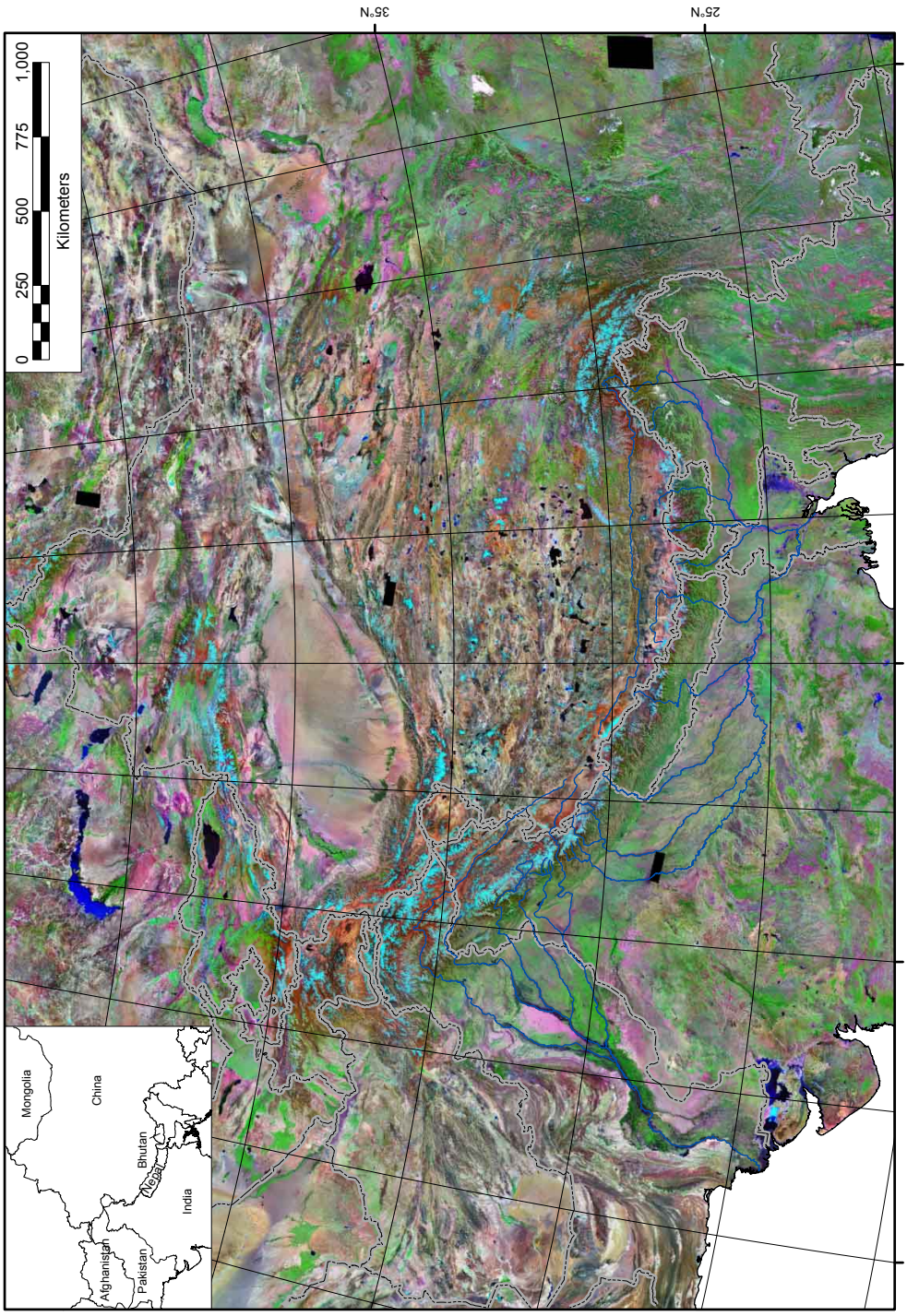

Figure 2.2: Landsat TM mosaic of the Greater Himalaya (data provided by the NASA and their Earth Science Enterprise Scientific Data Purchase Program). This image uses the Landsat TM channels 7, 4, 1 (R, G, B), and thus light blue colors represent glaciers, green vegetation, lakes are dark blue and black, and the remaining colors depict lithologies.

external parts of the orogen, these units are (1) the Indus suture zone, containing the ophiolites of the Neo-Tethys ocean; (2) the Tethyan Himalaya, containing the Upper Proterozoic to Eocene sedimentary cover of the north Indian margin; (3) the Himalayan crystalline core zone, composed of high-grade metamorphic gneisses and migmatites; (4) the Lesser Himalaya, mainly comprised of low-grade Proterozoic sediments of the Indian plate; and (5) the Sub-Himalaya foreland basin, containing the Oligocene to Neogene detrital sediments derived from erosion of the orogen.

2.2 Oscillating Climate in the Asian Monsoon Domain

The monsoon is the dominant erosion agent in south- and southeastern Asia. In order to understand potential links between erosion processes and tectonics, we need to characterize and evaluate the role of the Asian monsoon. Here, I describe the basic concepts of the Asian monsoon, changing boundary conditions, and their oscillations through time.

The word monsoon is derived from the Arabic word for seasonal wind, and the distinguishing attribute of the monsoonal regions of the world is considered to be the seasonal reversal in the direction of the wind. Over 300 years ago, *Halley* [1686] suggested that the primary cause of the monsoon was the different heating between ocean and land. Thus, in the first-ever model proposed, the monsoon was considered to be a gigantic land-sea breeze. Differential heating of land and sea is still considered to be the basic mechanism for the monsoon by several scientists [e.g., *Webster and Chou*, 1980; *Fein and Stephens*, 1987; *Webster*, 1987; *Hastenrath*, 1994]. An alternative hypothesis considers the monsoon to be a manifestation of the seasonal migration of the intertropical convergence zone or the equatorial trough in response to the seasonal variation of the latitude of maximum insolation [e.g., *Riehl*, 1954; *Charney*, 1969; *Riehl*, 1979; *Gadgil et al.*, 2003].

The long-term evolution and variability of the monsoon can be attributed to changes in at least four types of large-scale forcing or boundary conditions: orbital parameters, mountain-plateau orography (tectonic), glacial-age surface boundary conditions and atmospheric CO_2 concentration [e.g., *Flohn*, 1957, 1969; *Hahn and Manabe*, 1975; *Webster and Chou*, 1980; *Webster*, 1987; *Clemens and Prell*, 1991; *Prell and Kutzbach*, 1992; *Rodwell and Hoskins*, 1995; *Hoskins and Rodwell*, 1995; *Wu and Zhang*, 1998; *Hsu and Liu*, 2003]. These amplify or dampen the seasonal processes of heating, latent heat transport and moisture convergence over the Asian continent, and thereby modify the strength of the summer monsoon circulation. *Prell and Kutzbach* [1992] suggest that the monsoon is most sensitive to elevation and radiation (orbital) changes. They conclude that at least half the modern elevations are a pre-requisite for strong monsoon circulations. Similarly, *Clemens and Prell* [1991] argue that solar insolation and latent heat released over the elevated Tibetan Plateau dominates monsoonal circulation. Comparisons to

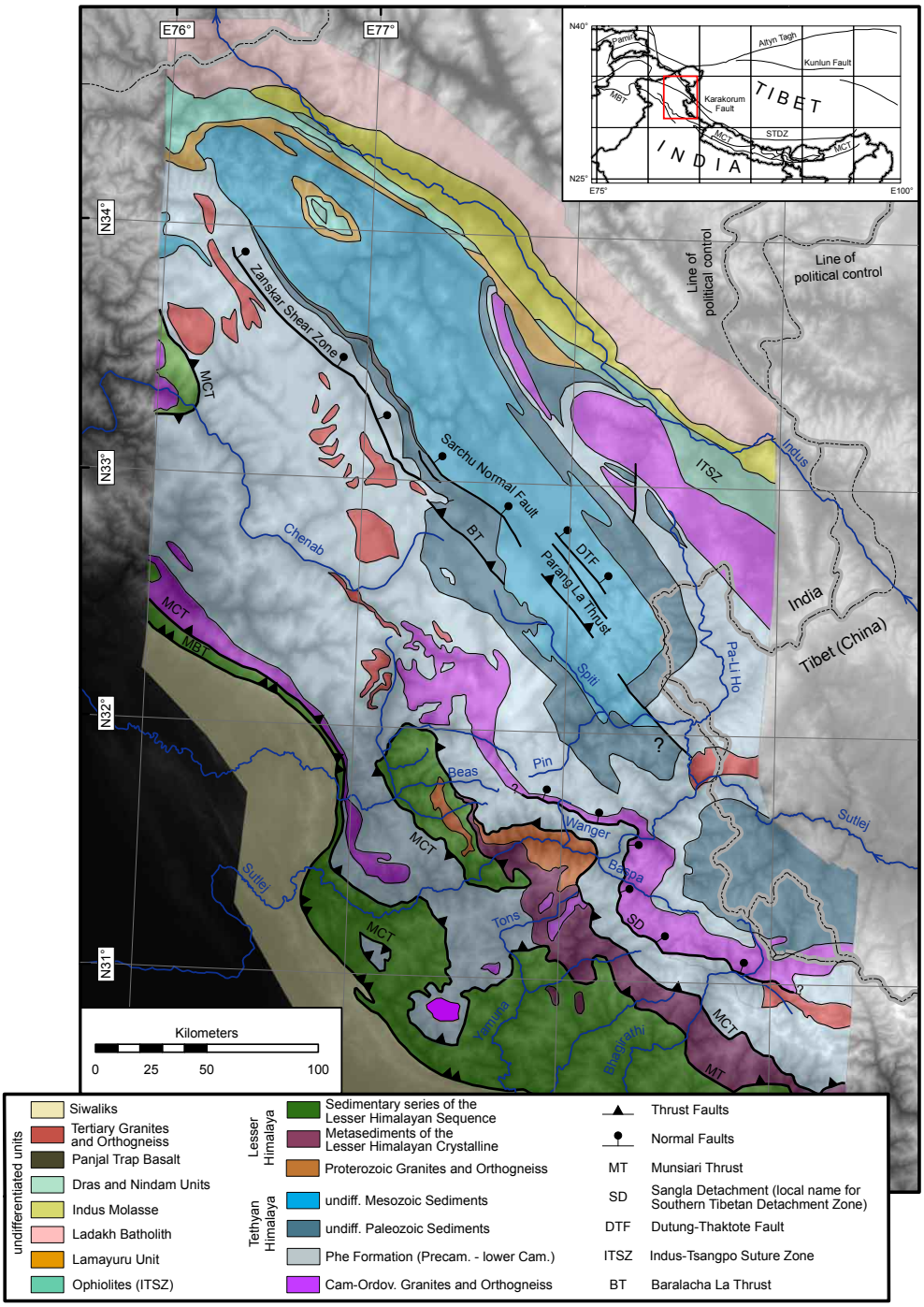

Figure 2.3: Geological Overview of the northwestern Himalaya. Simplified after *Wyss et al.* [1999].

paleoclimate data indicate that these conditions were achieved in the late Miocene [e.g., *Molnar*, 1997; *Zheng et al.*, 2000; *Zhisheng et al.*, 2001; *Dettman et al.*, 2001; *Guo et al.*, 2002; *Gupta and Thomas*, 2003; *Dettman et al.*, 2003]. Thus, synoptically, the high elevation of the Tibetan Plateau intensifies the differential heating between land and ocean, but also locally forces rain due to the orographic barrier along the southern slopes of the Himalaya [e.g., *Barros et al.*, 2000; *Bookhagen et al.*, 2005b]. This two-fold influence of the Tibetan Plateau is important with respect to the interaction between erosion processes and long-term, erosion-controlled landscape evolution.

The response of monsoon circulation and tropical precipitation to orbitally-controlled solar radiation changes was much larger than the response to changes of glacial-age boundary conditions [e.g., *Hahn and Manabe*, 1976; *Hahn and Shukla*, 1976]. Much of the climate change during the period between 12,000 and 6000 yr BP can be described as an amplified (weakened) seasonal cycle in response to the larger (smaller) seasonal radiation extremes of the northern (southern) hemisphere. Summers were warmer and winters colder in the northern hemisphere, but there was little change in annual average temperature [e.g., *Berger*, 1978; *Kutzbach and Guetter*, 1986; *Hastenrath*, 1994; *Overpeck et al.*, 1996]. However, because the nonlinear relationship between saturation vapor pressure and temperature, the sensitivity of the hydrologic cycle to orbital parameter changes was larger in summer than in winter (and in the tropics, rather than high latitudes); in the tropics, this led to a net increase in estimated annual average precipitation and precipitation minus evaporation [e.g., *Kutzbach and Guetter*, 1986; *Overpeck et al.*, 1996]. Both modern and ancient Indian summer monsoons are driven by differential heating and resulting trans-equatorial pressure differences, directly coupled with the insolation difference between the northern and southern subtropical hemispheres. Long-term records from marine sediment cores resemble a strong link between insolation and Indian summer monsoon strength [*Sirocko et al.*, 1996; *Overpeck et al.*, 1996; *Heusser and Sirocko*, 1997; *Clemens and Prell*, 2003; *Fleitmann et al.*, 2003; *Leuschner and Sirocko*, 2003].

Interannual fluctuations in monsoon rains are also accompanied by large changes in atmospheric heating on the scale of south Asia [e.g., *Fasullo and Webster*, 2003; *Rodwell and Hoskins*, 2001]. The scale and magnitude of these heating perturbations are such that they have the potential of influencing and responding to other modes of tropical variability such as the El Niño/Southern Oscillation (ENSO) (Fig. 2.4). However, the interaction of the monsoon with other large-scale climatologic features is very complex and is therefore difficult to interpret. Early investigations of teleconnections with the monsoon region reveal a moderate correlation between anomalies in rainfall during June-July-August-September (JJAS) and sea surface temperatures (SST) in the eastern tropical Pacific Ocean [e.g., *Walker*, 1923; *Barnett*, 1983; *Rasmusson and Carpenter*, 1983; *Shukla and Paolino*, 1983]. The physical nature of a monsoon-ENSO telecon-

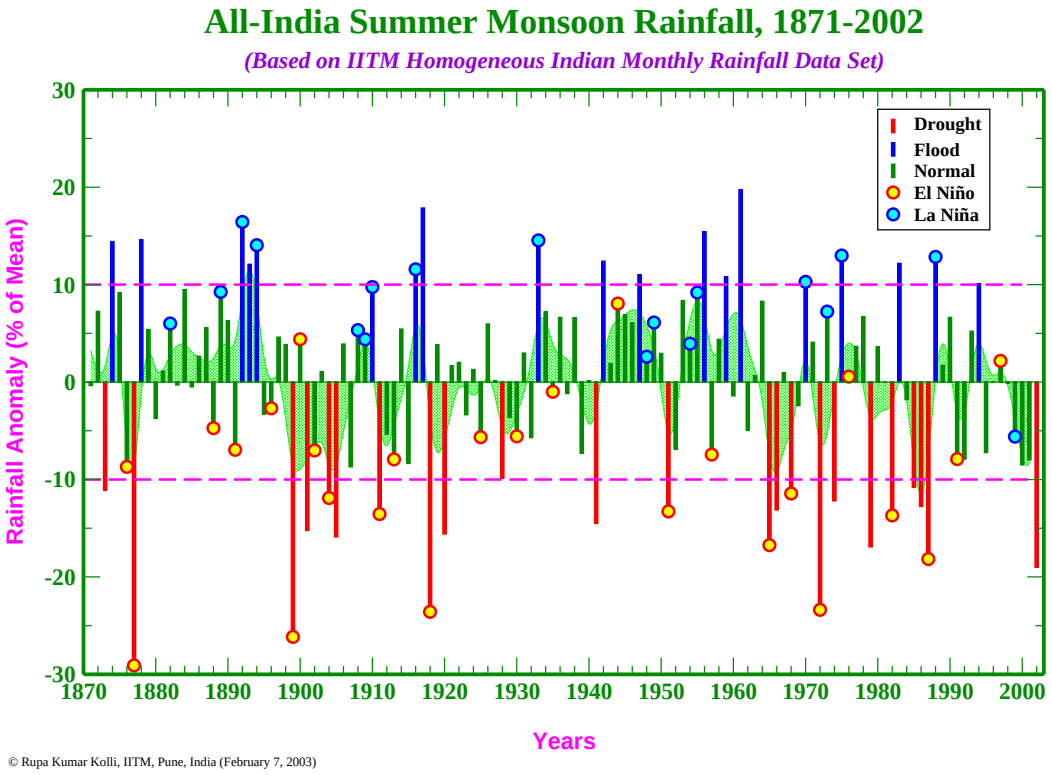

Figure 2.4: All India Summer Monsoon Rainfall from 1871–2002. Based on data from IITM, Pune. Rain gauges were mostly located in low-elevation regions in the Monsoon belt of India.

nection is often explained as an interaction between the Hadley circulation in the monsoon region with changes in moisture convergence driven by trade winds and a perturbed Walker circulation during ENSO [e.g., *Barnett*, 1983; *Rasmusson and Carpenter*, 1983; *Barnett*, 1984; *Webster and Yang*, 1992; *Ju and Slingo*, 1995; *Goswami*, 1998; *Lau and Bua*, 1998; *Fasullo and Webster*, 2002]. According to these theories, the net result of the interaction is a reduction in moisture transport into south Asia during El Nino events and an enhancement of convergence during La Nina events [e.g., *Sikka and Gadgil*, 1980; *Pant and Parthasarathy*, 1981; *Shukla and Paolino*, 1983; *Kumar et al.*, 1992; *Webster and Yang*, 1992; *Charles et al.*, 1997; *Krishnamurthy and Shukla*, 2000; *Slingo and Annamalai*, 2000; *Fasullo and Webster*, 2002]. One of the key features about the nature of the monsoon-ENSO interaction is the modification of moisture convergence in India and the Bay of Bengal regions during ENSO events due to both enhanced westerly vertical integrated moisture transport from the Arabian Sea and anomalous easterly vertical integrated moisture transport from the Pacific Ocean [e.g., *Fasullo and Webster*, 2002]. In terms of the

differential land-ocean heating model, a warm (cold) ENSO event results in a weaker (stronger) Asian monsoon, because of a lower (higher) temperature gradient. Similarly, in years of enhanced (reduced) winter snow cover in central Asia decreases (increases) the temperature difference and thus weakens (strengthen) the temperature gradient as the monsoonal driving force [e.g., *Hahn and Manabe*, 1976; *Meehl*, 1994].

2.3 Potential Erosion-Tectonic Feedbacks, Related Geomorphic Processes and Their Timescales

Recently it has been proposed that a positive feedback mechanism between erosion and tectonic uplift may exist [e.g., *Molnar and England*, 1990; *Burbank*, 1992; *Zeitler et al.*, 2001; *Koons et al.*, 2002; *Reiners et al.*, 2003]. The fundamental controlling factors of this hypothesis are erosional surface processes that are most likely dictated by climate. The coupled effects of topographic relief evolution and erosional unloading importantly influence the following: (1) isostatically compensated mountain summit elevation uplift and thus interpretation of landscape morphology in terms of tectonically-driven surface uplift; (2) spatial and temporal partitioning of tectonic and isostatic rock uplift, with potential direct feedback loops between zones of focused crustal strain; and (3) near-surface geothermal gradients through fast mass removal if no large tectonic structures are present, and thus interpretation of thermochronological data in terms of rock exhumation rates. The evolution of relief in response to climate change is particularly important in the debate over potential linkages between late Cenozoic uplift of the Himalayas and the Tibetan plateau and the onset of Quaternary glaciation [**?***Molnar*, 2004]. However, the link between surface erosion, uplift, and climatic variation is everything but trivial. For example, on short timescales more rainfall is argued to increase hillslope erosion, but simultaneously prevailing humid conditions increase vegetation cover and limit further erosion along steep slopes [e.g., *Lavé and Burbank*, 2004]. Thus, climatic oscillations may be a forcing factor for erosion [e.g., *Molnar et al.*, 1993; *Peizhen et al.*, 2001; *Molnar*, 2004]. Here, I summarize landscape response on various timescales and focus on annual to millennial periods that are the primary focus of this thesis.

On timescales embracing the late Cenozoic (10^6 years), it is argued that sediment accumulation rates of terrestrial sediment have increased in the past few million years both on and adjacent to continents, although not everywhere [e.g., *Molnar and England*, 1990; *Metivier and Gaudemer*, 1997, 1999; *Zheng et al.*, 2000; *Molnar*, 2004]. During these periods, erosion has apparently increased in elevated terrain regardless of when last tectonically active or what the character of the present-day climate is. If climate change triggered accelerated erosion, understanding the responsible mechanism(s) still remains an important challenge. Some obvious causes, such as a lowered sea level leading to both erosion of continental shelves and enhanced fluvial incision

on the continents, or increased glaciation, account for increased sedimentation in some areas. The erosional processes and mass removal, however, are strongly tied to climatic variations such as glacial and interglacial periods during the Quaternary. Paleoclimate archives and present measurements document oscillations on various magnitudes and frequencies, especially in the monsoon domain [e.g,. *Sirocko et al.*, 1993; *Wang et al.*, 2001; *Fleitmann et al.*, 2003; *Yuan et al.*, 2004]. However, the geomorphic and sedimentary response for these magnitude-frequency relationships is still largely unknown. It is argued that perhaps stable climates varied slowly and allowed geomorphic processes to maintain a state of equilibrium with little erosion until ∼3-4 Ma. In contrast, large climatic oscillations with higher frequencies (periods of 20,000–40,000 years) developed and may have prevented the landscape to reach equilibrium. However, there is no evidence as to which processes dominated sedimentary production and transport. For example, work from the northwest Argentine Andes suggests that transient hydrologically isolated, intramontane basins may develop that prevent effective mass removal from the orogen for several 10^5 to 10^6 years and thus limit the tectonic response to erosional unloading [e.g., *Sobel et al.*, 2003; *Hilley and Strecker*, 2004; *Hilley et al.*, 2004; *Hilley and Strecker*, 2005]. Alternatively, they may trigger out-of-sequence deformation due to headward erosion and intramontane basin capture.

On timescales spanning the Late Quaternary (10^5 years), the primary high-resolution climatic records are the Antarctic Vostok and Dome C ice cores that provide compelling evidence of the nature of climate, and of climate feedbacks, over the past 740,000 years [e.g., *Petit et al.*, 1997; *Augustin et al.*, 2004]. For example, it is known that glaciation occurred at various frequencies and that dominant periods changed throughout the Late Quaternary. However, the low temporal resolution of sedimentary records dilutes any signal from geomorphic processes and does not allow us yet to resolve a process-based climate-erosion interaction.

Thus, the younger climatic history encompassing the Late Pleistocene and Holocene provide the unique opportunity to study process interaction on annual to millennial timescales. On yearly timescales it is argued that extreme events dominate erosion and processes [e.g., *Tucker and Slingerland*, 1997; *Snyder et al.*, 2003]. Especially the landscape in arid regions is shaped during low frequency/high magnitude rainfall and flood events [e.g., *Coppus and Imeson*, 2002]. In the northwest Himalaya we find these arid regions leeward of orographic barriers in excess of 4 km elevation. There, increased shallow hillslope-erosion processes are observed during abnormal monsoon years. Millenial-scale monsoonal variation wash out and fill river valleys [e.g., *Pratt et al.*, 2002; *Pratt-Sitaula et al.*, 2004; *Bookhagen et al.*, 2005a]. River alluviation is linked to landsliding as observed in other orogens as well [e.g., *Dethier and Reneau*, 1996; *Reneau and Dethier*, 1996; *Trauth et al.*, 2000]. Processes between these timescales differ significantly and may have self-regulating effects. For example, during the intensified monsoon phase in the

early Holocene, sediment evacuation increased until a threshold was reached that triggered deep-seated mass movements and resulted in the formation of landslide-dammed, transient basins [e.g., *Bookhagen et al.*, 2003, 2005a]. These strongly nonlinear responses on short timescales suggest that the interaction between erosion and climate on longer periods is extremely complex and will need further investigation to be fully assessed and understood.

3. ABNORMAL MONSOON YEARS (AMY) AND THEIR CONTROL ON EROSION AND SEDIMENT FLUX IN THE HIGH, ARID NORTHWEST HIMALAYA

Abstract

The interplay between topography and Indian summer monsoon circulation profoundly controls precipitation distribution, sediment transport, and river discharge along the Southern Himalayan Mountain Front (SHF). The Higher Himalayas form a major orographic barrier that separates humid sectors to the south and arid regions to the north. During the Indian summer monsoon, vortices transport moisture from the Bay of Bengal, swirl along the SHF to the northwest, and cause heavy rainfall when colliding with the mountain front. In the eastern and central parts of the Himalaya precipitation measurements derived from passive microwave analysis (SSM/I) show a strong gradient, with high values at medium elevations and extensive penetration of moisture along major river valleys into the orogen. The end of the monsoonal conveyer belt is near the Sutlej Valley in the NW Himalaya, where precipitation is lower and rainfall maxima move to lower elevations. This region thus comprises a climatic transition zone that is very sensitive to changes in Indian summer monsoon strength. To constrain magnitude, temporal, and spatial distribution of precipitation, we analyzed high-resolution passive microwave data from the last decade and identified an abnormal monsoon year (AMY) in 2002. During the 2002 AMY, violent rainstorms conquered orographic barriers and penetrated far into otherwise arid regions in the northwest Himalaya at elevations in excess of 3 km asl. While precipitation in these regions was significantly increased and triggered extensive erosional processes (i.e., debris flows) on sparsely vegetated, steep hillslopes, mean rainfall along the low- to medium elevations was not significantly greater in magnitude. This shift may thus play an important role in the overall sediment flux toward the Himalayan foreland. Using extended precipitation and sediment flux records for the last century, we show that these events have a decadal recurrence interval during the present-day monsoon circulation. Hence, episodically occurring AMYs control geomorphic processes primarily in the high-elevation, arid sectors of the orogen, while annual recurring monsoonal rainfall distribution dominates erosion in the low- to medium elevation parts along the SHF.

3.1 Introduction

Climate change, climate variability, and short-lived extreme weather events exert control on hillslope and transport processes, and hence profoundly impact character and rates of surface

processes and therefore landscape development [e.g., *Molnar and England*, 1990; *Baker and Kale*, 1998; *Coppus and Imeson*, 2002; *Hartshorn et al.*, 2002; *Dadson et al.*, 2003; *Snyder et al.*, 2003]. Along the Southern Himalayan Mountain Front (SHF), interannual variations in Indian Summer monsoon strength strongly influence sediment flux and river discharge to the foreland [*Sah and Mazari*, 1998; *Paul et al.*, 2000; *Barnard et al.*, 2001]. However, the link between precipitation distribution, erosional hillslope processes (e.g., landsliding, debris flows), and sediment transport in the mountainous regions along the SHF is poorly constrained, and the impact of short-lived, abnormal monsoon events on landscape evolution has not been quantified. This is important, because voluminous debris flows, rock falls, slope failures, and massive effects on infrastructure document a link between short-lived climate and surface-process phenomena. Particularly in high mountain terrains, a better assessment and understanding of the connection between extreme climatic events and surface-process response is desirable, but often difficult to achieve due to the lack of adequate monitoring possibilities. A synoptic comparison of rainfall data and its spatial variability in remote mountainous regions can be accomplished, however, by using high-resolution, satellite-borne passive microwave data.

In this study we show that the Sutlej Valley region (78°E, 31°N) of the northwest Himalaya comprises a climatic transition zone that is very sensitive to the strength of the Indian Summer Monsoon (ISM). The availability of rain-gauge, discharge and suspended sediment-flux data makes this region an ideal environment to study the impacts of monsoonal precipitation on landscape-shaping processes. We processed and calibrated passive microwave data of the last decade to constrain temporal and spatial variations in rainfall and identified an abnormal monsoon year (AMY) in 2002. During the 2002 monsoon season exceptionally strong rainfall events that were not observed in the last decade, affected the usually arid, high-elevation regions of the upper Sutlej Valley. In this orographically shielded region, sediment production and mean basin denudation rates are low during the presently weak ISM circulation. Only during AMYs moisture penetrates farther into the orogen, amplifies erosive hillslope processes, such as debris flows, and increases fluvial sediment flux. In order to quantify the effect of shifting precipitation patterns on landscape evolution, we analyzed river discharge, sediment-transport and rainfall measurements, as well as satellite imagery before and after the AMY 2002 monsoon season.

Our results show a pronounced increase in mean basin denudation rates for these abnormal, recurring events. More importantly, amplified erosive hillslope processes that were triggered during AMYs dominate channel formation and fluvial network evolution in the arid, high-elevation sectors. While sediment efflux from this orographically shielded region was enhanced, total sediment flux toward the Himalayan foreland is still controlled by erosion of topographically-forced rainfall in the large monsoonal belt along the SHF. Thus, the present-day, weak monsoon circulation mainly affects areas between 1–3 km elevations. However, studies of proxies for monsoonal

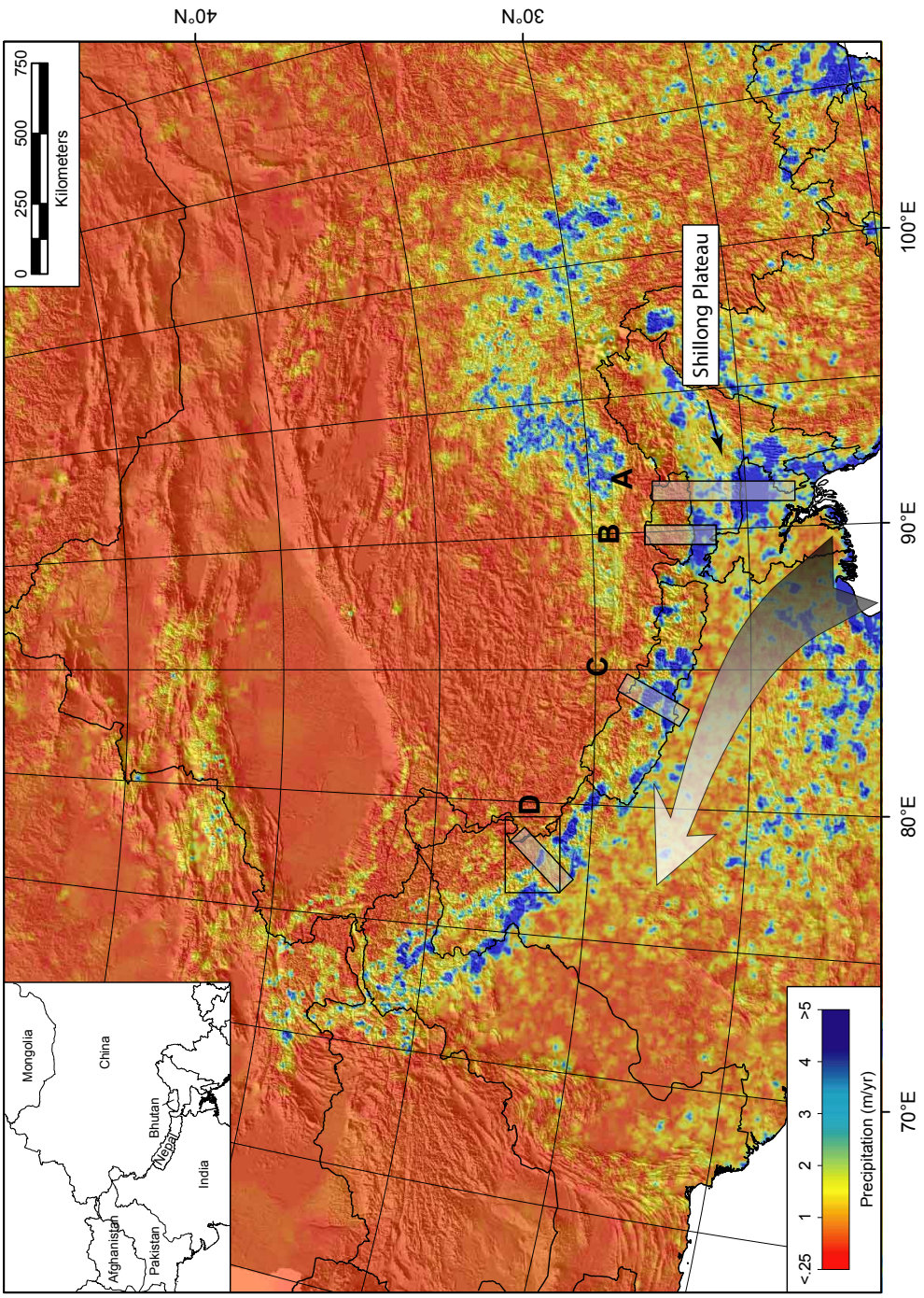

Figure 3.1: Mean annual precipitation for the Himalayan region based on passive microwave SSM/I data, analyzed for a 10-year time period (1992–2001, where data were available) during the Indian Summer Monsoon (June–August). Large arrow indicates moisture transport from the Bay of Bengal along the Southern Himalayan Front. Swath profiles (Fig. 3.5) are outlined by black boxes with gray shading. Profiles (from E to W) are: (A) Shillong-Plateau and Eastern Bhutan, (B) Sankosh River in Western Bhutan, (C) Kali Gandaki River in Central Nepal, and (D) Sutlej River, NW Himalaya. Plain, black box indicates location of Fig. 3.6.

precipitation distribution strongly suggest enhanced orogenward moisture migration into the high, arid regions in the late Pleistocene and early Holocene [e.g., *Gasse et al.*, 1991; *Bookhagen et al.*, 2005a]. During these periods, sediment flux toward the Himalayan foreland and adjacent oceans may have been dominated by material that was easily eroded from the shielded, high-elevation sectors. In this paper, we explore the geomorphic processes and influence on sediment flux on annual and event timescales to document the importance of AMYs on landscape shaping processes.

3.2 The Indian Summer Monsoon (ISM)

The ISM is part of a larger phenomenon called the InterTropical Convergence Zone (ITCZ). The ITCZ separates the wind circulation of the northern and southern hemispheres [e.g., *Webster and Chou*, 1980; *Gadgil et al.*, 2003]. This zone migrates north and south with the annual changes of the sun's declination and is located where the NE and SE trade winds converge. It is also characterized by strong upward motion of air and heavy, convective rainfall, as a result of intense solar heating during the boreal summer. The high topography of the Tibetan Plateau and latent heat released by the condensation of moisture amplifies the relative warming of the Asian landmass compared to the surrounding oceans and hence helps to establish the ISM circulation [e.g., *Webster et al.*, 1998; *Gadgil et al.*, 2003]. Inter-annual variations of ISM strength mainly result from deflections of this thermal gradient (e.g., through sea-surface temperatures during El Niño/Southern Oscillation and Asian winter snow cover distribution) [e.g., *Charles et al.*, 1997; *Clark et al.*, 2000]. General moisture transport during the ISM is controlled by the strong thermal divergence caused by the low-pressure cell over the Tibetan Plateau and high-pressure over the surrounding oceans, producing north- to northwestward, counterclockwise humid eddies originating in the Bay of Bengal [e.g., *Webster et al.*, 1998; *Shrestha*, 2000; *Lang and Barros*, 2002]. The monsoonal vortices are deflected and swirl along the SHF to the NW, causing heavy monsoonal precipitation from convection cells, when colliding with the mountain front (Fig. 3.1).

Primary control on the path of the monsoonal vortices and hence, moisture transport, is guided by the prevailing wind direction and speed during the ISM [*Lang and Barros*, 2002]. However, on medium to small spatial scales (10^2–10^4 km^2), local topography governs moisture migration along topographic barriers and into deeply incised valleys perpendicular to the mountain front (Fig. 3.1). The influence of orography can be attributed primarily to localized disturbances of the vertical structure of the atmosphere. Such disturbances exert important control acting either as barriers, elevated heat sources and sinks, or concentrated areas of high roughness [e.g., *Bergeron*, 1960; *Smith*, 1979b, a; *Barros and Lattenmaier*, 1994]. In addition to destabilizing the atmosphere, airflow over such topographic barriers leads to the ascent of

relatively water-rich, warm air from lower elevations. The forced ascent of moist air enhances condensation, the formation and growth of clouds, and ultimately, controls the triggering, duration, and intensity of precipitation events at high elevations. For example, the E-W oriented Shillong Plateau located to the south of the SHF forms a ∼2 km-high barrier, which forces high amounts of rainfall (∼5 m/yr) on the south, whereas leeward areas along the SHF receive ∼1 m/yr (Fig. 3.1). During the ISM, condensation on the windward side is initiated when a wet air parcel from the Bay of Bengal can no longer hold water in the vapor phase. As moisture-rich air masses move up in the atmosphere along the orographic barrier, pressure decreases and volume expands. Simultaneously, temperature and saturation vapor pressure decrease due to the conservation of energy and the proportionality between pressure and temperature of an ideal gas [e.g., *Barros and Lattenmaier*, 1994]. This interplay between low-level moist air flows and topography controls the amount and distribution of rainfall. Comparable conditions, although with lower amounts of precipitation, exist along the entire SHF.

The high rainfall amounts during the ISM thus exercise strong control on river discharge and consequently sediment transport, leading to major flooding and sediment deposition south of the orographic barriers.

3.3 Determining precipitation

To constrain the amount and distribution of rainfall in the Himalaya, and particularly the Sutlej region with sufficiently high resolution, we used passive microwave data from the Special Sensor Microwave/Imager (SSM/I) of the polar-orbiting Defense Meteorological Satellite Program (DMSP). The SSM/I satellite, which has been in operation since 1987 [*Hollinger*, 1990], has the unique ability to penetrate through cirrus clouds and sense the emitted and scattered radiation caused by raindrops and precipitation-sized ice particles, respectively. In the early stages of SSM/I data analysis, studies were limited to oceanic regions, because the determination of rainfall by passive microwave measurements is based on low frequency/emission techniques, and hence estimation was more direct over ocean than over land. In this study, however, high frequency/scattering techniques are used. The primary method for land-rainfall retrieval uses an 85 GHz scattering-based algorithm [e.g., *Grody*, 1991; *Kummerow and Giglio*, 1994a, b; *Ferraro*, 1997] to obtain daily land precipitation with a spatial resolution of 156.25 km^2 (footprint of 12.5 km). The rain signature needs to be separated from other surfaces exhibiting similar characteristics, such as snow cover, deserts and semiarid regions [*Grody*, 1991; *Ferraro et al.*, 1998]. Overviews of the varying techniques for rainfall retrieval from the SSM/I are presented by [*Wilheit et al.*, 1994; *Petty*, 1995]. Many of the algorithms suffered from the improper delineation of rain areas from other surfaces that exhibit similar microwave signatures, resulting in erroneous

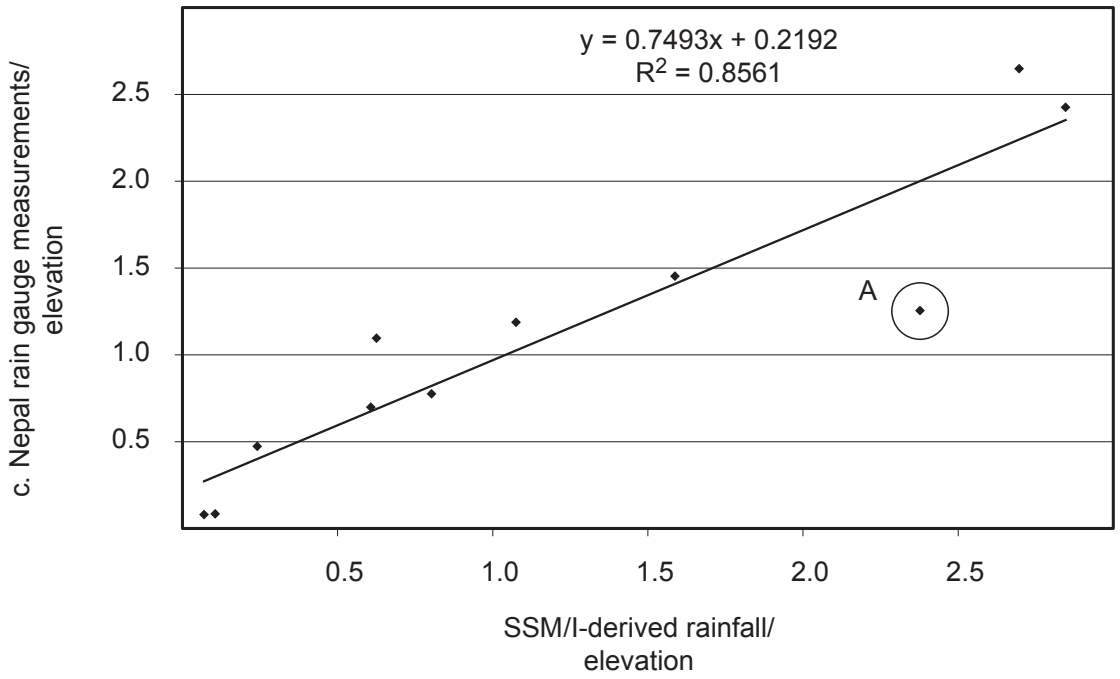

Figure 3.2: Ratios of rainfall estimations and elevation. We plot the ratio of central Nepal rain gauges and elevation (see *Lang and Barros* [2002] and Tab. 3.1 more information) vs. the ratio of SSM/I-derived rainfall and elevation for the same time interval (June to September, 1999 and 2000). We average all measurements from spot gauges that lie within the ∼150 km^2 SSM/I grid cell and divide it by the averaged elevation. The datasets show a good correlation despite their different spatial resolutions. A circled outlier labeled A (included into the regression analysis) is caused by a different grid cell elevation and not by a significant difference in rainfall amount (rain gauge elevation of ∼1300 m asl with 1627 mm/yr vs. 750 m asl and 1790 mm/yr of the SSM/I grid cell).

excessive monthly rainfall amounts [*Ferraro et al.*, 1998]. To avoid these problems, we identified critical regions such as glaciers, ice and snow fields using screening techniques suggested by Grody [*Grody*, 1991]. In addition, we applied a supervised classification algorithm on a Landsat TM mosaic for the complete Himalayan region to determine these critical areas more reliably. We then processed the marked regions in a different way by taking into account the surface characteristics.

We focused on processing data for the summer monsoon months, because more than 80% of precipitation along the SHF falls during the ISM [*Shrestha*, 2000]. In addition, the increased snow cover during winter would necessitate extensive screening to distinguish snow from overland precipitation. Where available, we analyzed data for the three summer monsoon months (June to August) between 1992 and 2002 (Fig. 3.1). This information was first calibrated with local rainfall measurements from the northwest Himalaya [*Beas Bhakra Management*, 2001; *Jaiprakash Company*, 2002, unpublished company data]. In order to understand and quantify precipitation

Station Nr.	JJAS mean rain for 1999 and 2000 [mm]	SSM/I-derived rainfall [mm]	Mean station elevation [m]	SSM/I grid cell elevation [m]	Precipitation deflection (%)
13	1281	1870	528	657	-31.52
16	1315	1240	1200	1982	6.01
4,8,11,12	3373	3500	1274	1298	-3.63
1,18	1627	1790	1297	753	-9.12
3,19	3842	4215	2644	2656	-8.86
2,17,20	1278	850	2702	3526	50.31
9	3503	3560	2950	3312	-1.60
5,15	2698	2410	3478	3002	11.95
6	302	550	3562	5212	-45.09
7	339	280	4220	4021	21.07
14	3100	2450	4435	4035	26.53

Table 3.1: Comparison of SSM/I-derived precipitation and rainfall-gauge measurements in central Nepal [*Lang and Barros*, 2002; *Barros et al.*, 2000]. Stations correspond to single point measurements, whereas passive microwave data average rainfall over an area of ∼150 km^2. To compare the two spatially different datasets we examine the rain-gauge data with the corresponding SSM/I cell during the same time interval. Precipitation is strongly dependent on elevation in this part of the Himalaya, as shown by the swath profile in Fig. 3.3. Precipitation deflection describes the deviation between these dataset, and most of the deflections in the highly correlated data can be attributed to spatial differences and variations in mean elevation between passive microwave and rain-gauge datasets. The 2 datasets are highly correlated; differences can be attributed to the spatial difference and the variation in mean elevation of the passive microwave and rain-gauge datasets. For example, stations 4, 8, 11, 12 all fall into one SSM/I grid cell, cover the same mean elevation, pertain to the same climatic regime, and hence show similar precipitation values. In contrast, stations 2, 17, 20 show the influence of two climatic settings: The wet, southern and the dry, northern part in the rain shadow of the Annapurna. Station 17 is the dry station that correlates very well with the SSM/I-derived precipitation. Here, the SSM/I-derived precipitation is lower, because dry regions cover a larger area of this grid cell. JJAS stands for June, July, August, September rainfall. The elevations were taken from Hydro1K dataset (1 km^2 resolution) and averaged over SSM/I measurement area (156.25 km^2).

changes along the SHF we compare our calibrated data with gauge stations in a similar remote environment in central Nepal [*Barros et al.*, 2000; *Lang and Barros*, 2002] (Fig. 3.2 and Tab. 3.1). Although, the datasets are spatially inconsistent (point measurement vs. corresponding SSM/I grid cell of approx. 150 km^2) they still demonstrate the validity of the applied remote-sensing technique. Precipitation in these areas is strongly dependent on elevation and thus we plot the ratio of precipitation amount and elevation for both datasets (Fig. 3.2, 3.3 and Tab. 3.1) additional information in the electronic appendix). The rain gauges in central Nepal document a nocturnal peak [*Barros et al.*, 2000], which is not reflected in the SSM/I data because of limited temporal coverage. We emphasize that errors of 15–35% are associated with total precipitation amounts, while relative values are more accurate. Low precipitation values (<300 mm/yr) are associated with larger errors due to the interference from screening algorithms, whereas medium

to high precipitation (approx. >750 mm/yr) from convection cells is very well represented. Precipitation in the Himalayan foreland may be underestimated because it can be forced by very small convection cells with strong vertical velocity fields that are not correctly represented by the scales used in this study [*Lang and Barros*, 2002]. Furthermore, the contribution of stratiform precipitation is larger, characterized by widespread slow ascent velocity fields, which is not very accurately captured with passive microwave analysis. For these reasons, we focus on the valley- and orogen-scale moisture transport, where precipitation from heavy convection cells is the predominant rain type.

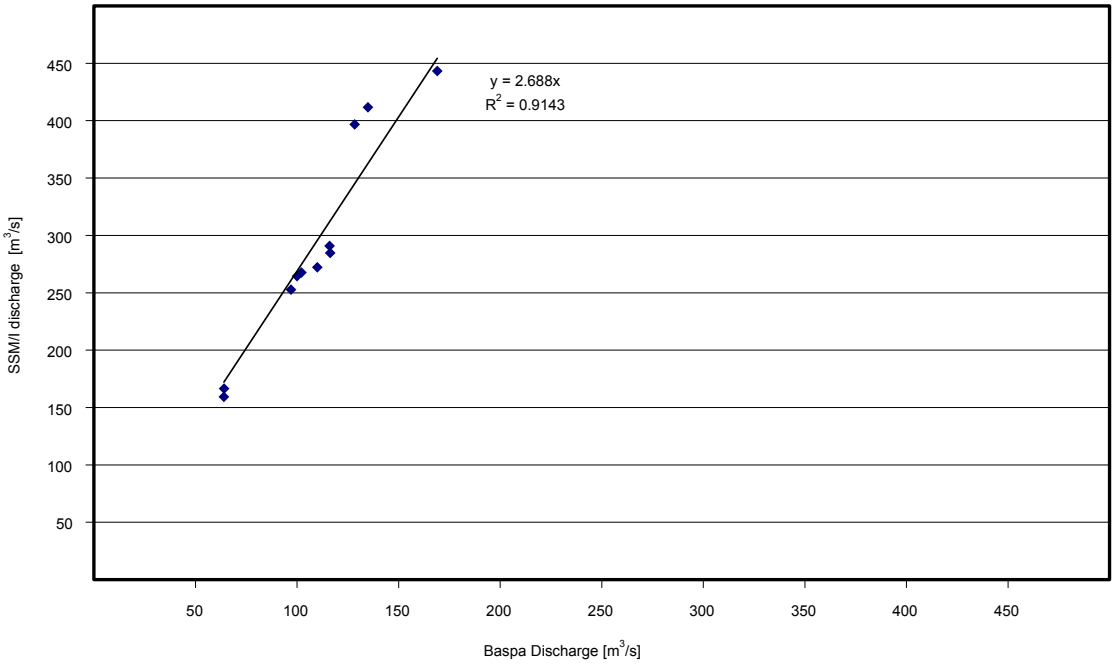

Figure 3.3: SSM/I-computed discharge based on annual precipitation estimates from 1993–2002 and integrated over the drainage basins with topography derived from a 30 m digital elevation model. Satellite-derived discharge is consistently higher than gauged data. We attribute this to overestimations of precipitation in the glacier-covered parts of the catchment, lack of evapo-transpiration and seepage assumptions during fluvial transport, and discontinuous gauge measurements.

We extended our decadal dataset to the middle of the last century using rain-gauge observations in the vicinity of the Sutlej River region with the Global Historical Climatologic Network [GHCN Version 2, *Peterson and Vose*, 1997] and stations maintained by the B.B.M.B. [*Beas Bhakra Management*, 2001, , personal communication]. In addition, daily suspended sediment transport and river-discharge measurements are available at a few stations along the Sutlej River and also along the Baspa River, a major tributary in the transitional zone between the humid and arid parts of the orogen [*Beas Bhakra Management*, 2001; *Jaiprakash Company*, 2002, unpublished company data]. The Baspa gauge data covers 35 years of measurements, while data

along the main stem only provide a 20-year record. These data were used to calculate sediment flux and mean basin denudation rates. Daily suspended sediment transport in mg/l is available during the ISM months, while measurements during winter indicate very low values. Bedload transport has been neglected, because studies in similar partially glaciated, steep environments show that the total transported sediment amount consists only of 6% bedload [*Bhutiyani*, 2000]. However, bedload-transport rates are difficult to measure and we thus consider our erosion rates to be only minimum values.

ASTER (Advanced Spaceborne Thermal Emission and Reflection Radiometer) satellite images taken before and after the 2002 AMY were used to identify reactivated and newly formed channels on hillslopes. We analyzed the three visible bands (VNIR) of the ASTER sensor. This data is highly correlated and we used Principal Component Analysis (PCA) to transform the different bands to a set of uncorrelated output bands, which are ordered by decreasing variability. The main use of PCA is to reduce the dimensionality while retaining as much information as possible [e.g., *Richards*, 1994]. This step was taken to minimize the divergence in surface reflectance because the ASTER images were taken at different seasons and times of day. We filtered and removed homogenous regions with non-relevant information (i.e., glaciers and shadows from surrounding mountains) to enhance contrast, thus making it easier to locate changes between satellite images, taken before and after the 2002 AMY.

3.4 Moisture and precipitation gradients during the ISM

We identified two precipitation gradients that fundamentally influence vegetation and erosional geomorphic processes along the SHF. Precipitation gradually decreases with distance from the Bay of Bengal (from E to W) and decreases leeward of orographic barriers, toward the Tibetan Plateau (from S to N). To illustrate the topographic control on precipitation, four representative swath profiles perpendicular to the Himalayan orogen were created (Fig. 3.5). The Shillong Plateau (∼1.5 km) constitutes the most prominent orographic barrier (Fig. 3.1, 3.6). The southern flank of the plateau is the wettest inhabited place on earth (Cherrapunji, District Meghalaya) at 1300 m asl with a record of 9.3 m rainfall during one month in July 1861, Indian Meteorological Department). An orographic rain shadow thus exists and results in much drier conditions to the north of the Shillong Plateau in E Bhutan compared to regions to the east and west along the SHF. In contrast, rainfall in the Sankosh Valley region of W Bhutan (Fig. 3.5B) just to the W of the dry part along the SHF receives high precipitation (∼3.5 m/yr) with maximum amounts of up to ∼5 m/yr. There precipitation is forced by low to medium elevations of 0.5 to ∼2 km. Moisture transport in the Kali Gandaki region (central Nepal, Fig. 3.5C) is strongly controlled by valley topography. Medium amounts of rain (∼2.3 m/yr) are forced on the SHF,

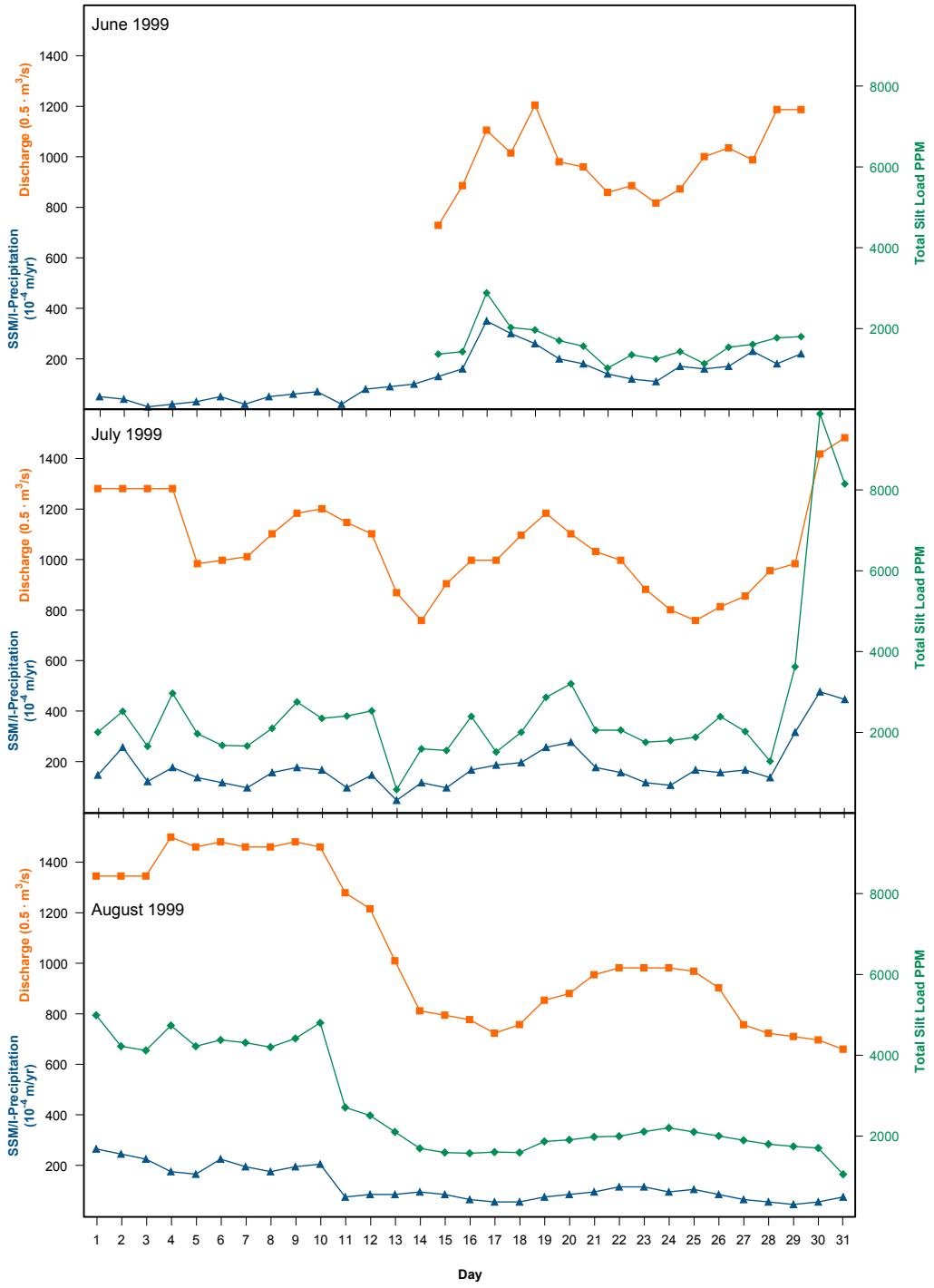

Figure 3.4: Sutlej River discharge and sediment flux for the Indian summer Monsoon 1999 (June–August) at Karchham near the Baspa-Sutlej confluence. Precipitation was derived from calibrated passive microwave data and shows daily values. SSM/I measurements were taken from a single grid cell (∼150 km^2) including Karchham. Suspended sediment flux is measured twice a day and only represents material with low densities (∼1.4 g/cm^3).

whereas moisture migrates into the orogen through the Kali Gandaki River to the E of the swath profile (Fig. 3.1). Here, wet air condensates on the orographic barrier to form a second precipitation peak at ∼150 km north of the mountain front (Fig. 3.5C). Interestingly, heavy, wet air masses do not easily overcome moderately elevated ranges, similar to the orographic barrier of the Shillong Plateau (Fig. 3.5A). Above a mean elevation of 3 km asl, precipitation decreases and north of the main Himalayan barrier, with peaks above 5 km, very little precipitation is observed (Fig. 3.5B and Fig. 3.5C). Therefore, during summer under present conditions, moisture only reaches the dry Tibetan Plateau primarily by migrating upstream through river valleys, thereby circumventing orographic obstacles (Fig. 3.1).

In contrast to the high amounts of precipitation in the eastern and central parts of the SHF, rainfall in the Sutlej Valley region is characterized by lower ISM precipitation and maxima at lower elevations (Fig. 3.5D). Moisture migrates along the valley to condensate along the main topographic barrier at moderate altitudes of about 2.5 km asl (Fig. 3.6). There, the decadal SSM/I-derived ISM mean rainfall does not exceed 1.5 m/yr and regions to the NE are left dry (<0.3 m/yr). For example, the village of Sangla in the Baspa Valley is in a semi-arid corridor where rain-gauge measurements result in ∼0.2 m/yr during the ISM of the last decade. However, during the 2002 AMY, precipitation migrated farther into the orogen and increased rainfall amounts up to ∼0.8 m/yr in the Baspa Valley (Fig. 3.5D, 3.7). Interannual variations in precipitation and resulting river discharge in the study region during the last decade were not subject to large amplitude changes (Fig. 3.9). There exists a large, but constant offset between the rain-gauge data and SSM/I precipitation estimates. Similar to observation in central Nepal, we assume that most of the rainfall occurred at high elevations on the hillslopes [*Barros et al.*, 2000]. Thus gauge stations along the valley bottom that were used to calibrate passive microwave data do not capture the orographic rainfall effects. However, SSM/I rainfall integrated over the catchment area shows a linear correlation with discharge measured in the Baspa River near Sangla (see information in the electronic appendix). Mean SSM/I ISM rainfall for the Sangla grid-cell during the last decade was 0.65 m/yr and increased to 1.5 m/yr during the 2002 AMY (Fig. 3.9).

The rainfall anomaly map (Fig. 3.8) clearly demonstrates that wet air traveled along river valleys to bypass orographic barriers and reach scarcely vegetated, normally arid regions (<0.3 m/yr rain) of the internal part of the Himalaya. For example, rainfall migrated along the Chandra and Bhagirati rivers to reach the Baspa River and the upper Spiti River, two major tributaries of the Sutlej (Fig. 3.8). In these areas, heavy rainstorms in late August and September of the 2002 AMY amplified river discharge and sediment flux while moisture precipitated at high elevations along the windward sides of topographic barriers. Thus, the arid, high-elevation regions received precipitation in excess of 200% of the annual mean during non-AMY years (Fig. 3.8). We thus

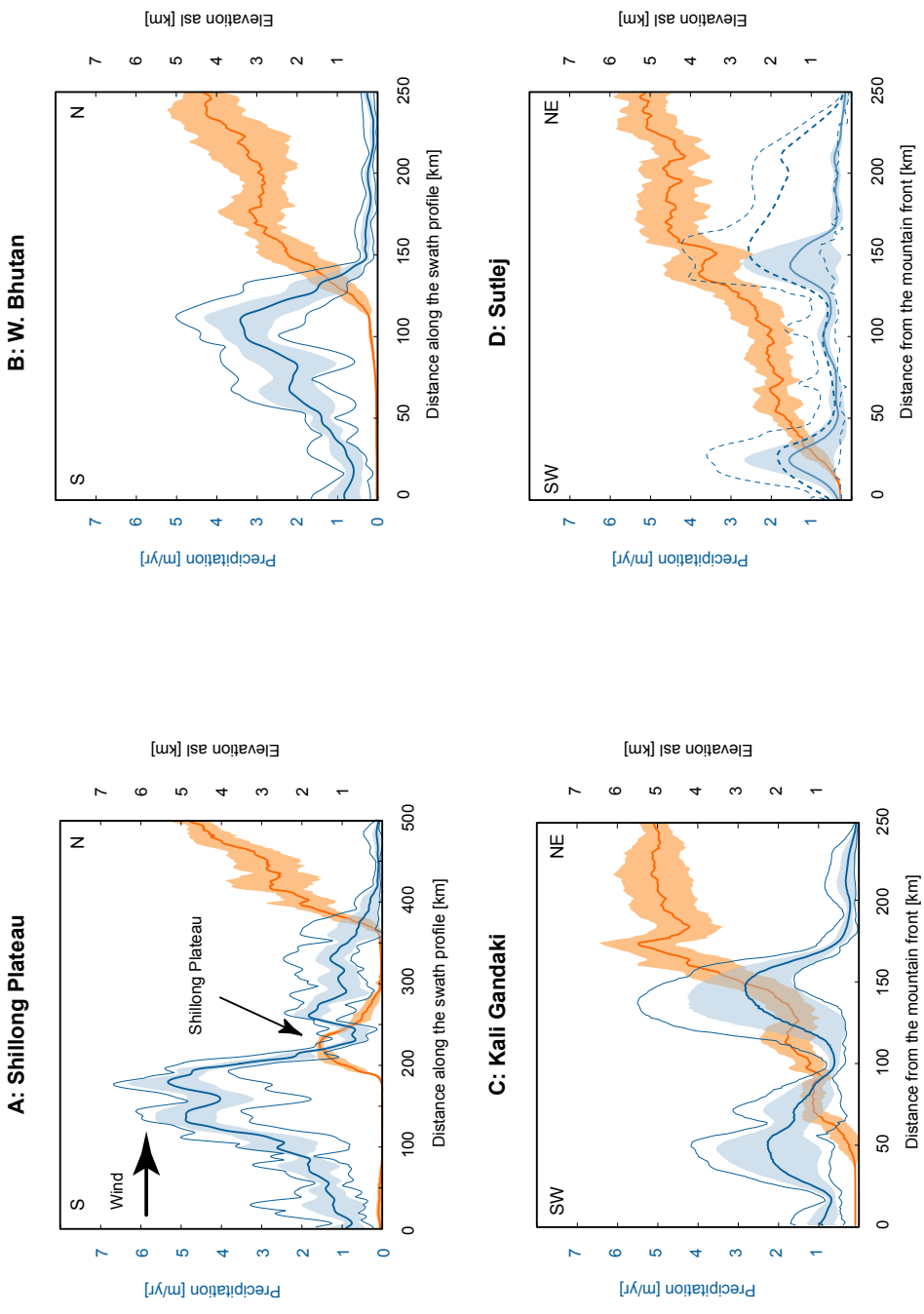

Figure 3.5: Topographic and precipitation swath profiles, see Fig. 3.1 for locations. Swath profiles are 80 km wide and centered along river valleys, perpendicular to the mountain front. Topography (orange) derived from HYDRO1K dataset (USGS) and precipitation (blue) from passive microwave data. Bold lines indicate mean values, shading denotes $\pm 2\sigma$ ranges, and thin lines minimum and maximum annual rainfall. Prevailing wind direction during monsoon season is from S-SE to N-NW. Note high amounts of rainfall on the windward side of orographic barriers. Along the Sutlej Valley, bold dashed line indicates annual precipitation during the 2002 AMY and thin dashed lines minimum and maximum values.

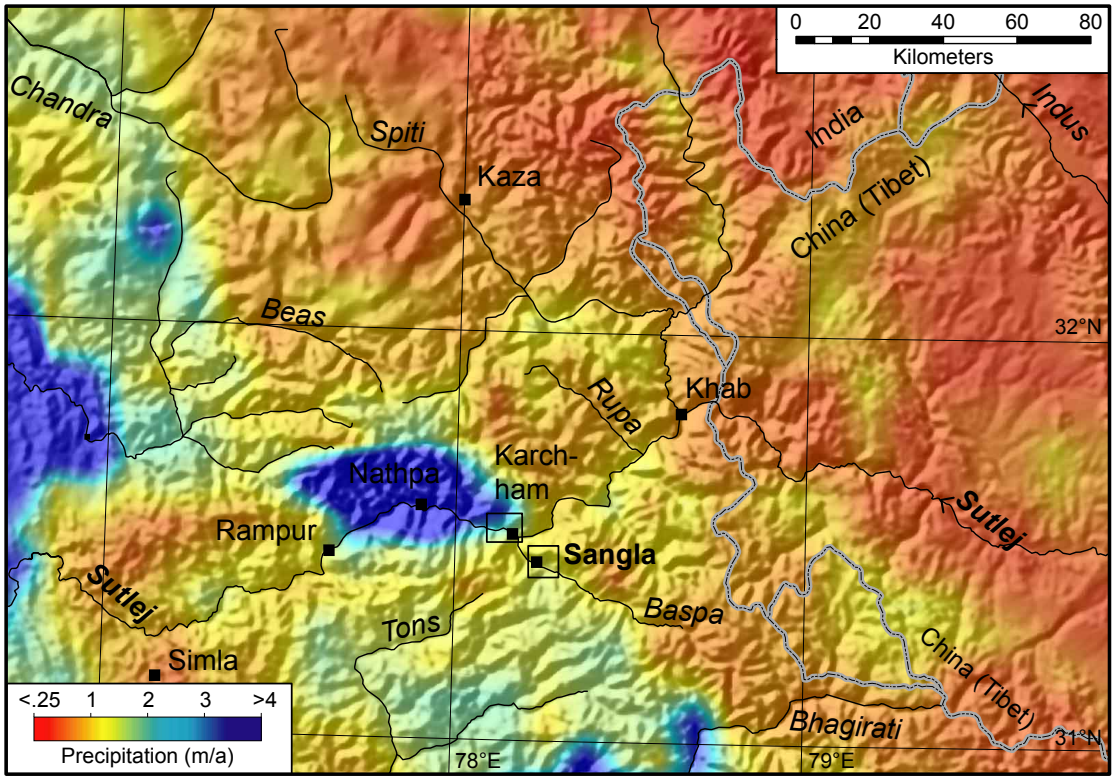

Figure 3.6: Normal monsoonal precipitation distribution (based on averaged 10-year analysis). Mean ISM precipitation and shaded relief of the Sutlej River region. Topography is based on GTOPO30 (USGS), and precipitation was derived from calibrated SSM/I passive microwave data that were smoothed for this output. Black boxes outlines region of Fig. 3.12, 3.13.

expect the geomorphic response (e.g., erosional hillslope processes) and resulting sediment transport to be much more pronounced during such extreme climatic, abnormal years. In contrast, rainfall in the low and medium-elevation regions (<3 km asl) was only moderately enhanced by about 25-50%. Although we cannot precisely reconstruct spatial migration of moisture for the time predating SSM/I measurements, we were able to identify the same contrasting pattern throughout the last 50 years using rain gauges in the Sutlej Valley [*Beas Bhakra Management*, 2001; *Jaiprakash Company*, 2002, unpublished company data] and adjacent regions [*Peterson and Vose*, 1997].

On a synoptic scale we are able to define two compartments of monsoonal precipitation: High rainfall amounts along the orographic barriers of the SHF and moderate amounts in the Indian plains to the south. While precipitation patterns in the lowlands are extensively covered by investigations by *Shrestha* [2000] and *Parthasarathy et al.* [1992], we concentrated on areas affected by orographic rainfall. These regions have not received much attention, and precipitation quantification is restricted to a limited number of local studies because of the lack of adequate data [e.g.,

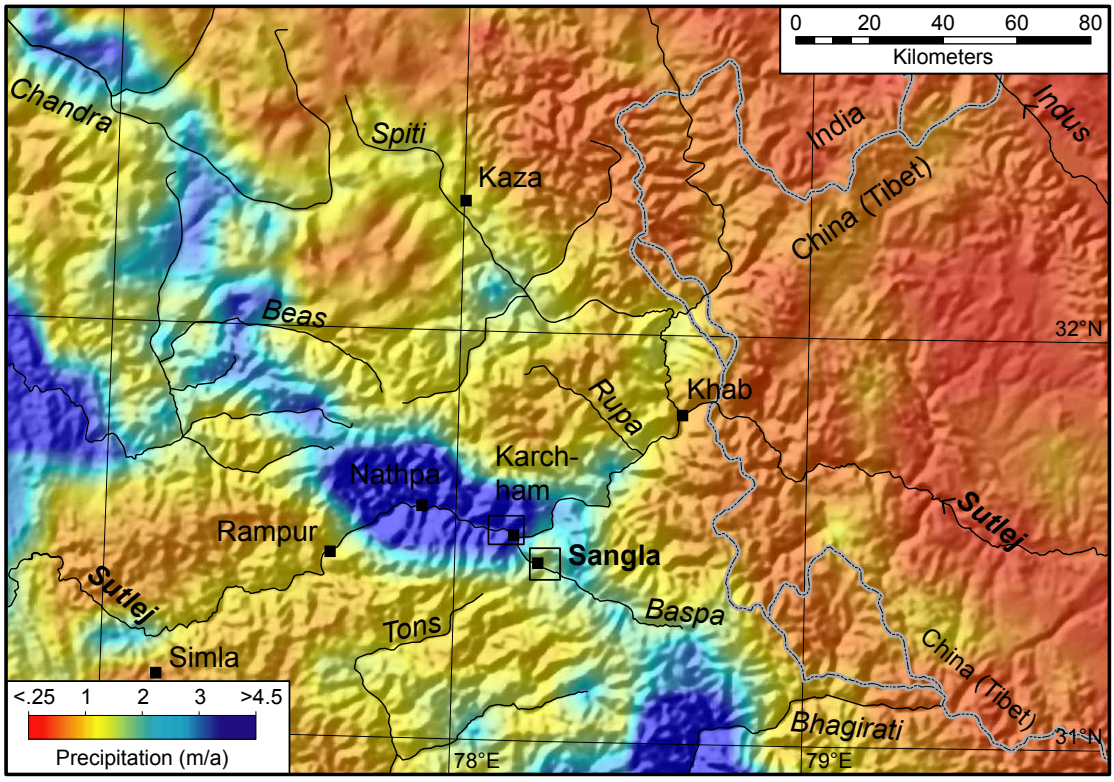

Figure 3.7: Abnormal monsoon year (AMY) of 2002 (averaged for 3 months, where data available). Mean ISM precipitation and shaded relief of the Sutlej River region. Topography is based on GTOPO30 (USGS), and precipitation was derived from calibrated SSM/I passive microwave data that were smoothed for this output. Black boxes outlines region of Fig. 3.12, 3.13.

Barros et al., 2000; *Lang and Barros*, 2002]. It is noteworthy that the two rain compartments show very different behavior with respect to the inter-annual variations and precipitation distribution during the ISM circulation. For example, the 2002 AMY was characterized by a negative rainfall anomaly over the Indian plains, whereas the arid mountainous regions were affected by torrential rainfall and major flooding (Fig. 3.7; International Red Cross Annual Report, 2002; Indian Meteorological Department; United Nations Office for the Coordination of Humanitarian Affairs (OCHA)). In addition, the onset of the ISM in 2002 was delayed by several weeks, before violent, active monsoon phases transported moisture from the Bay of Bengal to the Indian plains and the SHF. Hence, a first order control on rainfall amount on the Indian continent is exerted by large-scale atmospheric modulations (e.g., in relation to ENSO) and changes in sea surface temperatures [e.g., *Charles et al.*, 1997; *Shrestha et al.*, 2000; *Slingo and Annamalai*, 2000; *Gadgil et al.*, 2003], while tectonically created topography plays an important role in forcing and focusing orographic rainfall. Interestingly, precipitation patterns caused by orographic forcing along large river valleys in the medium elevations of the SHF have remained rather stationary during

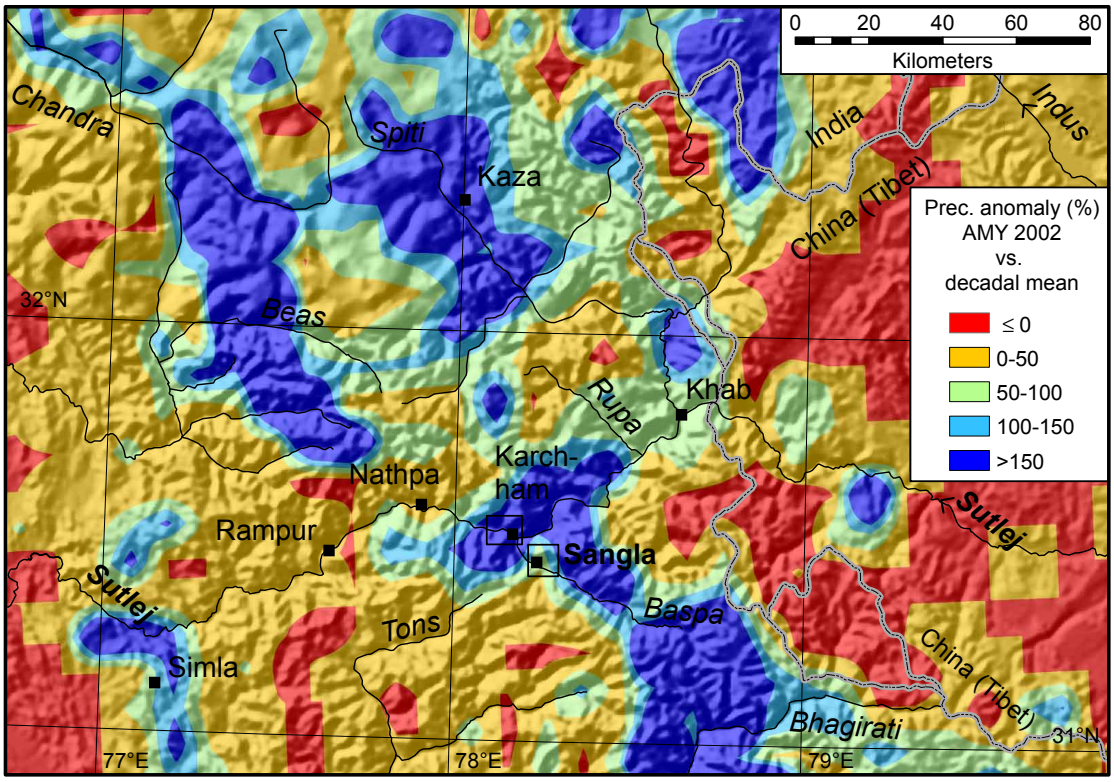

Figure 3.8: Precipitation anomaly map (in percent) showing the magnitude changes between decadal mean and 2002 AMY. Positive anomalies depict more rain during the 2002 AMY, i.e. a 100% anomaly represents the double amount of precipitation. The dominant effect of topography on precipitation distribution is best demonstrated in the middle region of the Sutlej Valley, where moderate amounts of precipitation (3 m/yr) fall in convective cells. Only during the 2002 AMY moist air masses penetrate northeastward into the orogen through the Beas, Chandra and Bhagirati valleys, and generate greater amounts of precipitation in the commonly dry areas of the Spiti, Baspa and Sutlej rivers. Black boxes outlines region of Fig. 3.12, 3.13.

at least the last decade despite high ISM-strength variations. Thus, precipitation as an effective erosion agent might have played a significant control on localized denudation along the medium elevation sectors of the SHF on a geologic time scale [e.g., *Hodges et al.*, 2004; *Thiede et al.*, 2004].

3.5 Precipitation patterns and sediment flux in the NW Himalaya

The significantly different spatial distribution of precipitation during an abnormal monsoon year derived from high-resolution passive microwave data (Fig. 3.8) can be used to further explore the links between erosional hillslope processes and strong rainfall events. In semi-arid to arid mountainous environments, high-magnitude, low-frequency events commonly dominate both

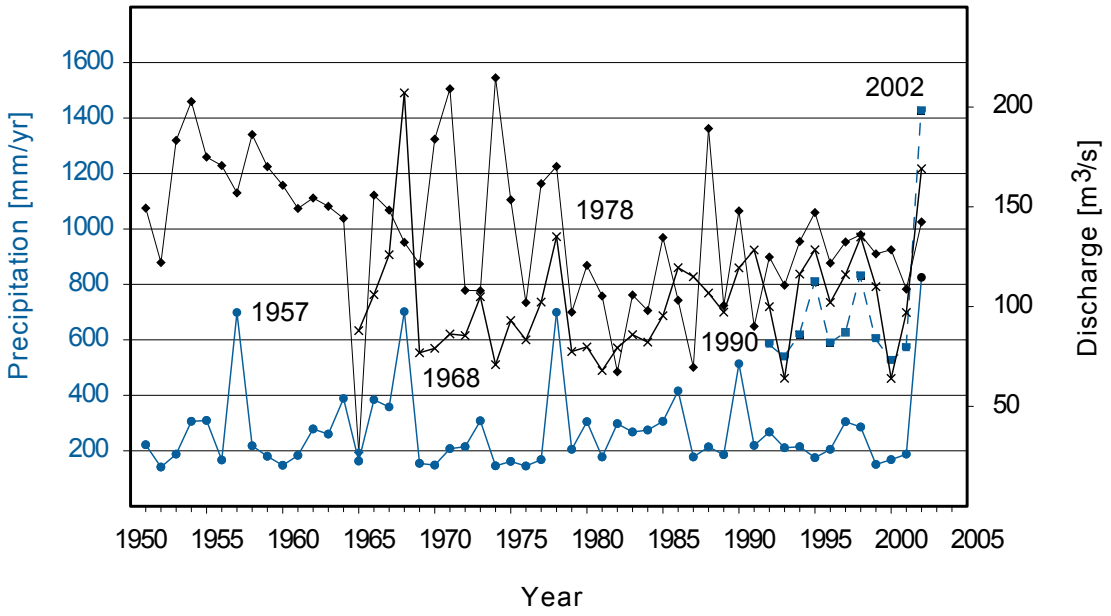

Figure 3.9: Rain-gauge measurements (solid line, dots) and SSM/I-derived precipitation (dashed line, squares) for the village of Sangla (Baspa Valley). Simla rain-gauge data is shown as a representative station for the low- to medium elevation regions (solid line, triangles). Mean annual Indian Summer Monsoon (ISM) rainfall for Sangla is low (∼0.28 m/yr) during the last 50 years but indicate AMYs in 1957, 1968, 1978, 1990, and 2002. Baspa River discharge (gray line, crosses) since 1965 shows similar events. Mean ISM SSM/I rainfall is 0.65 m/yr in the vicinity of the village Sangla during the last decade, while AMY estimations are significantly increased.

river-channel processes and hillslope erosion [e.g., *Wolman and Miller*, 1960; *Mulligan*, 1998; *Osterkamp and Friedman*, 2000]. Consequently, during extreme climatic events the relations between high precipitation and hillslope processes, channel erosion, and sediment transport play a fundamental role in shaping arid, mountainous landscapes. However, only few studies have been published that illustrate impacts of high intensity rainfall events on channels in such environments [e.g., *Coppus and Imeson*, 2002]; in fact, knowledge about erosion processes taking place during abnormal strong events is very limited and often based on deduction. Here, we combine field and satellite observations, river-discharge data, information on sediment flux, and precipitation measurements during the 2002 AMY to identify processes leading to enhanced hillslope erosion during strong climatic events. We demonstrate the validity of the SSM/I-derived precipitation for the summer Monsoon season 1999. In 1999, we could obtain daily river discharge and suspended-sediment flux data and compare them to calibrated passive microwave precipitation (Fig. 3.4) [*Beas Bhakra Management*, 2001; *Jaiprakash Company*, 2002].

The Sutlej River is an integral part of the Indus catchment and comprises the third largest drainage area in the Himalaya and southern Tibet. Before entering India, it drains 43,500 km^2

Figure 3.10: Remnants of a debris-flow in the village of Sangla, Baspa Valley during the 2002 AMY (31.8.2002). White dashed lines indicate location of destroyed road. Note levee material related to debris flow showing the thickness of the flow.

on the Tibetan Plateau. However, due to the aridity in Tibet, this large drainage-basin area does not result in significant discharge and sediment flux into the Himalayan region. In crossing the regions of the Tethyan sediments, Higher and Lower Himalayan Crystalline sectors, and units of the Lesser Himalaya, the Sutlej River rapidly descends from almost 4 km to 0.2 km asl in the Himalayan foreland. Along its course, transient climatic and related geomorphic boundaries exist that develop in response to the changing monsoonal conditions. Thus, depending on the strength and stage of the ISM, characteristic landscape compartments evolve with highly divergent rainfall, vegetation cover, and hillslope processes.

We distinguish between the humid, low to medium elevation parts (1–$\sim$2.5 km asl) that are characterized by high sediment production (HSP) during high-frequency/low-magnitude rainfall events, and the upstream, arid, high-elevation regions ($>\sim$3 km asl) defined by low sediment production (LSP) during normal ISM years. During these typical monsoon years, mean ISM daily river discharge and sediment load in the Sutlej at Rampur (HSP) are on the order of 800 m^3/s and 2.5 g/l (Tab. 3.2). Here, and approximately 60 km upstream, erosional hillslope processes during the monsoon season dominate mass wasting into the channels, and sufficient runoff ensures sediment removal [e.g., *Sah and Mazari*, 1998; *Paul et al.*, 2000; *Barnard et al.*, 2001].

	Normal Monsoon Conditions				**AMY 2002**			
	High-Sediment Production (HSP)		Low-Sediment Production (LSP)		High-Sediment Production (HSP)		Low-Sediment Production (LSP)	
SSM/I Rainfall (m/yr)	1.5		0.3		1.7		0.75	
JJA-Monsoon Average Discharge [m^3/s]	Nathpa (Sutlej)	790 ±10	Khab (Sutlej)	∼225	Nathpa (Sutlej)	ND	Khab (Sutlej)	ND
			Sangla (Baspa)	96 ±20			Sangla (Baspa)	169
	Rampur (Sutlej)	850 ±13	Kar-chham (Sutlej)	380 ±24	Rampur (Sutlej)	900	Kar-chham (Sutlej)	ND
JJA-Monsoon Suspended Sediment Flux [g/l]	Nathpa (Sutlej)	1.7 ±0.3	Khab (Sutlej)	∼0.15	Nathpa (Sutlej)	ND	Khab (Sutlej)	ND
			Sangla (Baspa)	0.95 ±0.15			Sangla (Baspa)	1.23
	Rampur (Sutlej)	2.5 ±0.8	Kar-chham (Sutlej)	1.2 ±0.3	Rampur (Sutlej)	2.9	Kar-chham (Sutlej)	ND

Table 3.2: Summary of precipitation, discharge and suspended sediment flux data for the Sutlej Valley region during normal monsoon conditions and the abnormal monsoon year (AMY) 2002. High sediment production (HSP) region denotes the area between 1 and 2.5 km elevation, while the low sediment production (LSP) region lies above 3 km elevation leeward of orographic barriers. Measurements from Sangla, Baspa were taken from *Jaiprakash Company* [2002], other data is from the *Beas Bhakra Management* [2001]. Standard deviations are given in 2σ, ND indicates no data was available, and JJA stands for June-July-August precipitation.

In contrast, mean ISM river discharge and silt load in the LSP area at Khab, south of the Sutlej-Spiti confluence, are ∼225 m^3/s and ∼0.15 g/l, respectively. Thus, regions along the Sutlej Valley that are always exposed to the high ISM rainfall regime show constantly high sediment flux (Tab. 3.2). During the 2002 AMY, precipitation increased only by a small percentage in these sectors (Fig. 3.8) and did not result in significantly enhanced sediment transport. The humid, HSP compartment with mean elevations between 1–2.5 km thus tends to compensate slightly higher rainfall. In contrast, the Baspa River basin is located in the LSP, high-elevation semi-arid region (>∼3 km asl). It has a 35-year average ISM discharge (excluding AMYs) of 96 m^3/s (2σ±20 m^3/s), while the 2002 AMY is characterized by ∼169 m^3/s (Fig. 3.9; Tab. 3.2). Sediment-load measurements in the Baspa River show similar distinctions from 0.95 g/l and

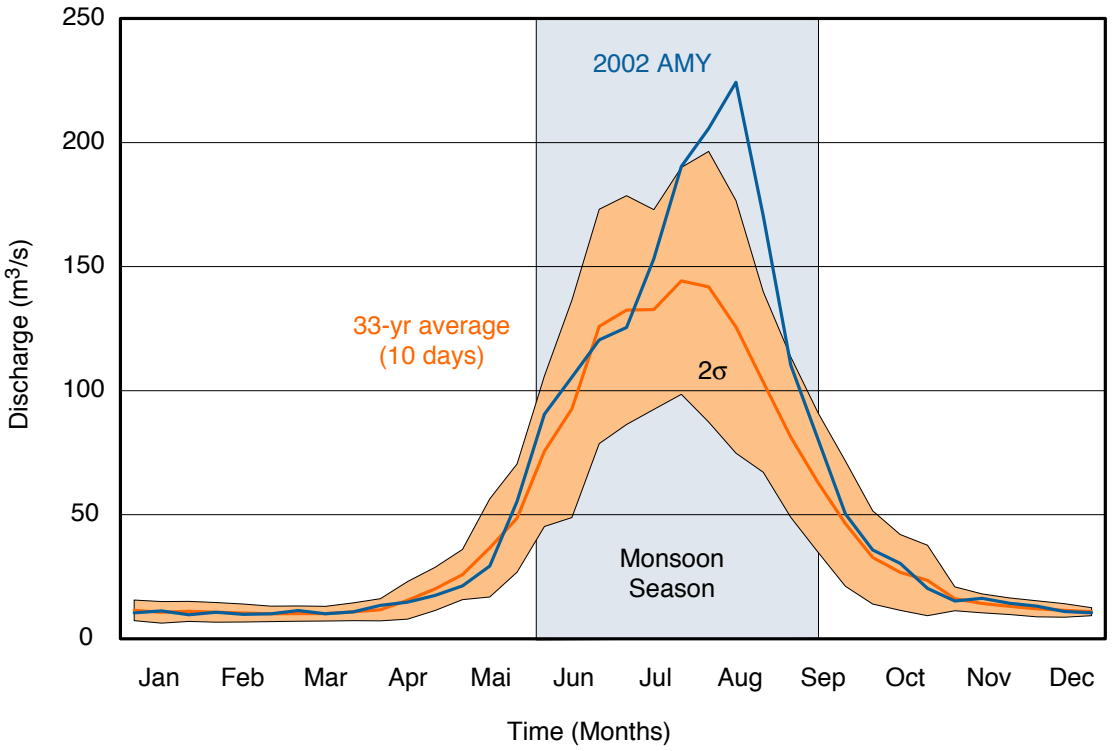

Figure 3.11: Discharge measurements of the Baspa Valley for a 33-year period. We compare averaged 10-day measurements for the last 32 years with the abnormal monsoon year in 2002.

~1.23 g/l during the 2002 AMY [*Jaiprakash Company*, 2002, unpublished company data]. These values are mean ISM (June–August) amounts based on daily measurements – extreme events after heavy rainstorms can have significantly higher values and exert a crucial control on the amount of evacuated sediment. The 2002 AMY value is also a minimum estimation, because daily measurements were difficult to obtain and were not collected during and after heavy rainstorms while rivers were flowing rapidly. However, we expect transported grain sizes to be significantly larger during the AMY 2002 when peak discharges of up to 500 m^3/s must have significantly increased the shear stress acting on the riverbed to overcome the threshold of motion [e.g., *Hartshorn et al.*, 2002].

In order to calculate annual sediment-transport rates for the Baspa basin, we multiply river discharge (96 m^3/s) and suspended sediment flux (0.95 g/l) for the monsoon season (3 months). About 60% of the annual discharge and 85% of the annual sediment flux occurs during the summer monsoon months June to August. A total of $7.1 \cdot 10^5$ t/yr sediment is carried by the Baspa River, which corresponds to 937 $t/(yr \cdot km^2)$ for the drainage area (757 km^2). We then estimate mean basin-denudation rates by applying a density for the suspended sediment of 1.4 t/m^3 to convert mass into volume. Mean basin denudation in the Baspa catchment is ~0.7±0.14 mm/yr, while

during the 2002 AMY the rate more than doubled to ∼1.5 mm/yr. We emphasize that these values represent only minimum mean basin denudation rates, because bedload transport has not been included and suspended sediment transport was not measured continuously during the 2002 monsoon season. In addition, we assumed a low bulk density for the suspended sediment and thus only considered a small fraction of the transported sediment in suspension. However, the differences in rates clearly demonstrate the impact of AMYs on mean basin lowering in the high-elevation parts of the northwestern Himalaya.

We relate enhanced sediment flux in the fluvial system to enhanced erosional slope processes that result from heavy rainfall (Fig. 3.11). For example, representative for enhanced hillslope erosion in this region, a large debris flow was triggered during several hours of heavy rainfalls in the Baspa Valley at the end of August 2002. The debris flow traveled from high elevation, and carved a preexisting channel within the village of Sangla (Fig. 3.10). Numerous similar observations were made in the neighboring Sutlej, Rupa and Spiti valleys. In these locations, the AMY-related rainfall primarily affected vegetation-free hillslopes, increased pore-water pressure, and destabilized steep, regolith-mantled slopes that eventually generated debris flows.

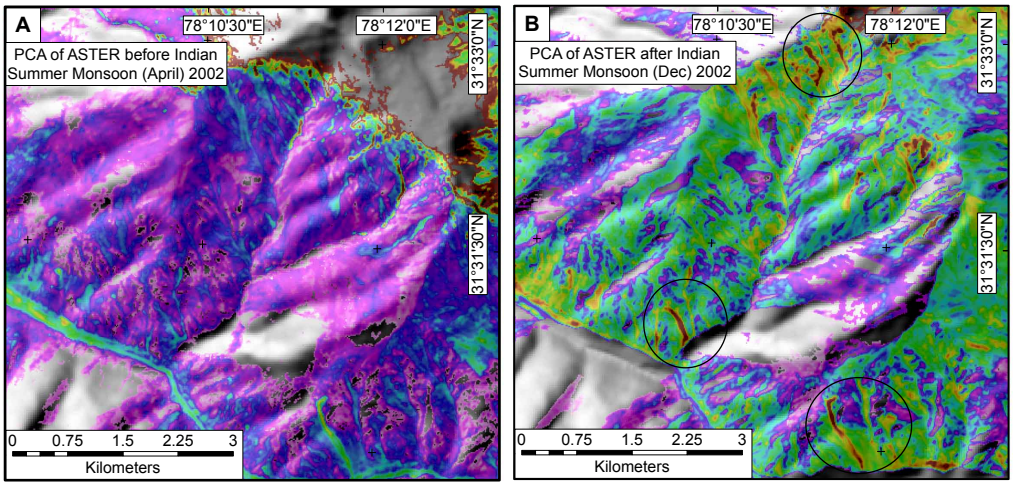

Figure 3.12: Principal Component analysis (PCA) of ASTER Images before (April 9, A) and after (December 8, B) the 2002 AMY event (locations are shown on Fig. 3.6). Prior to PCA, the satellite data have been filtered to show more contrast by removing shadows and large snow fields along the peaks. We show the first axis of PCA that aligns along the highest variance of the all three input bands. Purple, blue, and green colors indicate low variance, whereas rivers, newly formed, and reactivated channels along the hillslopes have higher reflectances values (brown colors). Black circles outline newly formed or reactivated debris flow. These false-color images do not represent the original, natural color and were draped over shaded-relief topography.

From laboratory, field, and theoretical studies of sediment transport mechanics it is well known that sediment transport by free-surface flow, seepage and shallow mass movements does not occur until a threshold of flow strength is exceeded [e.g., *Yalin*, 1977; *Snyder et al.*, 2003].

More recently, studies of watersheds in the western United States support the theory originally proposed by Horton [*Horton*, 1945] that a similar erosion threshold also controls the location of channel heads in some drainage basins [e.g., *Dietrich et al.*, 1992; *Montgomery and Dietrich*, 1992]. These studies suggest that channels form where the shear stress generated by surface flow during storms exceeds the threshold to entrain and transport sediment particles.

During the 2002 AMY, the threshold of flow strength was clearly exceeded along scarcely vegetated, steep hillslopes in arid and semi-arid regions of the Himalaya, and new channel formation in the headwaters through debris flows could be observed. If new channel formation during extreme climate events is regionally relevant, then the extent of the channel network should be particularly sensitive to changes in climate [e.g., *Tucker and Slingerland*, 1997]. To assess the spatial distribution of new channel formation, we compared the three VNIR (Visible Near Infra Red) bands of the ASTER sensor taken before and after the 2002 AMY, on April 9 (Fig. 3.12, 3.13) and December 8 (Fig. 3.12, 3.13, 3.14), respectively. In order to enhance output quality, sharpen the image and reduce dimensionality, we applied principal component analysis (PCA) on the three input bands and show only the first component. The PCA rotates the input bands and aligns them along their axes of highest variance [e.g., *Richards*, 1994]. Newly formed and eroded pre-existing channels on these false-color images have a higher reflectance and data variance. Thus, PCA represents a tool to identify recently active areas. We circled and identified changes in the satellite images taken in December after the 2002 AMY (Fig. 3.12, 3.13, 3.14). In the field we found these channels to be the transport tracks for debris from the hillslopes. Despite the 15 m spatial resolution of the VNIR bands of ASTER images, we primarily observe reactivated and limited newly incised channels through debris flows. Not all flows reached the main stem and thus did not immediately supply more sediment to the river. An increase in debris-flow activity in the arid, high-elevation part, was not observed during the previous normal ISM seasons, and also not in the HSP region during the AMY. Despite the imaginable inactivity of old channels during normal ISM conditions, we observe that they funnel even small amounts of runoff during weaker monsoon years. Thus, the initiation, carving, and reactivation of channels increases the erosion potential through collecting runoff and potentially focusing erosion during normal monsoon years in small parts of the hillslopes [e.g., *Tucker and Slingerland*, 1997].

Based on these observations, we refer to the arid to semi-arid region as a geomorphic threshold area, where scarcely vegetated, steep hillslopes and channel networks are very sensitive to climatic changes [e.g., *Montgomery and Dietrich*, 1992; *Tucker and Slingerland*, 1997]. The rainfall threshold that triggers shallow hillslope erosion therefore lies between 0.3 m/yr and 0.7 m/yr. In contrast, the humid, vegetated medium-elevation regions do not show a significant increase in hillslope processes during the same time period. We argue that the dense, protective organic layer effectively intercepts precipitation and possibly reduces direct runoff and thus armors these

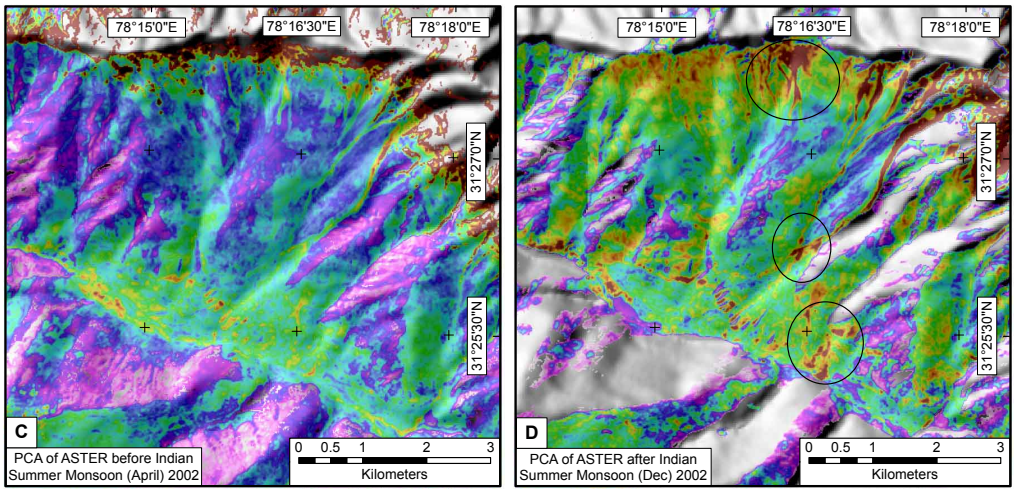

Figure 3.13: Principal Component analysis (PCA) of ASTER Images before (April 9, A) and after (December 8, B) the 2002 AMY event (locations are shown on Fig. 3.6). We show the first axis of PCA that aligns along the highest variance of the all three input bands. Purple, blue, and green colors indicate low variance, whereas rivers, newly formed, and reactivated channels along the hillslopes have higher reflectances values (brown colors). Black circles outline newly formed or reactivated debris flow. These false-color images do not represent the original, natural color and were draped over shaded-relief topography.

environments. Although we observe a moderate increase in rainfall in these HSP regions and Sutlej River discharge during the 2002 AMY, a comparable increase in sediment flux did not take place compared to the high-elevation LSP compartment. Thus, increased material was derived from the arid, high-elevation areas, although presenting only a fraction of total sediment transport to the foreland basins during the 2002 AMY. Analogous to present-day conditions produced by AMYs, this phenomenon may have been much more pronounced during longer-lasting intensified monsoon phases in the geologic past [e.g., *Goodbred and Kuehl*, 2000; *Pratt et al.*, 2002; *Bookhagen et al.*, 2005a].

While we spatially linked moisture transport and erosion process distribution in detail during the 2002 AMY, we were also able to identify similar, extreme events during the last century. For example, Sangla ISM rainfall rates in the Baspa Valley (Fig. 3.9) indicate conditions similar to the 2002 AMY in 1957, 1968, 1978, and weaker event in 1990 [*Beas Bhakra Management*, 2001; *Peterson and Vose*, 1997, unpublished company data]. Baspa discharge is available since 1965 and also shows significantly increased river discharge in AMYs [*Beas Bhakra Management*, 2001, unpublished company data] (Fig. 3.9). If a decadal recurrence interval is assumed, the influence of these abnormal monsoon years on mean basin denudation is roughly 20% in the arid parts of the Sutlej Valley. However, high-resolution satellite observations unfortunately do not exist for earlier events and we are unable to reconstruct detailed moisture transport for this time.

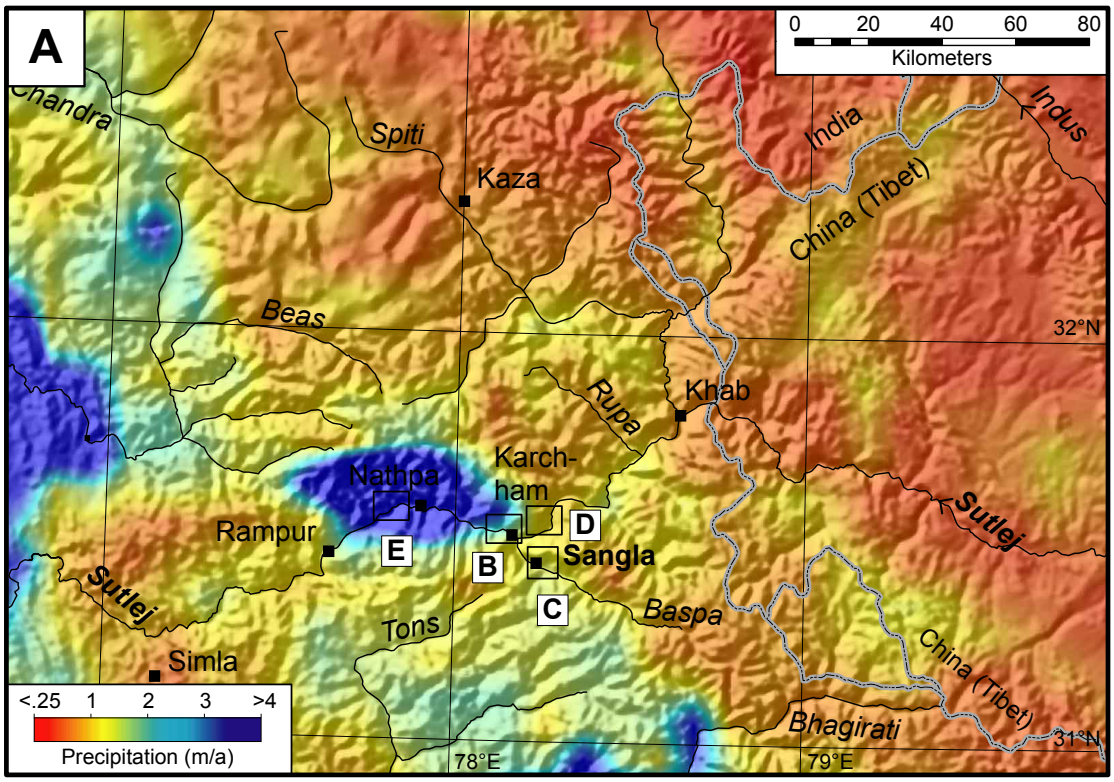

Figure 3.14: Location map for Principal Component Analyses. This figure is based on SSM/I-derived precipitation distribution from 1992-2001, excluding the abnormal monsoon year 2002.

Although the mechanistic principle underlying these short-term climatic perturbations is not yet well understood and matter of ongoing debate [e.g., *Gadgil et al.*, 2003; *Slingo and Annamalai*, 2000; *Webster et al.*, 1999], the potential effect of extreme monsoon events on erosional surface processes and their impact on sediment production is evident, resulting in effective hillslope erosion and increased sediment evacuation. This causative relationship in turn, may explain the higher sediment transport to the Bay of Bengal during longer lasting, intensified monsoon phases in the younger geologic past and may represent an important process in the erosion of the Himalayan orogen [e.g., *Gadgil et al.*, 2003; *Bookhagen et al.*, 2005a].

Despite active seismicity in the Himalaya and the possible seismic triggering of large landslide masses [e.g., *Keefer*, 1994], earthquakes apparently only play a minor role in directly supplying increased sediment amounts to rivers in regions with strong monsoon seasons [e.g., *Owen et al.*, 1996; *Hovius et al.*, 2000; *Barnard et al.*, 2001]. Although comparison to other studies is difficult due to the complex geologic setting, *Barnard et al.* [2001] examined sediment flux during the monsoon season in 2000 and after the M_s 6.6 1999 earthquake in Garhwal, ~150 km E of the Sutlej Valley. Surprisingly, only a small overall contribution of earthquake-induced vs.

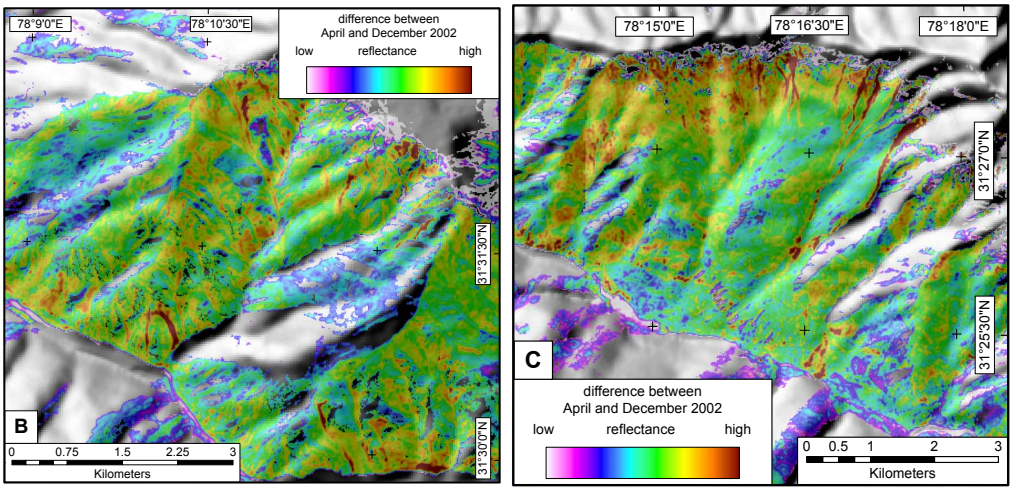

Figure 3.15: Principal component analysis (PCA) anomalies of two regions in the Sutlej Valley (see Fig. 3.14 for locations). We performed PCA on the three VNIR bands of the ASTER sensor, and focus on the first output band, which has the highest variance. The PCA was applied to images taken before and after the abnormal monsoon year 2002. We then normalized the output and subtracted the 'April' (before) from the 'December' image (after monsoon). This simple method is based on the fact that newly eroded channels and other geomorphic features that have higher reflectances. Thus, brown colors indicate the regions where changes occurred, while blue to green colors indicate little or no difference between the images. Figure B and C are located in the low sediment production region (LSP) in high elevation (continued on Fig. 3.16).

monsoon-triggered mass transport was detected. Similar results were obtained by *Owen et al.* [1996] after the M_s 7.0 1991 Garhwal earthquake. Their study showed that equivalent landscape lowering due to earthquake- and rainfall-induced mass movements was ∼0.007 and 0.02 mm, respectively. However, it may be cautioned that there might be a time lag between earthquake-induced processes and sediment removal during major precipitation events, thus considerably delaying sediment transport to lower elevations [*Lavé and Burbank*, 2004]. However, similar to other tectonically active orogens, it can be assumed that earthquakes are an important factor for sediment production in the humid, medium elevation regions [*Hovius et al.*, 2000]. In any case, our results imply that denudation and more importantly, erosional hillslope processes in the arid, high-elevation regions of the Himalaya are strongly controlled by extreme storm events during abnormal monsoon years.

3.6 Conclusion

We investigated synoptic and valley-scale precipitation gradients in the Himalayas using passive microwave data. Moisture is transported from the Bay of Bengal along the Southern Himalayan Mountain Front to the northwest and results in E-W and N-S precipitation gradients. Topog-

raphy exerts a strong control on rainfall along the mountainous regions and during enhanced monsoonal circulation. In this event, deeply incised river valleys oriented normal to the Himalayan arc provide thoroughfares for moist air to be carried into arid areas of the orogen. Interannual variations in precipitation penetration strongly depend on the characteristics of the Indian Summer Monsoon circulation. For the year 2002 we identified an abnormal monsoon year (AMY) for the northwest Himalaya, when rain migrated far into the orogen and reached regions shielded by orographic barriers. These typically arid sectors are characterized by steep, sparsely vegetated and regolith-mantled hillslopes and represent geomorphic threshold areas. During abnormal strong rainfall events, these slopes respond with enhanced erosional processes. We identify debris flows in the upper catchment regions as effective geomorphic erosion agents that are triggered by unusually high rainfall intensities. Suspended sediment transport measurements reveal that more than twice as much sediment may be evacuated by rivers in these dry regions of the orogen during high climatic variations. The increased sediment load in mountain streams documents significantly enhanced mean basin denudation rates in the arid sectors of the northwest Himalaya. In contrast, the low to medium-elevation portions of the orogen are characterized by smaller rainfall-magnitude changes during the AMY, and do not show increased but overall high denudation rates. We argue that this might be a result of the protective organic layer that effectively intercepts precipitation and modulates runoff on densely vegetated slopes. While we documented the relationship between the migration of precipitation far into the orogen and sediment-production processes only in the northwest Himalaya, we suggest that similar processes also occur along the entire southern Himalayan mountain front, where topographic barriers allow penetration of moisture to higher-elevation, arid sectors.

3.7 Acknowledgements

This work was supported by the German Research Foundation (DFG STR371/11-1). The success of this project was made possible through the support of many Indian friends and colleagues. We particularly thank A.K. Jain and S. Singh, both of I.I.T. Roorkee, India for their help. We gratefully acknowledge K. Haselton for his support on SSM/I data processing. We thank P. van der Beek, D. Burbank, B. Dietrich, and N. Hovius for constructive reviews and discussions. Daily sediment transport and river discharge measurements were provided by Dr. Narendra Singh of Jaiprakash Hydroelectric Power Industries Limited, New Delhi (India) for the Baspa River, a major tributary of the Sutlej. We appreciate discussions with L. Schoenbohm and E. Sobel. SSM/I and ASTER data were obtained from the NASA Pathfinder Program for early Earth Observing System (EOS) products.

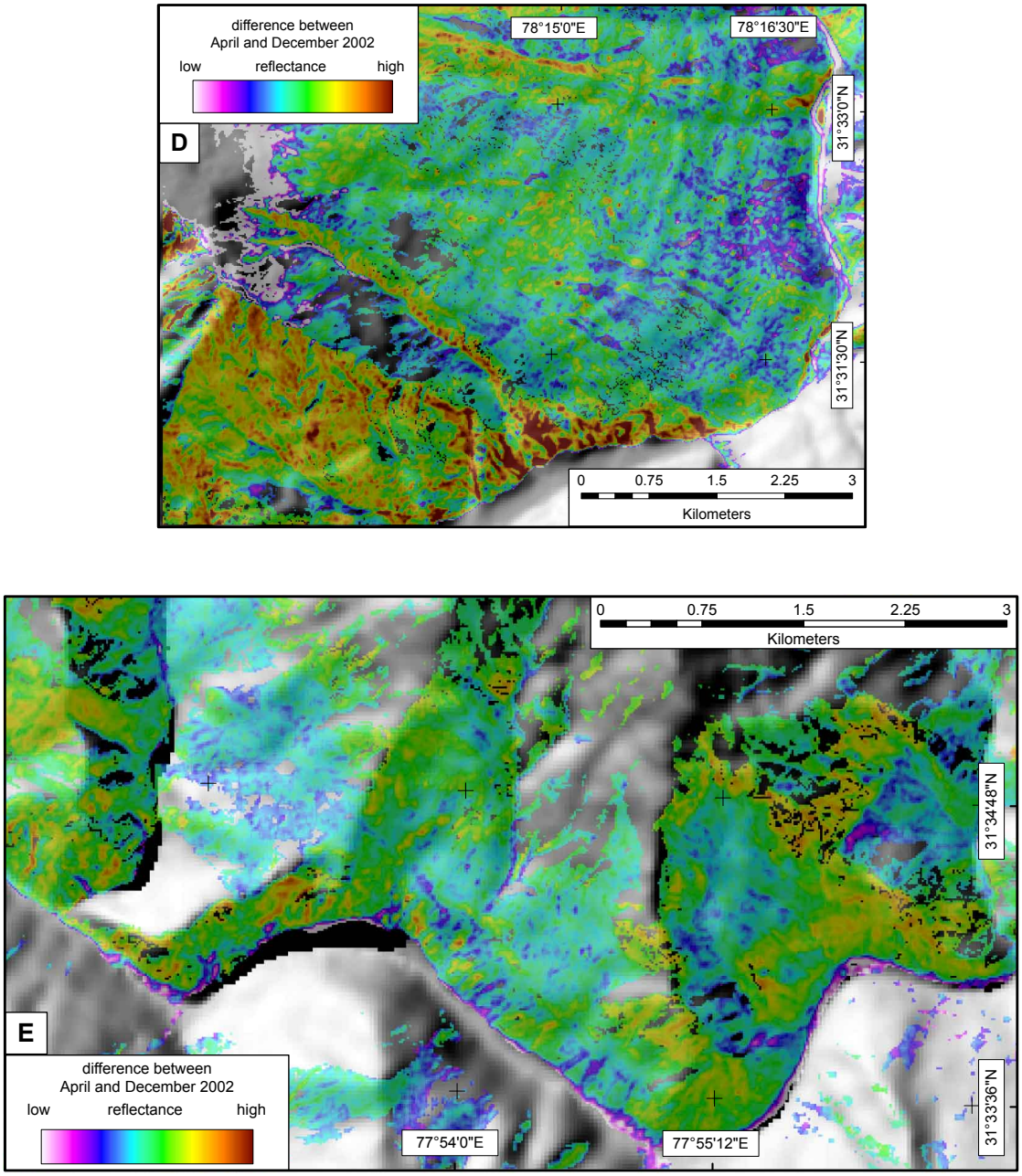

Figure 3.16: Figure D is located in the Low Sediment Production (LSP) area, while Figure E lies in the high sediment production (HSP) area. Interestingly, the low vegetated, steep hillslopes of the LSP show a more pronounced erosional response to increased precipitation than the humid, medium-elevation HSP sector. Thus, the landscape in the high-elevation parts is more sensitive to changes in climate (see Fig. 3.15 for extensive description).

4. LATE QUATERNARY INTENSIFIED MONSOON PHASES CONTROL LANDSCAPE EVOLUTION IN THE NORTHWEST HIMALAYA

Abstract

The intensity of the Asian summer-monsoon circulation varies over decadal to millennial time scales and is reflected in changes in surface processes, terrestrial environments, and marine sediment records. However, the mechanisms of long-lived (2–5 k.y.) intensified monsoon phases (IMPs), the related changes in precipitation distribution, and their effect on landscape evolution and sedimentation rates are not yet well understood. The arid high-elevation sectors of the orogen correspond to a climatically sensitive zone that currently receives rain only during abnormal (i.e., strengthened) monsoon seasons. Analogous to present-day rainfall anomalies, enhanced precipitation during an IMP is expected to have penetrated far into these geomorphic threshold regions where hillslopes are close to the angle of failure. We associate landslide triggering during IMPs with enhanced precipitation, discharge, and sediment flux leading to an increase in pore-water pressure, lateral scouring of rivers, and oversteepening of hillslopes, eventually resulting in failure of slopes and exceptionally large mass movements. Here, we use lacustrine deposits related to spatially and temporally clustered large landslides (>0.5 km^3) in the Sutlej Valley region of the northwest Himalaya to calculate sedimentation rates and to infer rainfall patterns during late Pleistocene (29–24 ka) and Holocene (10–4 ka) IMPs. Compared to present-day sediment-flux measurements, a fivefold increase in sediment-transport rates recorded by sediments in landslide-dammed lakes characterized these episodes of high climatic variability. These changes thus emphasize the pronounced imprint of millennial-scale climate change on surface processes and landscape evolution.

4.1 Introduction

Climate change at variable time scales exerts a profound control on hillslope and fluvial transport processes and hence on landscape development [e.g., *Hancock and Anderson*, 2002; *Hartshorn et al.*, 2002]. In the Himalaya, monsoonal circulation has varied at millennial, centennial, and decadal time scales [e.g., *Clemens et al.*, 1991; *Clemens and Prell*, 1991; *Altabet et al.*, 2002], and corresponding changes in precipitation distribution have left strong imprints on landscape evolution and sedimentation [e.g., *Goodbred and Kuehl*, 2000; *Prins and Postma*, 2000; *Barnard et al.*, 2001; *Pratt et al.*, 2002; *Bookhagen et al.*, 2005b].

The Indian summer monsoon results from a thermal gradient between a low-pressure cell over

Tibet and high pressure over the oceans, producing counterclockwise moisture transport from the Bay of Bengal along the southern Himalayan front toward the northwest [e.g., *Hastenrath*, 1994; *Lang and Barros*, 2002]. There, at the termination of the northwestward monsoonal moisture transport near the Sutlej Valley region (Fig. 4.1) rainfall amounts under normal conditions are less compared to regions farther east, and affect areas along the southern Himalayan front between 1 and 3 km elevation, [*Lang and Barros*, 2002; *Bookhagen et al.*, 2005b]. In this segment of the Himalaya, orographic barriers (>4.5 km in elevation) block moisture of the present-day, weak monsoonal circulation, resulting in an arid, high-elevation region to the north. Only during abnormal (i.e., strengthened) monsoon years rainfall penetrates more than 75km farther into the orogen to reach these areas, which have hillslopes near the threshold angle for failure [*Bookhagen et al.*, 2005b]. Due to its position near the terminus of the monsoon conveyer belt, the northwestern Himalaya is thus a climatically sensitive zone where changes in the strength of the monsoonal circulation system and their influence on hillslope processes can be evaluated (Fig. 4.1).

To unravel environmental changes during longer (>2 k.y.) intensified monsoon phases (IMPs) and to evaluate their influence on geomorphic processes and rates, we studied large (>0.5 km^3) landslides that impounded drainages of the Sutlej River network in the northwest Himalaya and the associated transient lacustrine basins in order to determine erosion and sedimentation rates. We thus use the landslide clusters as indicators of former rainfall distribution and sediment transport in the climatically sensitive zones. It is important to note that precipitation patterns of present-day, abnormal monsoon years mimic the spatial distribution of late Pleistocene and Holocene landslide clusters observed in the Sutlej River and its tributaries. This relationship suggests an intensification of surface processes in the arid parts of the orogen over at least decadal to millennial time scales due to an increase in available moisture during IMPs.

4.2 Methods

We are confident to have identified all large landslide deposits (>0.5 km^3) through extensive satellite imagery analysis (Corona, Landsat ETM+, and ASTER [Advanced Spaceborne Thermal Emission and Reflection Radiometer]) and detailed field observations in the Sutlej Valley region. Absolute age control for onset and duration of landslide-related lacustrine deposition is provided by AMS (accelerated mass spectrometry) ^{14}C dates on charcoal and plant remains from the bottom and top layers of the lake sediments (Tab. 4.1). Where absolute age control could not be obtained, deposits were correlated with adjacent dated units on the basis of stratigraphic relationships, such as superposition of fluvial terraces by landslide debris and associated lake sediments. Only late Pleistocene and Holocene large mass-movement deposits and their related basin fills were found. The amount of eroded sediment, longitudinal river profiles, and

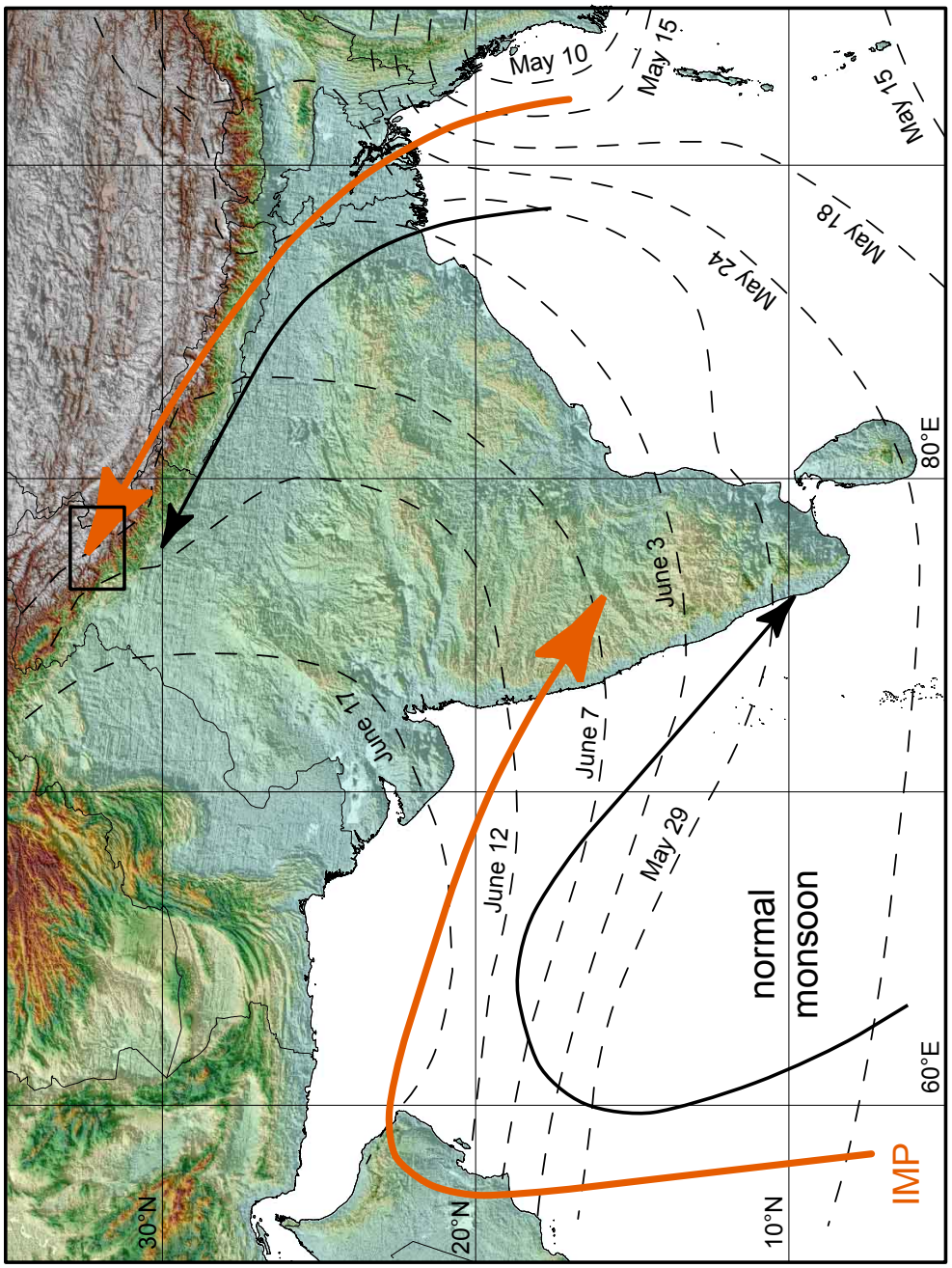

Figure 4.1: Main wind directions during Indian summer monsoon (southwest monsoon). Thin, black arrows indicate present-day, weak monsoonal wind directions. Bold, orange arrows show prevailing wind directions of a strong monsoon inferred to represent intensified monsoon phases (IMPs) during late Pleistocene and Holocene. Dashed lines depict temporal evolution of Indian summer monsoon and its northwestward propagation. Dates of rainfall onset are compiled from passive-microwave satellite observation and rain-gauge measurements [*Bookhagen et al.*, 2005b; *Hastenrath*, 1994; *Parthasarathy et al.*, 1992]. Black box outlines Sutlej Valley region (Fig. 4.4).

river geometry differ significantly in the late Pleistocene and Holocene data sets. For example, Holocene landslide deposits have retained pronounced knickpoints and are still being downcut, while Pleistocene deposits have been nearly obliterated and river profiles lack knickpoints. We calculated sedimentation rates for two Holocene landslide-related paleolakes of comparable size but different geographic setting by combining age information and volumetric measurements from a digital elevation model (DEM). DEMs were derived from digitized contour lines of 1:25,000 topographic maps and orthorectified ASTER satellite images. The quality of the digitized and ASTER-derived DEM was tested against elevation measurements by differential GPS (Global Positioning System) and altimeter readings and yielded consistent results. Pre-landslide topography and stream gradients were reconstructed by removing landslide deposits from the DEMs and connecting upstream and downstream channel sections by a simple river profile. The uncertainties introduced by this method are small, because the reconstructed topography in the steep and narrow bottom parts of the landslide-dammed valleys leads to insignificant differences in the paleolake-volume calculations. We assume that sedimentation rates of landslide-dammed lakes represent upstream denudation rates, whereas all fluvially transported material is being deposited in the lake basin. Multiple landslides in single drainage basins strongly affect catchment areas upstream of landslide dams. For example, three Holocene landslide deposits in the Baspa Valley truncate each other (Fig. 4.4). Hence, mean basin-erosion rates derived from lake-sedimentation rates were adjusted for smaller river catchment areas. Present-day summer-monsoon precipitation distribution was derived from 10 years of passive microwave data (Special Sensor Microwave/Imager, SSM/I) [*Bookhagen et al.*, 2005b].

4.3 Intensified Monsoon Phases (IMPs)

The IMPs in the northwest Himalaya may be the result of orbital and/or terrestrial forcing by intensifying the monsoonal circulation through a steeper ocean-land thermal gradient [*Clemens et al.*, 1991; *Clemens and Prell*, 1991; *Hastenrath*, 1994]. This provides greater moisture transport into the continent and also increases precipitation leeward of orographic barriers, when rainfall increases abruptly once it has overcome the moisture-saturation threshold [*Bookhagen et al.*, 2005b]. Consequently, in the dry, high-elevation sectors of the Sutlej Valley region enhanced rainfall may lead to significant changes in erosional surface processes.

Late Pleistocene (ca. 29–24 ka) and Holocene (ca. 9–4 ka) IMPs were previously identified by several authors (Fig. 4.5). For example, in the northwest Himalaya, Tibet, and South China, numerous lacustrine deposits indicate humid intervals between ca. 29 and 25 ka [e.g., *Fang*, 1991; *Kotlia et al.*, 2000] as well as during the Holocene [e.g. *Gasse et al.*, 1991]. In addition, marine records covering these two periods document enhanced terrigenous input and monsoon-

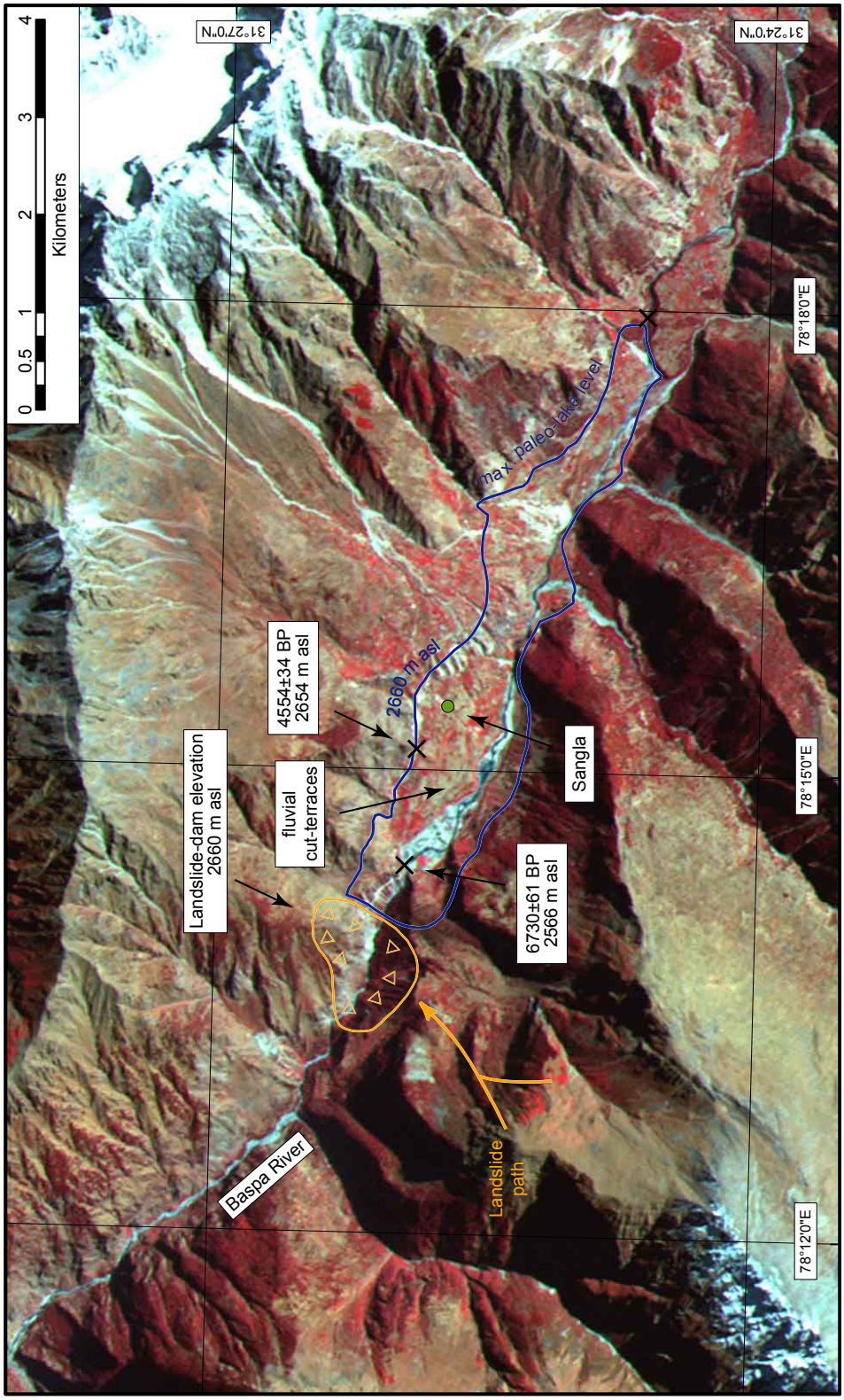

Figure 4.2: ASTER (Advanced Spaceborne Thermal Emission and Reflection Radiometer) satellite image of Sangla, Baspa Valley. Baspa River is flowing from East to West. Reconstructed landslide area is shown in orange, landslide-dammed lake area outlined in blue. We dated lake sediments using charcoal found in the bottom and top layers of the lake sediments. Photograph 4.3 was taken from the southeastern end of the paleolake extent (marked with black cross).

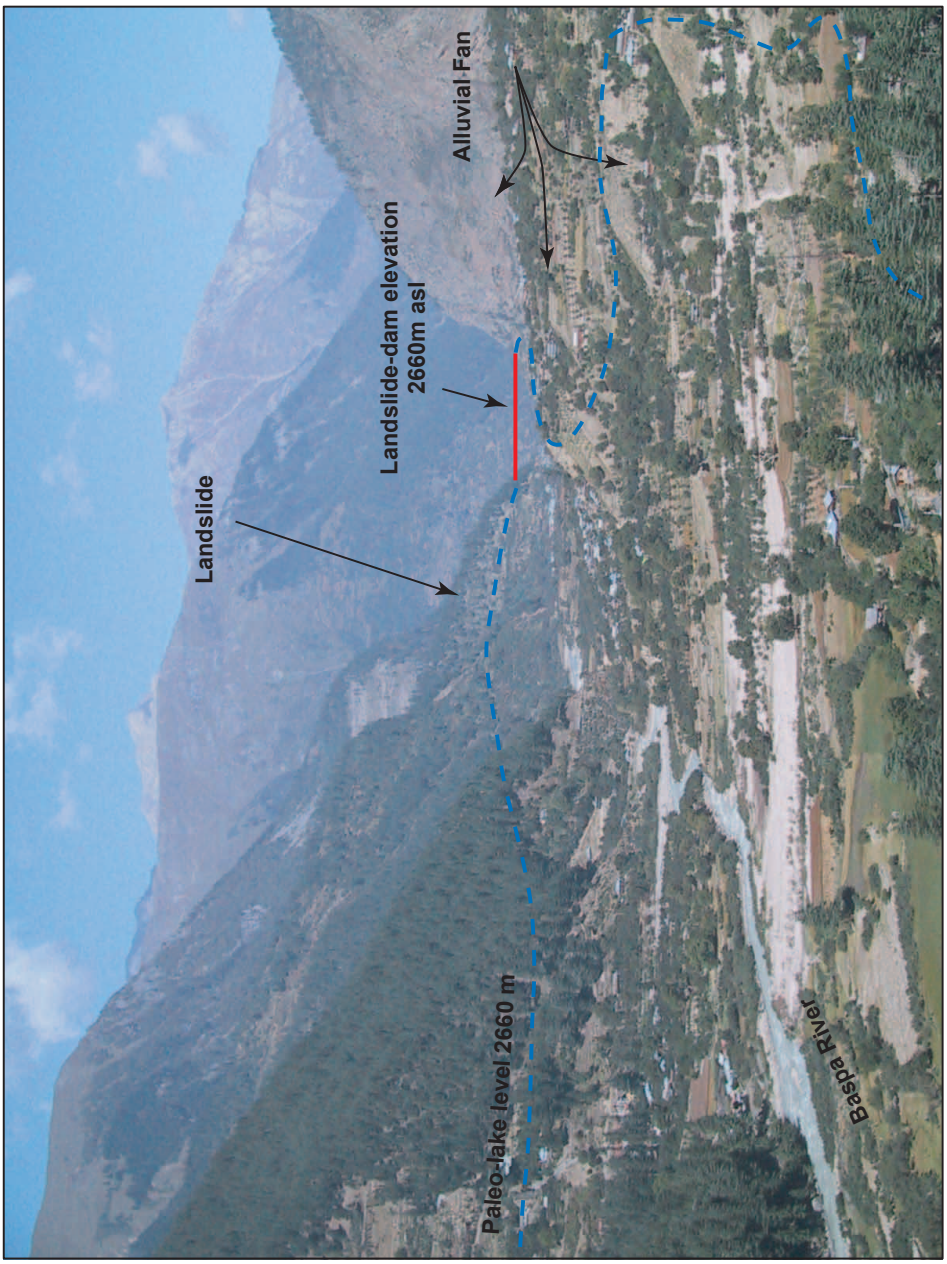

Figure 4.3: Photograph of the landslide at Kuppa, near Sangla in the Baspa Valley. Location of observer is given in Fig. 4.2. Not the break-off surface in the back of the picture.

related increased upwelling off the west coast of India [e.g. *Prins and Postma*, 2000; *Thamban et al.*, 2002]; increased sedimentation rates during the Holocene IMP are also known from the Bay of Bengal [*Goodbred and Kuehl*, 2000]. Humid conditions related to a strong southwest monsoon have been inferred [e.g., *Phillips et al.*, 2000] from the expansion of glaciers in the Nanga Parbat regions during the early to middle Holocene. Increased moisture transport during the late Pleistocene and Holocene has also been reported for the southern tip of the Arabian peninsula [e.g., *Bray and Stokes*, 2003; *Fleitmann et al.*, 2003]. Although the IMPs are well documented, processes and rates of erosion and sediment production, as well as the role of transient sediment storage in fluvial systems, remain largely unknown for these intervals of increased humidity.

4.4 Landslides and Lake Sediments

In the Sutlej Valley region, 13 large landslide deposits (>0.5 km^3) and lacustrine sediments constitute the vestige of enhanced hillslope erosion and valley impoundment during IMPs in late Pleistocene (at or after 28.8 cal. k.y. B.P.) and Holocene time (8.8–4 cal. k.y. B.P.) time (Tab. 4.1). Field observations, radiometric dating, and stratigraphic and geomorphic correlations allow reconstruction of paleolake surfaces, landslide volumes, and the temporal evolution of sedimentation and erosion.

The Holocene Kuppa (Baspa Valley) and Sichling (Spiti Valley) lake deposits behind former landslide barriers (Fig. 4.4 and Tab. 4.1) are well suited for an assessment of process rates in this region. Sedimentation rates for the Kuppa landslide are based on 2370±86 yr of lake existence, catchment area upstream of the landslide (115 km^2), reconstructed area of the paleolake (5.6 km^2), and the volume of associated deposits ($\sim 1.15 \cdot 10^9$ m^3). Borehole data [*Jaiprakash Company*, 2002, personal communication] indicate that an additional 50m of organic material underlies the presently exposed lake sediments. We associate this layer with deposition immediately after landsliding, when riparian vegetation and plants from the hillslopes were deposited in the newly formed basins. This undated, but short time period constitutes less than 5% of the total lake-sediment volume. The lacustrine strata comprise clay-rich layers and irregular intercalations of fine-sand layers, 1–6 mm and 1–3 mm thick, respectively. In the proximal parts of the basin, interfingering coarse alluvial-fan sediments document a dynamic, more erosive environment than today in which large alluvial fans grew with rising lake level. The highest fan elevation always coincides with the highest lake level and, hence it can be inferred that the landslide barriers were higher or at least as high as these deposits. Similarly, calculations for the Sichling landslide are based on 2550±80 yr of lake existence, 1372 km^2 catchment area, and a paleolake-sediment volume and area of $\sim 1.6 \cdot 10^9$ m^3 and 4.7 km^2, respectively.

During the Holocene IMP, basin-denudation rates for the duration of the lakes were 4.3±0.4

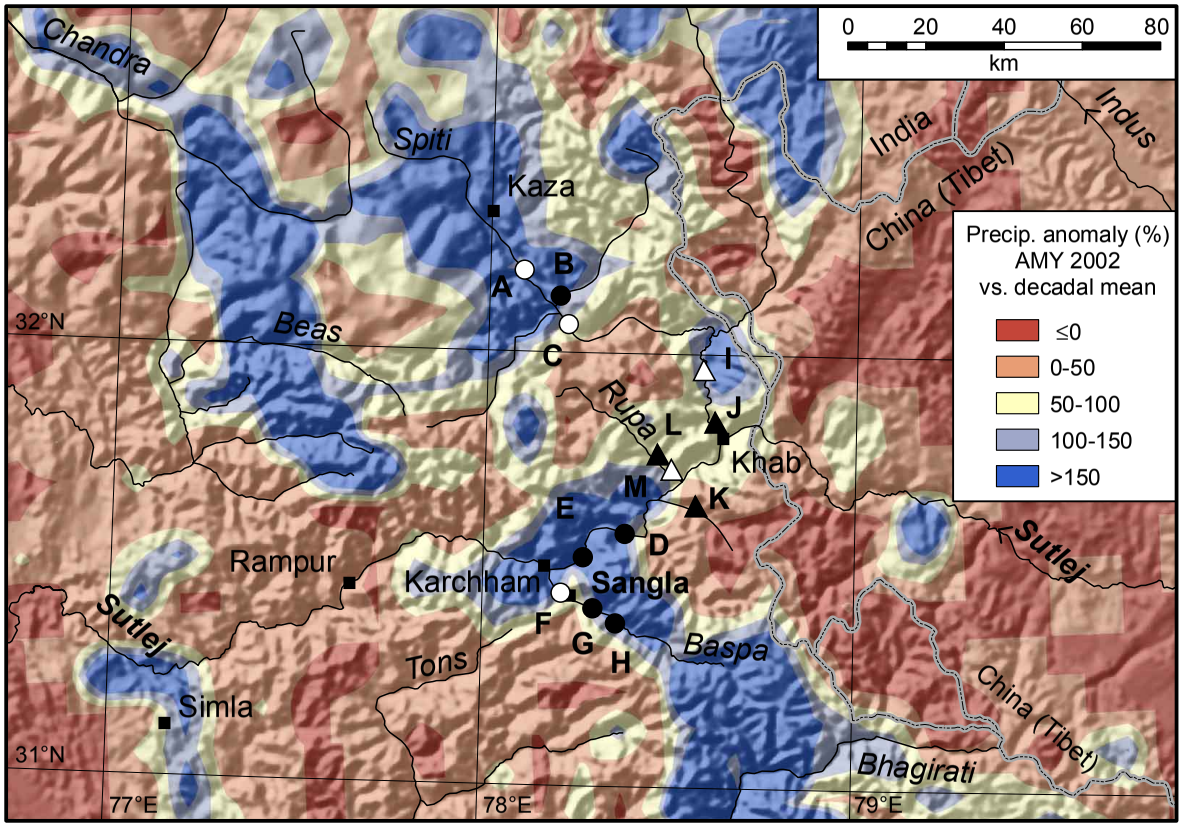

Figure 4.4: Precipitation anomalies draped over shaded relief of Sutlej Valley region. Topography based on GTOPO30 (U.S. Geological Survey) and precipitation anomalies from a 10 yr record of passive microwave data [*Bookhagen et al.*, 2005b]. Precipitation anomaly map (in percent) depicts magnitude changes between decadal mean (1992–2001) and an abnormal monsoon year (AMY; i.e., strengthened monsoon intensity) in 2002. Positive anomalies (blue) show more rain during 2002 AMY, i.e., a 100% anomaly represents a doubling of precipitation. During an AMY, moist air masses penetrate northeastward into the orogen through the Beas, Chandra, and Bhagirati Valleys and generate high amounts of precipitation in commonly dry areas of Spiti, Baspa, and Sutlej Valleys. Locations of late Pleistocene (triangles) and Holocene (circles) landslides and lacustrine sediments are shown; white symbols indicate radiocarbon-dated deposits, and black symbols denote landslides and their related lacustrine sediments dated by stratigraphic correlation. Letters indicate landslides and associated lacustrine deposits for which more detailed information is available (Tab. 4.1).

#	Land-slide	^{14}C date [yr B.P.]		Calibrated age (1σ) [yr B.P.]		Land-slide location	Land-slide volume [10^9 m^3]	Area of dammed lake [10^6 m^2]	Vol. of lake sed. [10^9 m^3]	Catch-ment area [10^6 m^2]	Basin averaged precipitation rate [mm/a]	
		bottom	top	bottom	top						Modern	AMY
A	Kaza (Spiti)	N.D.	2749±62	N.D.	2860±70	78°05.5'E 32°10.5'N	0.5	2.9	0.4	1975	250	575
B	Lingti (Lingti)	mid Holocene	N.D.	N.D.	N.D.	78°12.4'E 32°08.1'N	0.3	3.4	0.5	1026	175	375
C	Sichling (Spiti)	7926 ±38	5286±35	8711±68	6158±12	78°10.5'E 32°06.7'N	1.4	4.7	1.6	4393/ 1372	175	375
D	Akpa (Sutlej)	mid Holocene	N.D.	N.D.	N.D.	78°23.5'E 31°34.8'N	0.5	4.5	0.7	29,064	175	175
E	Rekong Peo (Sutlej)	mid Holocene	N.D.	N.D.	N.D.	78°14.8'E 31°30.9'N	1.0	5.4	0.9	29,418	175	175
F	Kuppa (Baspa)	6730 ±61	4554±34	7594 ±27	5297 ±17	78°14.3'E 31°26.0'N	0.6	5.6	1.2	757/115	100	850
G	Rak-chham (Baspa)	mid Holocene	N.D.	N.D.	N.D.	78°16.5'E 31°24.9'N	0.5	2.6	0.4	601/72	100	775
H	Khor-gala (Baspa)	mid Holocene	N.D.	N.D.	N.D.	78°18.9'E 31°24.3'N	0.4	1.5	0.1	657	100	775
I	Chango (Spiti)	25,120±245 24,960±300 25,430±550	N.D.	28,570±920 28,590±920 28,920±1160	N.D.	78°35.6'E 32°04.1'N	1.0	31.5	5.5	7846	175	750
J	Khab (Spiti)	late Pleis-tocene	N.D.	N.D.	N.D.	78°37.8'E 31°49.4'N	0.8	3.5	0.3	8257	175	750
K	Tirang (Tirang)	late Pleis-tocene	N.D.	N.D.	N.D.	78°35.5'E 31°42.5'N	0.4	2.5	0.2	328	125	350
L	Rupa II (Rupa)	late Pleis-tocene	N.D.	N.D.	N.D.	78°28.1'E 31°45.8'N	0.5	3.5	0.2	480	175	400
M	Shaso (Rupa)	24,040±285	N.D.	27,130±540	N.D.	78°30.5'E 31°43.3'N	0.6	2.2	0.3	555	175	425

Table 4.1: List of landslide-dammed lakes in the Sutlej Valley region. Column 1 indicates landslide location on Figure 4.4. Calibration of ^{14}C dates after *Stuiver et al.* [1998] and *Voelker et al.* [1998] (B.P. = 1950, N.D. = No Data). The catchment area and basin averaged precipitation rates were determined for the area upstream of the landslide-dam. AMY denotes abnormal monsoon year [*Bookhagen et al.*, 2005b].

mm/yr for the Kuppa landslide and ∼0.5±0.05 mm/yr for Sichling. Where available, we compared present-day suspended-sediment measurements and Holocene sediment infill in the Baspa and Spiti Valleys. Modern, mean basin denudation rates at Kuppa are 0.7 mm/yr during normal monsoon seasons and increase to 1.6 mm/yr during abnormal (i.e., strengthened) monsoon years [*Bookhagen et al.*, 2005b]. Hence, IMP basin erosion rates are at least 5 times greater than the average modern rate and more than twice as large as rates during abnormal monsoon years. In the more arid Spiti Valley (Sichling landslide) IMP mean basin denudation rates are six times greater than present rates on the order of 0.08 mm/yr.

4.5 Discussion

Under present conditions, there is a clear relationship between abnormal (i.e., strengthened) monsoon years, northward moisture penetration into the arid parts of the orogen, and enhanced surface-process rates [*Bookhagen et al.*, 2005b]. Although these observations only constrain the relationship between precipitation distribution and surface processes in the Sutlej Valley region, coeval phenomena are documented for other areas in the northwest Himalaya as well [e.g., *Barnard et al.*, 2001; *Paul et al.*, 2000]. These data suggest that episodic moisture transport into the arid sectors of the orogen is also a fundamental process on longer time scales acting along the southern flank of the orogen [e.g., *Goodbred and Kuehl*, 2000; *Pratt et al.*, 2002]. The present-day process of spatially shifting precipitation patterns may thus serve as a model for explaining higher rainfall, increased runoff, and enhanced sediment production in the arid sectors during IMPs in the late Pleistocene and Holocene.

The steep hillslopes in the arid, high-elevation parts of the northwest Himalaya are sparsely vegetated, and during abnormal monsoon years, enhanced precipitation controls shallow hillslope erosion [*Bookhagen et al.*, 2005b]. However, during longer-lasting IMPs, the increased pore-water pressure, enhanced sediment flux and higher frequency of flood events are expected to have created favorable conditions for deep-seated landsliding. It is important to note that studies relating the influence of extreme climatic events to erosion rates in river basins similar in size to the Spiti and Baspa tributaries document channel widening rather than incision during extreme floods [e.g., *Hartshorn et al.*, 2002]. In fact, modeling studies and field observations show that increased runoff and sediment transport result in lateral scouring, undercutting, and subsequent oversteepening of hillslopes [e.g., *Hancock and Anderson*, 2002]. We thus posit that, if such humid conditions were sustained over several millennia, as during an IMP, enhanced precipitation would have led to higher pore pressures, increased lateral scouring, and hillslope instability. Ultimately, these processes may have caused exceptionally large bedrock landslides that are not triggered under present conditions. After the establishment of voluminous landslide barriers, material

stripped off hillslopes was stored in these transient basins, before the material was eroded again during ensuing times of lower climatic variability with reduced rainfall and sediment flux.

Analogous observations relating humid phases and landslide triggering have been described in the southwestern United States [e.g., *Dethier and Reneau*, 1996; *Reneau and Dethier*, 1996]. Alternatively, it could be argued that massive landsliding may have been triggered by seismicity [e.g., *Keefer*, 1994]. However, despite active seismicity in the Himalaya, these events apparently only play a minor role in supplying increased sediment amounts to rivers in regions with strong monsoon seasons [e.g., *Owen et al.*, 1996; *Paul et al.*, 2000; *Barnard et al.*, 2001].

In summary, our data show that higher precipitation is coupled with increased mass wasting and significantly higher sediment flux during IMPs in the currently arid, high-elevation regions of the northwest Himalaya. The large landslides and associated lake deposits therefore constitute the vestige of enhanced hillslope erosion and valley impoundment during phases of increased humidity (Fig. 4.5). It is interesting to note that the mass movements not only cluster in time, but also in space. Large landslide deposits occur in the semiarid to arid climatic transition zone that receives increased precipitation only during abnormal (i.e., strengthened) monsoon years (Fig. 4.4).

4.6 Conclusion

We temporally linked intensified monsoon phases (IMPs) with the occurrence of large landslides and documented a strong influence of long-lasting, intensified monsoon circulations on landscape evolution. During IMPs in late Pleistocene and Holocene time, moisture migrated into the high, arid parts of the northwest Himalaya and dramatically enhanced the sediment flux compared to present-day, weaker monsoon conditions. The corresponding increase in averaged basin-erosion rates during these episodes was linked to increased precipitation and amount of material stripped off the hillslopes. Increased moisture migration is expected to have raised pore pressures along the poorly vegetated hillslopes, eventually leading to massive landsliding in the high-elevation sectors of the orogen. Thus, enhanced sediment evacuation toward the Himalayan foreland and the formation of transient basins are strongly controlled by higher climatic variability during IMPs and lead to fundamentally different geomorphic transport and erosion processes. The causative relationship between wetter climate and landsliding explains the absence of large mass movements in the arid, high-elevation regions under both present conditions and during the weak summer-monsoon phases of the Last Glacial Maximum. Thus, the locations of these exceptionally large landslides might serve as a proxy for paleo-moisture migration in the interior part of the Himalayas.

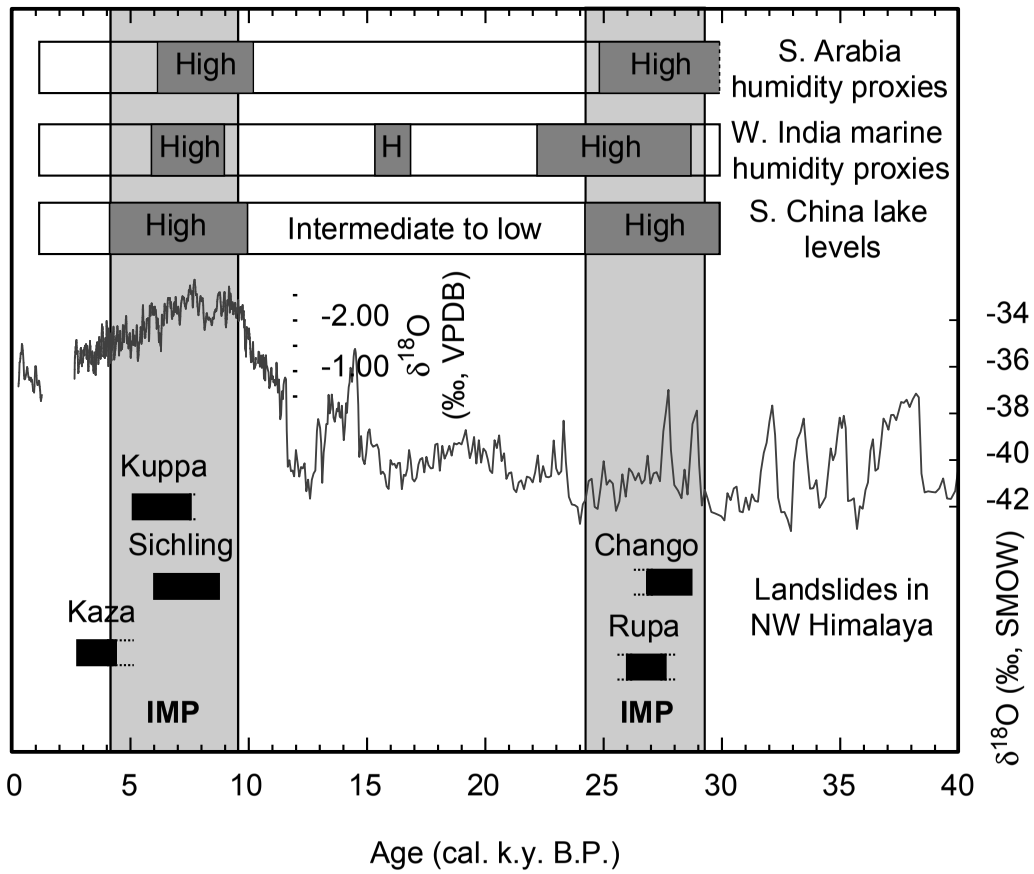

Figure 4.5: Late Pleistocene and early Holocene intensified monsoon phases (IMPs). Information on δ^{18}O measurements (VPDB–Vienna Peedee belemnite; SMOW–standard mean ocean water) is merged from GISP2 [*GISP*, 1997] and high-resolution, Holocene speleothem data from the southern Arabian Peninsula [*Fleitmann et al.*, 2003]. Speleothem data indicate a strengthened southwest monsoon during late to middle Holocene. Multiple, past humid phases in the desert of southern Arabia (S. Arabia humidity proxies) show two distinctive wet intervals [*Bray and Stokes*, 2003]. Humidity proxies from the north and east Arabian Sea (W. India marine humidity proxies) show intensified summer monsoons [*Prins and Postma*, 2000; *Thamban et al.*, 2002]. Independently derived chronologies of humid phases in adjacent areas (S. China lake levels) from lake highstands and pollen records emphasize regional importance of these humid intervals [e.g., *Fang*, 1991; *Gasse et al.*, 1991]. Black boxes mark existence of landslide-dammed lakes in greater Sutlej Valley region, black lines outside the boxes signify age uncertainties (see Tab. 4.1 for a complete list)

4.7 Acknowledgements

This work has been supported by the German Research Foundation (DFG STR371/11-1 to M. Strecker). The success of this project was made possible through the support of many Indian friends and colleagues, especially A.K. Jain and S. Singh (I.I.T. Roorkee). We gratefully acknowledge fruitful discussions with A. Barros, P. Blisniuk, B. Dietrich, G. Haug, G. Hilley, and E. Sobel. Reviews by D. Burbank, A. Densmore, and N. Hovius were highly appreciated. SSM/I and ASTER data were obtained from the NASA Pathfinder Program for early Earth Observing System (EOS) products.

5. HOLOCENE MONSOONAL DYNAMICS AND FLUVIAL TERRACE FORMATION IN THE NORTHWEST HIMALAYA, INDIA

Abstract

Cosmogenic radionuclide exposure ages of cut-and-fill river-terrace surfaces from the lower Sutlej Valley, northwest Himalaya, document the close link between Indian Summer Monsoon (ISM) oscillations and fluvial incision. During the early Holocene ISM optimum, precipitation was stronger and moisture penetrated farther into the orogen leading to amplified sediment flux from erosion off vegetation-free hillslopes and remobilization of formerly lodged glacigenic deposits in the high-elevation, internal parts of the orogen. Contrary to common concepts linking fluvial incision of terrace systems to increased precipitation and runoff, we demonstrate that less moisture during centennial oscillations of the ISM system results in lower sediment supply, allowing flux-undersaturated rivers to incise episodically. This choked the wide, low-gradient valleys in the southern Himalayan front with debris, locally up to 120 m thick. Incision and channel abandonment between ISM onset at 9.7 ka BP and today coincides with centennial-long, drier intervals in the oscillating monsoonal system.

5.1 Introduction

Abrupt climate changes are known from the geologic record [*Thompson et al.*, 2000; *Altabet et al.*, 2002; *Fleitmann et al.*, 2003; *Gupta and Thomas*, 2003], but their effect on the fluvial transport system remains unknown. The Indian Summer Monsoon (ISM) exerts a profound control on erosional hillslope processes, river discharge, and sediment flux along the southern Himalayan front. The ISM circulation transports moisture from the Bay of Bengal along the mountains to the northwest, and rainfall decreases gradually along its way [*Shrestha et al.*, 2000; *Shrestha*, 2000; *Bookhagen et al.*, 2005b]. In the eastern Himalaya, rainfall penetrates far into the orogen along river valleys and annual precipitation amounts are on the order 5 m/yr. In contrast, the northwestern regions near the Sutlej Valley (78°E, 31°N) receive 2.5 m/yr and rainfall does not migrate far into the Himalaya but focuses on the mountain front. Thereby, the strength of the ISM determines precipitation amounts, while orography controls precipitation distribution. In a recent, abnormally strong monsoon year in 2002, rainfall migrated far into the Sutlej Valley and initiated debris flows in the normally arid, high-elevation parts of the northwestern Himalaya.

These shallow, erosional hillslope processes significantly increased fluvial suspended sediment transport into the Himalayan foreland. Similarly, millennial-long intensified monsoon phases in the late Pleistocene and early Holocene were characterized by increased sediment transport and deep-seated landsliding in the internal, high-elevation regions of the Sutlej Valley [*Bookhagen et al.*, 2005a]. Thus, the Sutlej Valley at the end of the monsoonal conveyer belt provides an ideal location to analyze the impact of short (<10 to 10^2 years) and long-term (>10^4) ISM oscillations.

The oscillating ISM mainly affects the boundaries of three distinctive climatic and geomorphic segments along the Sutlej River (Fig. 5.1, 5.2): (1) the semi-humid, low-elevation (<1 km asl), low-gradient and wide river valleys with moderate rainfall (1 m/yr), (2) the wet, medium-elevation (1–3 km asl), steep areas with high rainfall (3 m/yr), and (3) the arid, high-elevation (>3 km asl), steep regions with low rainfall (<0.2 m/yr). Thus, a change in ISM strength impacts rainfall amount and rainfall distribution, and increases erosional processes primarily in the arid, high-elevation regions. Interestingly, sediment evacuation from this high-elevation region is restricted to abnormal monsoon years where precipitation reaches orographically-shielded areas and enhances sediment mobilization [*Bookhagen et al.*, 2005b]. It is thus most likely that during long-lasting (10^2 to 10^3 years), intensified monsoon phases precipitation continuously reached these regions and caused significant enhanced fluvial sediment transport. While the oscillating ISM during the early to mid Holocene was overall stronger than today, several centennial-long intervals of reduced rainfall, such as during the 8.2 kyr event, can be detected [*Gasse et al.*, 1991; *Fleitmann et al.*, 2003; *Yuan et al.*, 2004]. Here, we analyze the influence of this oscillating shifting precipitation patterns on sediment flux, fluvial erosion, and depositional processes.

5.2 Data sets and Methods

In the low-elevation Sutlej Valley, a massive conglomeratic fill, about 120 m above the present baselevel, is found between Rampur and Luhri over a distance of ∼75 km, immediately downstream of the narrow, high-gradient gorges (Fig. 5.1). There are no aggradational terraces in the humid, medium-elevation regions. Stratigraphy of the infill shows a stepless, uninterrupted deposition, and provenance of the pebbles suggests source regions from the medium- to high-elevation regions of the Sutlej Valley. Sculpted into this deposit are six fluvial terraces that occur at successively lower elevations between the highest surface at 1020 m and the present stream at 900 m asl (Fig. 5.2). The cosmogenic nuclide ages thus define the abandonment following fluvial incision and were averaged over both isotopes (Tab. 5.1). We surveyed these fluvial cut-and-fill terraces using a differential GPS and determined their exposure ages with cosmogenic nuclide radioisotopes (^{10}Be, ^{26}Al) on gravels from the surfaces. Clasts were crushed and sieved to a uni-

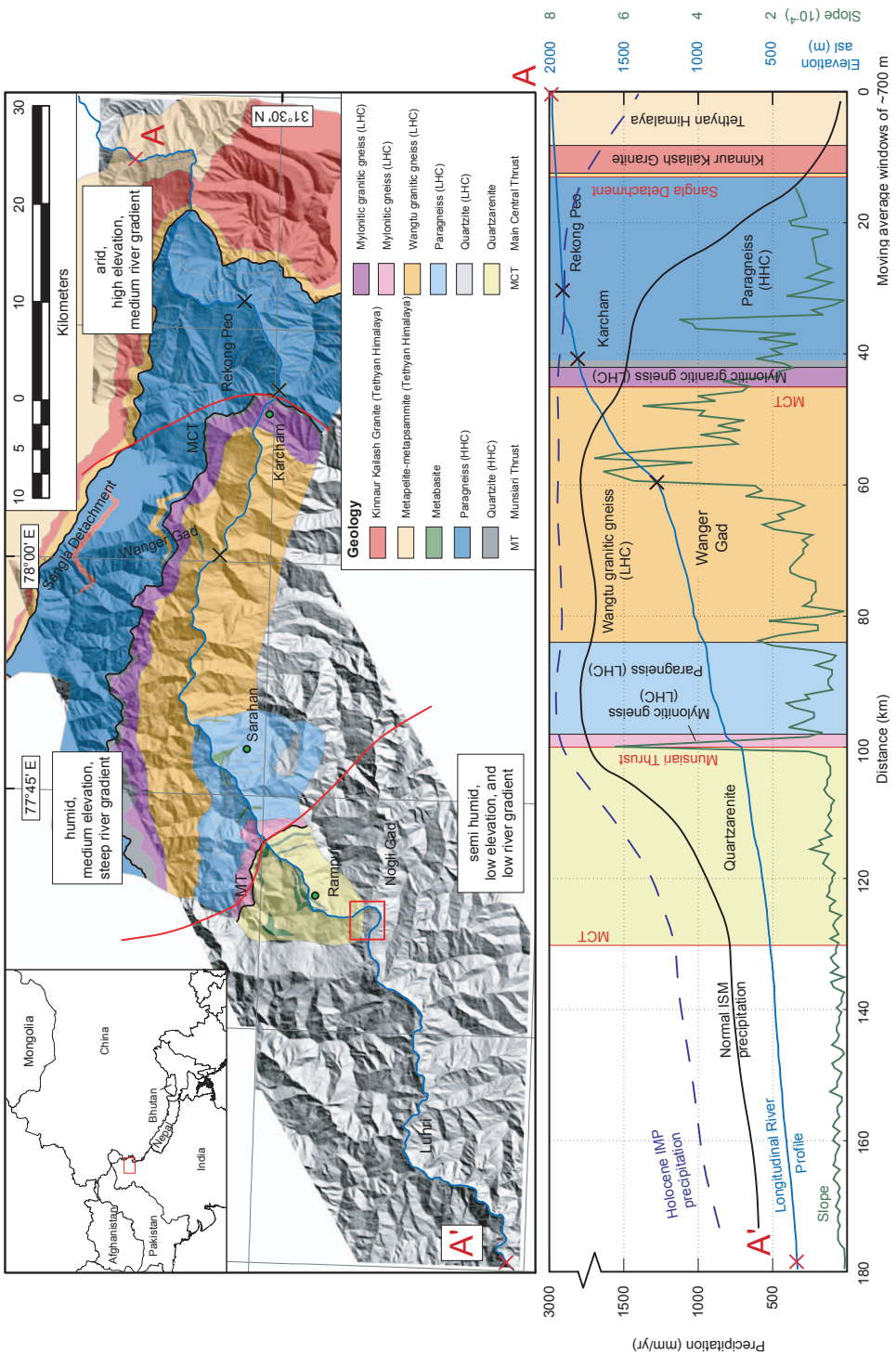

Figure 5.1: Geological map and longitudinal river profile of the Sutlej River. Topographic profile and slopes are obtained from a digital elevation model, created from digitized 20m contour lines. Normal Indian Summer Monsoon (ISM) precipitation was taken from calibrated SSM/I-derived data [*Bookhagen et al.*, 2005b]. Inferred paleo precipitation during the Holocene Intensified Monsoon Phase (IMP) has been derived from landslide distribution [*Bookhagen et al.*, 2005a]. Red box south of Rampur in the Geological map outlines region of Fig. 5.2.

Sample	Elevation [m asl]	Height above modern grade [m]	^{10}Be age [ky]	± [ky]	^{26}Al [10^3 atoms per 1 g qtz]	± [ky]	^{26}Al age [ky]	± [ky]	Mean age (^{10}Be and ^{26}Al) [ky]	± [ky]
BB1	1020	120	9.5	0.3	587.7	20.2	9.8	0.3	9.7	0.5
BB2	1005	105	8.0	0.3	493.8	26.2	8.3	0.4	8.2	0.5
BB3	1005	105	8.4	0.5	488.6	38.7	8.2	0.7	8.3	0.8
BB4	1005	105	9.8	0.2	495.2	28.9	9.9	0.6	9.8	0.6
BB5	1005	105	9.5	0.2	296.8	25.3	9.8	0.8	9.7	0.9
BB6	1005	105	10.3	0.3	160.6	16.4	8.3	0.9	9.3	0.9
BB7	1005	105	11.4	1.9	78.7	10.2	11.2	1.5	11.3	2.4
BB8	965	65	6.3	0.3	368.4	17.3	6.2	0.3	6.3	0.4
BB9	920	20	2.9	0.2	185.1	10.5	3.2	0.2	3.1	0.3
BB10	892	6	2.4	0.2	159.2	21.5	2.8	0.4	2.6	0.4
BB11	893	7	2.3	0.1	134.0	10.2	2.4	0.2	2.3	0.2

Table 5.1: List of processed cosmogenic nuclide samples near Rampur (Averi). Production calculation after *Lal* [1991], with corrected values [*Nishiizumi et al.*, 1989; *Clark et al.*, 1995]. We included muon production calculation for depth-dependent profile [*Granger and Muzikar*, 2001; *Granger and Smith*, 2000]. Density of terrace conglomerates: $\rho = 1.9$ g/cm^3, attenuation length $\Lambda = 160$ g/cm^2. Al and Be production rate (atoms/yr) are 31.1 and 5.1, respectively [*Clark et al.*, 1995]. For each sample, we added 0.3 mg of ^{9}Be carrier (6.7E19 atoms/mg).

form size of 125–500 μm, and clean quartz from these samples was isolated by chemical leaching [*Kohl and Nishiizumi*, 1992]. We added 0.3 mg of Be carrier to a 100 g sample of quartz and dissolved in 3:1 HF:HNO_3. Aluminum concentrations were determined by Inductively Coupled Plasma-Atomic Emission Spectrometry (ICP-AES) on an aliquot of the dissolved sample. Al and Be were separated by ion chromatography and precipitated as metal hydroxides which were then oxidized to Al_2O_3 or BeO. The ratio of the radionuclide to the stable isotope was determined by accelerator mass spectrometry at Lawrence Livermore National Laboratory [*Davis et al.*, 1990]. ^{10}Be concentrations were determined relative to an ICN standard and ^{26}Al to an NBS standard, both prepared by K. Nishiizumi. ^{10}Be/Be ratios were corrected for interference from ^{10}B. The measured ratios of both ^{10}Be and ^{26}Al were corrected for process blanks treated in the same way as the samples. We collected a total of 25–30 quartz-rich clasts on the conglomeratic terrace surfaces to account for pebble-specific exposure history. We also collected material from large, single boulders with fluvial erosion marks (e.g., potholes). In addition, samples from a 2-m-deep depth profile show no initial radionuclide inheritance (Fig. 5.3). All ages are given with 1σ errors. Errors on the model ages were calculated by propagating the analytical uncertainties together with a 6% error on the production rates [*Stone*, 2000] and 3.3% and 2.8% uncertainties for the decay constants of ^{10}Be and ^{26}Al, respectively [*Gosse and Phillips*, 2001]. To account for the decreased production rates at depth, the ages of subsurface samples are depth-corrected

with $\rho = 1.9 \pm 0.2$ g/cm^3 and $\Lambda = 160 \pm 10$ g/cm^2. We included muon production calculation for depth-dependent profile [*Granger and Smith*, 2000; *Granger and Muzikar*, 2001].

To decipher the role of ISM oscillations in changing precipitation regimes, we use oxygen isotope ratios (δ^{18}O) measured in a stalagmite from Southern Oman. Previous work in southern Arabia demonstrates that δ^{18}O values are inversely related to the amount of rainfall, primarily via an 'amount effect' [*Burns et al.*, 1998; *Fleitmann et al.*, 2003]. Thereby, lower δ^{18}O values result from enhanced fractionation through increased thermal convection of humid air accompanied by increased precipitation. Thus, lower values indicate more precipitation, while higher values represent less precipitation. We then temporally compare cosmogenic nuclide age distribution with phases of relatively more or less precipitation.

5.3 Results and Discussion

Deposition of the terrace gravels was very rapid at the onset of the ISM in early Holocene at 9.8 ka BP. Overall, precipitation between 9.6 ka and 7.4 ka BP was stronger than today, with several pronounced low-intensity intervals in the early to mid Holocene [*Gasse et al.*, 1991; *Overpeck et al.*, 1996; *Fleitmann et al.*, 2003; *Yuan et al.*, 2004]. Our age determinations show that the highest terrace (T1, 120m above modern grade, amg) was abandoned at 9.7 ka (±0.3 ka) (Tab. 5.1). This surface is highly dissected and consists of isolated remnants along the present stream. We suggest that the formation of this terrace dates the evacuation of transiently stored, unconsolidated material from the high-elevation sectors of the Sutlej Valley. The second highest and most pronounced terrace surface T2 (110m amg) is 8.6 ka (±0.7 ka) and can be followed upstream into large tributaries as well. In places, fine-grained overbank deposits cover the terrace conglomerates near the valley flanks. We argue that these deposits indicate remnants of flood overspills, while the channel was incising. Only high flows would overcome the channel tops and deposit suspended sediments. The period between ∼8.7 and 8 ka was characterized by a low-frequency/high-amplitude, weak ISM phase [*Gasse et al.*, 1991; *Overpeck et al.*, 1996; *Fleitmann et al.*, 2003] and thus provided sufficient time to substantially change hydrologic conditions. Terrace level T3 was not sampled because of the poor preservation of the small relict surfaces. We propose, however that the formation of T3 occurred during a short, weak ISM phase around 7 ka. The third lowest terrace T4 is clearly distinguishable and 6.3 ka (±0.5 ka) old. Similar to T2, we observe overbank deposits that we associated with overspills during flood conditions while the channel was incising in middle of the wide river valley. These deposits are 6.6 cal ^{14}C ka (±0.1 ka). Again, abandonment of the pronounced T4 level coincides with a prominent low-frequency/high-amplitude, weak ISM phase. In contrast, we cannot identify such a character during the generally decreasing ISM between 6.2 and 3 ka, which may explain the lack of terrace

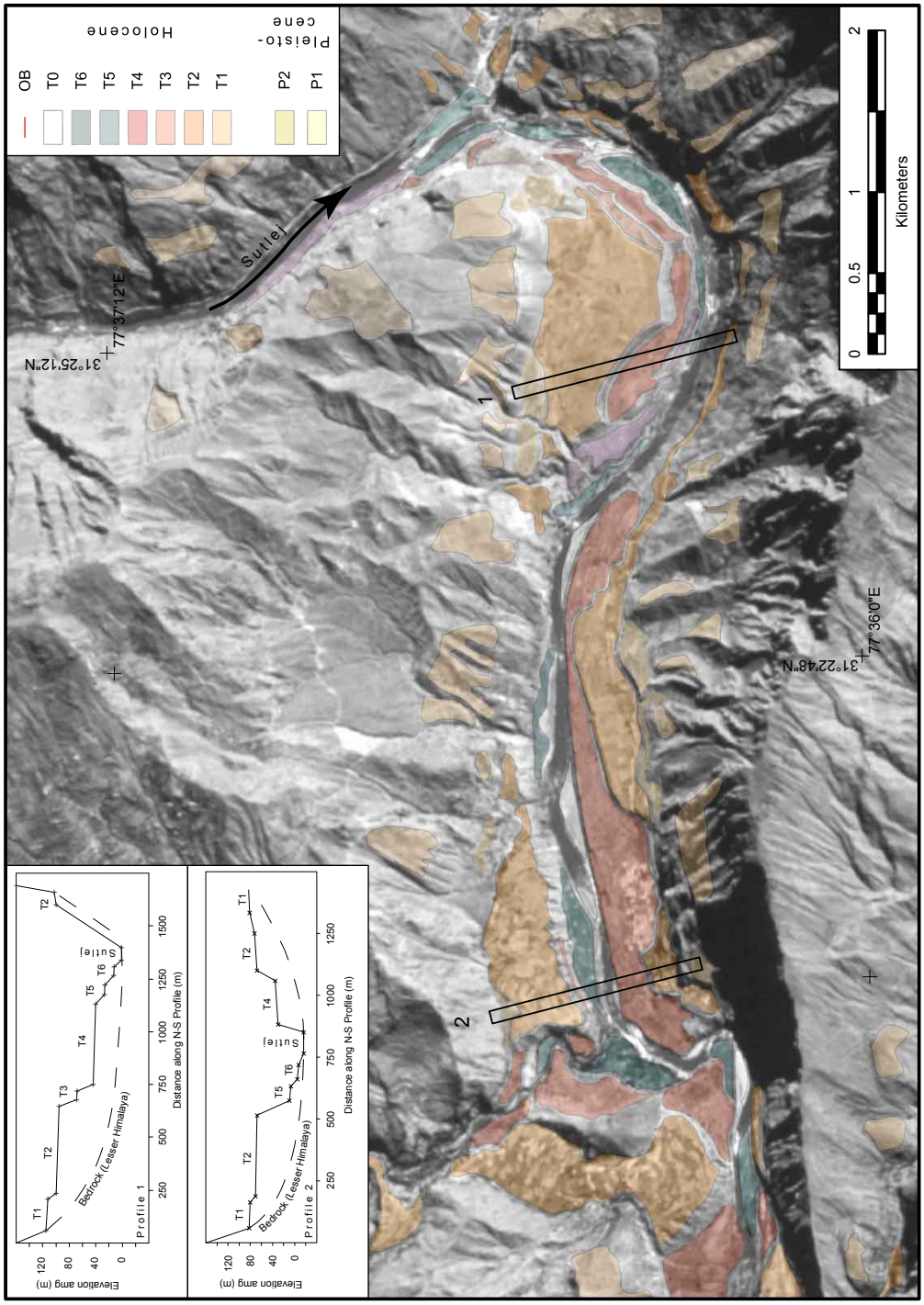

Figure 5.2: Fluvial cut-and-fill terrace sequence south of Rampur near Averi. Location outlined in Fig. 5.1. Terrace surfaces are colorcoded and draped over a Corona satellite image. Map inset denotes two topographic sections measured with differential GPS across the Sutlej River.

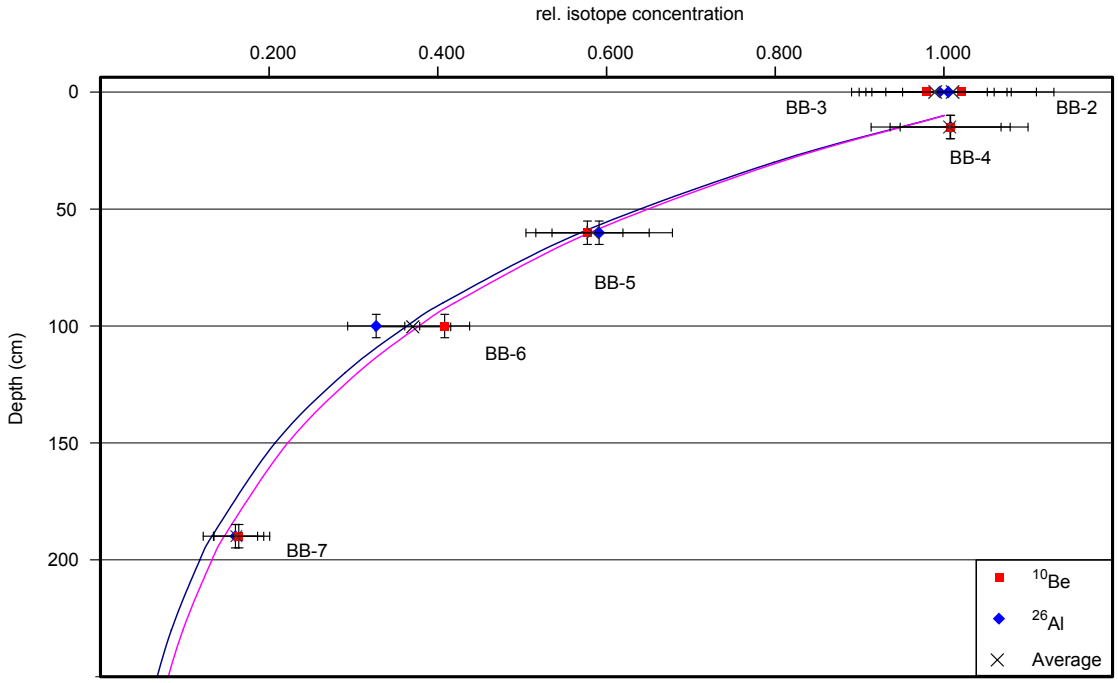

Figure 5.3: Depth profile (2m) on terrace surface T2 (see Fig. 5.2). Cosmogenic-nuclide exposure ages include measurement and scaling errors. Relative concentration is compared to max. theoretical concentration on the surface. Quartz-rich material for sample BB2 was collected from a single boulder (diameter of 2.3m) that showed pronounced fluvially-formed potholes. For sample BB3, 30 quartz-rich clasts from the surface were collected. Theoretical decay concentration were calculated for including muon production (pink) and without (blue).

formation in mid-Holocene time. The lower levels of T5 (25m amg) and T6 (10m amg) have ages of 3.1 ka (±0.1 ka) and 2.5 ka (±0.1 ka), respectively, and also only occur as isolated remnants. We relate them to late Holocene ISM oscillations, where conditions were as weak as during the present-day. Similar to the high-elevation, upstream areas, the Sutlej presently flows partly over bedrock in the low-elevation regions and has thus regained its base level prior to the rapid alluviation of the valley in early Holocene time.

Orogenward precipitation migration was more pronounced during the early Holocene when moisture traveled upstream large valleys to reach orographically shielded, arid areas including the Tibetan Plateau [*Gasse et al.*, 1991; *Overpeck et al.*, 1996; *Bookhagen et al.*, 2005a]. Accelerated rainfall fell on barren slopes, presumably causing a large increase in erosion [*Goodbred and Kuehl*, 2000; *Bookhagen et al.*, 2005a]. Furthermore, the increased runoff cut through freshly deposited glacial sediment, which had accumulated in the valley bottoms due to glacial and periglacial conditions during the Last Glacial Maximum (LGM) and the Younger Dryas, immediately before the onset of the ISM [*Owen et al.*, 2001, 2002; *Barnard et al.*, 2004]. These two sources of sediment in combination should have significantly increased the sediment load to the downstream, low-

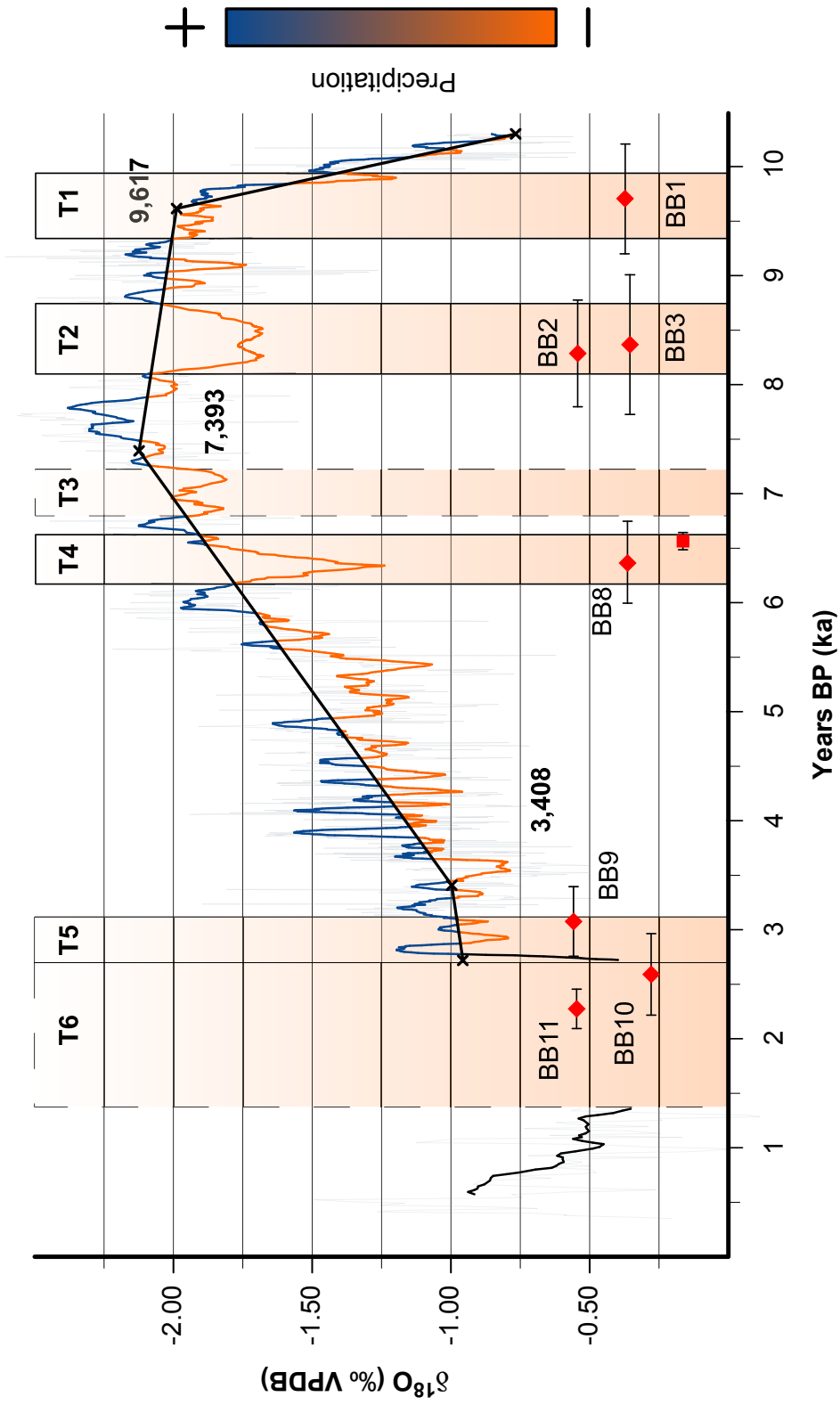

Figure 5.4: Holocene monsoonal oscillations (derived from δ^{18}O-measurement of speleothems [*Fleitmann et al.*, 2003]) and cosmogenic-nuclide exposure ages of fluvial cut surfaces. Orange regions outline centennial-long, weak monsoon phases. Terrace-surface abandonment ages were averaged over both isotopes (^{26}Al and ^{10}Be) and include measurement and scaling errors.

gradient channels leading to considerable aggradation there. Importantly, the rapid evacuation of the transiently stored, glacial sediments must have cleared the steep, narrow channels in the high-elevation parts and lowered the baselevel to allow bedrock incision. Baselevel lowering and increased pore-water pressures along the hillslopes help to explain deep-seated landsliding during the early Holocene in the high-elevation, internal parts of the orogen [*Bookhagen et al.*, 2005a]. During that time, basin-wide erosion rates were at least four times greater than at present [*Bookhagen et al.*, 2005b]. Thus, oscillations in the ISM and moisture migration into the orogen control sediment efflux from the Sutlej valley [*Bookhagen et al.*, 2005a, b]. Consequently, decreased precipitation and sediment flux at 9.7 ka BP lead to incision and the formation of cut-terrace level T1. Studies in the Marsyandi Valley, central Nepal [*Pratt et al.*, 2002], and our own observations in the Sutlej Valley suggest that these sediments were not entirely evacuated from the orogen. Instead, they were temporally stored in the wider, low-gradient sectors of these mountain streams, locally reaching more than 100 m in thickness. Thus, sediment flux and hydrologic regime in these parts of the Himalaya are strongly correlated with the migration of moisture. Deep penetration of precipitation into the orogen during strengthened ISM phases increased sediment production and transport toward the foreland, while weaker ISM periods were characterized by lower sediment flux [*Bookhagen et al.*, 2005b, a].

Our assessment of coeval channel abandonment and periods of reduced rainfall thus documents a two-tiered influence of climate changes on landscape evolution. First, the voluminous valley fill forming the substrate for the terrace surfaces in the low-gradient regions emphasizes the importance of increased precipitation and its influence on sediment removal and transient sediment storage derived from the high-elevation, threshold environments. Sediment storage in the Sutlej Valley also highlights a significant lag time between production and mobilization of sediment during a climatic transition period and the arrival of erosion products in foreland basins. Secondly, ensuing episodic incision and terrace formation herald a return to base level positions that had already existed immediately before alluviation and underscore the pronounced effects of centennial climate variability on geomorphic processes.

6. CONCLUSIONS

In order to test the hypothesis that there exist a link between climatic and erosion processes, I investigated mass-transfer rates and relief-forming processes on a variety of spatial and temporal scales. Erosion in the high-relief Himalaya is strongly dictated by monsoonal rainfall as documented by the present-day synoptic and valley-scale precipitation gradients in the Himalayas that were analyzed using passive microwave data. In this climatic regime moisture is transported from the Bay of Bengal along the southern Himalayan mountain front to the northwest and results in E-W as well as N-S precipitation gradients due to the Himalayan orographic barrier. Topography thus exerts a strong control on rainfall along the mountainous regions and guides moisture migration into deeper parts of the orogen during strengthened monsoonal circulation. The year 2002 was an abnormal monsoon year (AMY) for the northwest Himalaya, when precipitation migrated far into the orogen and reached arid regions normally shielded by orographic barriers. These sectors are characterized by steep, sparsely vegetated and regolith-mantled hillslopes and represent geomorphic threshold areas that are very sensitive to changes in environmental conditions. During abnormally strong rainfall events, hillslopes in this environment respond with enhanced erosion. I identified debris flows in the upper catchment regions as effective geomorphic erosion agents by comparing satellite images taken before (April) and after (December) the 2002 AMY. These images show that carving and reactivation of channels, and thus fluvial network evolution is significantly increased during these extreme events. In addition, mass transport rates measured by suspended sediments reveal that more than twice as much sediment may be evacuated by rivers in these dry regions of the orogen during episodes of high climatic variability. Despite an increase in erosion rates in the high-elevation parts of the Sutlej River during the 2002 AMY, mean basin lowering rates along the medium-elevation sectors are dominated by rainfall distribution during normal monsoonal years.

Analogous to periods characterized by extreme weather events I also link intensified monsoon phases (IMPs) on timescales of 10^3 to 10^4 years with the occurrence of large landslides during the late Pleistocene and early Holocene. I use the occurrence of exceptionally large landslides as proxy indicators for higher precipitation. During IMPs in late Pleistocene and Holocene time, moisture migrated continuously into the high, arid parts of the Sutlej Valley. Sedimentological data show that dramatically enhanced the sediment flux compared to present-day, weaker monsoon

conditions. The corresponding increase in averaged basin-erosion rates during these episodes is then thought to have been correlated with increased precipitation and higher amounts of material stripped off the hillslopes. Increased moisture migration is expected to have raised pore-water pressures along the poorly vegetated hillslopes, and increased sediment flux, provided erosion tools that aided lateral scouring and destabilization. This eventually caused massive landsliding in the high-elevation regions of the orogen. In addition, the onset of heavy monsoonal rainfall during the IMP at 9.7 ka BP removed the material stored along the rivers. Thus, the fluvial baselevel was lowered and rivers were able to incise into bedrock and erode laterally. Interestingly, we do not observe large landslides at other periods and more importantly, there are no large landslides in the medium-elevation region that regularly receives high rainfall. Hence, only the combination of material removal along the rivers and a pronounced increase in precipitation apparently leads to the formation of deep-seated landslides in this environment.

Relief in the steep, high-elevation parts was increased at the onset of the IMPs at $\sim$ 10 ka BP through extensive mass removal along the rivers, but was counteracted by landslide-dammed lakes that formed transient sediment traps. In contrast, relief in the low-elevation sectors was reduced during these times, because the Sutlej River exceeded its transport capacity in the low-gradient areas, leading to pronounced sediment accumulation. This 120m thick alluviation event was initiated 9.7 ka BP and records further fluvial and geomorphic responses to oscillating monsoonal conditions. Radiometric age determination using the cosmogenic nuclides ^{10}Be and ^{26}Al allow a further quantitative assessment of these processes. Cut terraces formed in this infill during centennial-long low precipitation phases, for example at 8.2 ka BP, and 6.3 ka BP. At these times, lower sediment flux allowed downcutting, while higher sediment flux due to higher precipitation prevented incision.

This relationship – fluvial incision during weaker monsoon periods versus aggradation during stronger monsoon phases – underscores the highly nonlinear responses of landscapes to climatic forcing. Erosion and sedimentation are thus not clearly correlated with wetter climates, but rather with climatic variability and its oscillating character.

BIBLIOGRAPHY

Allegre, C. J., et al., Structure and Evolution of the Himalaya-Tibet Orogenic Belt, *Nature*, *307*(5946), 17–22, 1984.

Altabet, M. A., M. J. Higginson, and D. W. Murray, The effect of millennial-scale changes in Arabian Sea denitrification on atmospheric CO2, *Nature*, *415*(6868), 159–162, 2002.

Anderson, R. S., Evolution of the Santa-Cruz Mountains, California, through Tectonic Growth and Geomorphic Decay, *Journal of Geophysical Research-Solid Earth*, *99*(B10), 20,161–20,179, 1994.

Augustin, L., et al., Eight glacial cycles from an Antarctic ice core, *Nature*, *429*(6992), 623–628, 2004.

Baker, V., and V. Kale, The role of extreme floods in shaping bedrock channels, in *Rivers Over Rock: Fluvial Processes in Bedrock Channels, Geophys. Monogr. Ser.*, vol. 107, edited by K. Tinkler and E. Wohl, pp. 153–165, AGU, Washington, D.C., 1998.

Barnard, P. L., L. A. Owen, M. C. Sharma, and R. C. Finkel, Natural and human-induced landsliding in the Garhwal Himalaya of northern India, *Geomorphology*, *40*(1-2), 21–35, 2001.

Barnard, P. L., L. A. Owen, and R. C. Finkel, Style and timing of glacial and paraglacial sedimentation in a monsoon-influenced high Himalayan environment, the upper Bhagirathi Valley, Garhwal Himalaya, *Sedimentary Geology*, *165*(3-4), 199–221, 2004.

Barnett, T. P., Interaction of the Monsoon and Pacific Trade-Wind System at Interannual Time Scales .1. The Equatorial Zone, *Monthly Weather Review*, *111*(4), 756–773, 1983.

Barnett, T. P., Interaction of the Monsoon and Pacific Trade-Wind System at Interannual Time Scales .3. A Partial Anatomy of the Southern Oscillation, *Monthly Weather Review*, *112*(12), 2388–2400, 1984.

Barros, A. P., and D. Lattenmaier, Dynamic Modeling of Orographically Induced Precipitation, *Reviews of Geophysics*, *32*(3), 265–284, 1994.

Barros, A. P., M. Joshi, J. Putkonen, and D. W. Burbank, A study of the 1999 monsoon rainfall in a mountainous region in central Nepal using TRMM products and rain gauge observations, *Geophysical Research Letters*, *27*(22), 3683–3686, 2000.

Beas Bhakra Management, B., The B.B.M.B. (Beas Bhakra Management Board) provided hydrological data for the Sutlej, Spiti and Baspa Valleys., 2001.

Berger, A. L., Long-Term Variations of Daily Insolation and Quaternary Climatic Changes, *Journal of the Atmospheric Sciences*, *35*(12), 2362–2367, 1978.

Bergeron, T., Operation and results of "Project Pluvius", in *Physics of Precipitation, Geophys. Monogr. Ser.*, vol. 5, edited by H. Weickmann, pp. 152–157, AGU, Washington, D.C., 1960.

Bhutiyani, M. R., Sediment load characteristics of a proglacial stream of Siachen Glacier and the erosion rate in Nubra valley in the Karakoram Himalayas, India, *Journal of Hydrology*, *227*(1-4), 84–92, 2000.

Bookhagen, B., R. Thiede, and M. Strecker, Late Quaternary Intensified Monsoon Phases control Landscape evolution in the NW Himalaya, in *Eos Trans. AGU*, vol. 84, pp. Abstract H41A–06, 2003.

Bookhagen, B., R. Thiede, and M. R. Strecker, Late Quaternary intensified monsoon phases control landscape evolution in the northwest Himalaya, *Geology*, *in press*, 2005a.

Bookhagen, B., R. Thiede, and M. R. Strecker, Abnormal Monsoon years and their control on erosion and sediment flux in the high, arid northwestern Himalaya, *Earth and Planetary Science Letters*, *in press*, 2005b.

Bray, H. E., and S. Stokes, Chronologies for Late Quaternary barchan dune reactivation in the southeastern Arabian Peninsula, *Quaternary Science Reviews*, *22*(10-13), 1027–1033, 2003.

Brozovic, N., D. W. Burbank, and A. J. Meigs, Climatic limits on landscape development in the northwestern Himalaya, *Science*, *276*(5312), 571–574, 1997.

Burbank, D. W., Causes of Recent Himalayan Uplift Deduced from Deposited Patterns in the Ganges Basin, *Nature*, *357*(6380), 680–683, 1992.

Burbank, D. W., Rates of erosion and their implications for exhumation, *Mineralogical Magazine*, *66*(1), 25–52, 2002.

Burbank, D. W., L. A. Derry, and C. Francelanord, Reduced Himalayan Sediment Production 8 Myr Ago Despite an Intensified Monsoon, *Nature*, *364*(6432), 48–50, 1993.

Burbank, D. W., A. E. Blythe, J. Putkonen, B. Pratt-Sitaula, E. Gabet, M. Oskin, A. Barros, and T. P. Ojha, Decoupling of erosion and precipitation in the Himalayas, *Nature*, *426*(6967), 652–655, 2003.

Burns, S. J., A. Matter, N. Frank, and A. Mangini, Speleothem-based paleoclimate record from northern Oman, *Geology*, *26*(6), 499–502, 1998.

Charles, C. D., D. E. Hunter, and R. G. Fairbanks, Interaction between the ENSO and the Asian monsoon in a coral record of tropical climate, *Science*, *277*(5328), 925–928, 1997.

Charney, J., The intertropical convergence zone and the Hadley circulation of the atmosphere, *Proc. WMO/IUCG Symp. Numer. Weather Predict. Jpn. Meteorol. Agency*, *III*, 73–79, 1969.

Clark, C. O., J. E. Cole, and P. J. Webster, Indian Ocean SST and Indian summer rainfall: Predictive relationships and their decadal variability, *Journal of Climate*, *13*(14), 2503–2519, 2000.

Clark, D. H., P. R. Bierman, and P. Larsen, Improving in situ cosmogenic chronometers, *Quaternary Research*, *44*(3), 367–377, 1995.

Clemens, S., W. Prell, D. Murray, G. Shimmield, and G. Weedon, Forcing Mechanisms of the Indian-Ocean Monsoon, *Nature*, *353*(6346), 720–725, 1991.

Clemens, S. C., and W. L. Prell, Late Quaternary Forcing of Indian-Ocean Summer-Monsoon Winds - a Comparison of Fourier Model and General-Circulation Model Results, *Journal of Geophysical Research-Atmospheres*, *96*(D12), 22,683–22,700, 1991.

Clemens, S. C., and W. L. Prell, A 350,000 year summer-monsoon multi-proxy stack from the Owen ridge, Northern Arabian sea, *Marine Geology*, *201*(1-3), 35–51, 2003.

Coppus, R., and A. C. Imeson, Extreme events controlling erosion and sediment transport in a semi-arid sub-andean valley, *Earth Surface Processes and Landforms*, *27*(13), 1365–1375, 2002.

Dadson, S. J., et al., Links between erosion, runoff variability and seismicity in the Taiwan orogen, *Nature*, *426*(6967), 648–651, 2003.

Davis, J. C., et al., LLNL/UC AMS facility and research program, *Nuclear Instruments and Methods in Physics Research*, *B52*, 269–272, 1990.

Dethier, D. P., and S. L. Reneau, Lacustrine chronology links late pleistocene climate change and mass movements in northern New Mexico, *Geology*, *24*(6), 539–542, 1996.

Dettman, D. L., M. J. Kohn, J. Quade, F. J. Ryerson, T. P. Ojha, and S. Hamidullah, Seasonal stable isotope evidence for a strong Asian monsoon throughout the past 10.7 m.y, *Geology*, *29*(1), 31–34, 2001.

Dettman, D. L., X. M. Fang, C. N. Garzione, and J. J. Li, Uplift-driven climate change at 12 Ma: a long delta O-18 record from the NE margin of the Tibetan plateau, *Earth and Planetary Science Letters*, *214*(1-2), 267–277, 2003.

Dietrich, W. E., C. J. Wilson, D. R. Montgomery, J. McKean, and R. Bauer, Erosion Thresholds and Land Surface-Morphology, *Geology*, *20*(8), 675–679, 1992.

England, P., and P. Molnar, Surface Uplift, Uplift of Rocks, and Exhumation of Rocks, *Geology*, *18*(12), 1173–1177, 1990.

Fang, J. Q., Lake Evolution During the Past 30,000 Years in China, and Its Implications for Environmental-Change, *Quaternary Research*, *36*(1), 37–60, 1991.

Fasullo, J., and P. J. Webster, Hydrological signatures relating the Asian summer monsoon and ENSO, *Journal of Climate*, *15*(21), 3082–3095, 2002.

Fasullo, J., and P. J. Webster, A hydrological definition of Indian monsoon onset and withdrawal, *Journal of Climate*, *16*(19), 3200–3211, 2003.

Fein, J., and P. Stephens, *Monsoons*, John Wiley and Sons, New York, 1987.

Ferraro, R. R., Special sensor microwave imager derived global rainfall estimates for climatological applications, *Journal of Geophysical Research-Atmospheres*, *102*(D14), 16,715–16,735, 1997.

Ferraro, R. R., E. A. Smith, W. Berg, and G. J. Huffman, A screening methodology for passive microwave precipitation retrieval algorithms, *Journal of the Atmospheric Sciences*, *55*(9), 1583–1600, 1998.

Finlayson, D. P., D. R. Montgomery, and B. Hallet, Spatial coincidence of rapid inferred erosion with young metamorphic massifs in the Himalayas, *Geology*, *30*(3), 219–222, 2002.

Fleitmann, D., S. J. Burns, M. Mudelsee, U. Neff, J. Kramers, A. Mangini, and A. Matter, Holocene forcing of the Indian monsoon recorded in a stalagmite from Southern Oman, *Science*, *300*(5626), 1737–1739, 2003.

Flohn, Large-scale aspects of the "summer monsoon" in south and East Asia, *J. Meteor. Soc. Japan*, *75*, 180–186, 1957.

Flohn, Contributions to a meteorology of the Tibetan Highlands, *Atmos. Sci. Paper*, (130), 120, 1969.

Gadgil, S., A. B. Shrestha, C. P. Wake, J. E. Dibb, and P. A. Mayewski, The Indian monsoon and its variability, *Annual Review of Earth and Planetary Sciences*, *31*(3), 429–467, 2003.

Gansser, A., *The Geology of the Himalayas*, Wiley Interscience, London, 1964.

Gansser, A., The significance of the Himalayan suture zone, *Tectonophysics*, *62*, 37–52, 1980.

Gasse, F., et al., A 13,000-Year Climate Record from Western Tibet, *Nature*, *353*(6346), 742–745, 1991.

GISP, The Greenland Summit Ice Cores [CD-ROM], 1997. Available from the National Snow and Ice Data Center, University of Colorado at Boulder, and the World Data Center-A for Paleoclimatology, National Geophysical Data Center, Boulder, CO. Also available online at: www.ngdc.noaa.gov/paleo/icecore/greenland/ summit/index.html., 1997.

Goodbred, S. L., and S. A. Kuehl, Enormous Ganges-Brahmaputra sediment discharge during strengthened early Holocene monsoon, *Geology*, *28*(12), 1083–1086, 2000.

Gosse, J. C., and F. M. Phillips, Terrestrial in situ cosmogenic nuclides: theory and application, *Quaternary Science Reviews*, *20*(14), 1475–1560, 2001.

Goswami, B. N., Interannual variations of Indian summer monsoon in a GCM: External conditions versus internal feedbacks, *Journal of Climate*, *11*(4), 501–522, 1998.

Granger, D. E., and P. F. Muzikar, Dating sediment burial with in situ-produced cosmogenic nuclides: theory, techniques, and limitations, *Earth and Planetary Science Letters*, *188*(1-2), 269–281, 2001.

Granger, D. E., and A. L. Smith, Dating buried sediments using radioactive decay and muogenic production of Al-26 and Be-10, *Nuclear Instruments & Methods in Physics Research Section B-Beam Interactions with Materials and Atoms*, *172*, 822–826, 2000.

Grody, N. C., Classification of Snow Cover and Precipitation Using the Special Sensor Microwave Imager, *Journal of Geophysical Research-Atmospheres*, *96*(D4), 7423–7435, 1991.

Guo, Z. T., et al., Onset of Asian desertification by 22 Myr ago inferred from loess deposits in China, *Nature*, *416*(6877), 159–163, 2002.

Gupta, A. K., and E. Thomas, Initiation of Northern Hemisphere glaciation and strengthening of the northeast Indian monsoon: Ocean Drilling Program Site 758, eastern equatorial Indian Ocean, *Geology*, *31*(1), 47–50, 2003.

Hahn, D. G., and S. Manabe, Role of Mountains in South Asian Monsoon Circulation, *Journal of the Atmospheric Sciences*, *32*(8), 1515–1541, 1975.

Hahn, D. G., and S. Manabe, Role of Mountains in South Asian Monsoon Circulation - Reply, *Journal of the Atmospheric Sciences*, *33*(11), 2258–2262, 1976.

Hahn, D. G., and J. Shukla, Apparent Relationship between Eurasian Snow Cover and Indian Monsoon Rainfall, *Journal of the Atmospheric Sciences*, *33*(12), 2461–2462, 1976.

Halley, E., An historical account of the trade winds and monsoons observable in the seas between and near the tropics with an attempt to assign a physical cause of the said winds, *Philos. Trans. R. Soc. London*, *16*, 153–168, 1686.

Hancock, G. S., and R. S. Anderson, Numerical modeling of fluvial strath-terrace formation in response to oscillating climate, *Geological Society of America Bulletin*, *114*(9), 1131–1142, 2002.

Hartshorn, K., N. Hovius, W. B. Dade, and R. L. Slingerland, Climate-driven bedrock incision in an active mountain belt, *Science*, *297*(5589), 2036–2038, 2002.

Hastenrath, S., *Climate Dynamics of the Tropics: An Updated Edition of Climate and Circulation of the Tropics*, Kluwer Academic Publishers, 1994.

Heusser, L. E., and F. Sirocko, Millennial pulsing of environmental change in southern California from the past 24 ky: A record of Indo-Pacific ENSO events?, *Geology*, *25*(3), 243–246, 1997.

Hilley, G. E., and M. R. Strecker, Steady state erosion of critical Coulomb wedges with applications to Taiwan and the Himalaya, *Journal of Geophysical Research-Solid Earth*, *109*(B1), 2004.

Hilley, G. E., and M. R. Strecker, Processes of oscillating basin filling and excavation in a tectonically active orogen, Quebrada del Toro, NW Argentina, *Geological Society of America Bulletin*, *in press*, 2005.

Hilley, G. E., M. R. Strecker, and V. A. Ramos, Growth and erosion of fold-and-thrust belts with an application to the Aconcagua fold-and-thrust belt, Argentina, *Journal of Geophysical Research-Solid Earth*, *109*(B1), 2004.

Hodges, K. V., Tectonics of the Himalaya and southern Tibet from two perspectives, *Geological Society of America Bulletin*, *112*(3), 324–350, 2000.

Hodges, K. V., C. Wobus, K. Ruhl, T. Schildgen, and K. Whipple, Quaternary deformation, river steepening, and heavy precipitation at the front of the Higher Himalayan ranges, *Earth and Planetary Science Letters*, *220*(3-4), 379–389, 2004.

Hollinger, J. P., Special Issue on the Defense Meteorological Satellite Program (Dmsp - Calibration and Validation of the Special Sensor Microwave Imager (Ssm/I), *Ieee Transactions on Geoscience and Remote Sensing*, *28*(5), 779–780, 1990.

Horton, R., Erosional development of streams and their drainage basins: Hydrophysical approach to quantitative morphology, *Geol. Soc. Am. Bull.*, *56*, 275–370, 1945.

Hoskins, B. J., and M. J. Rodwell, A Model of the Asian Summer Monsoon .1. The Global-Scale, *Journal of the Atmospheric Sciences*, *52*(9), 1329–1340, 1995.

Hovius, N., C. P. Stark, H. T. Chu, and J. C. Lin, Supply and removal of sediment in a landslide-dominated mountain belt: Central Range, Taiwan, *Journal of Geology*, *108*(1), 73–89, 2000.

Hsu, H. H., and X. Liu, Relationship between the Tibetan plateau heating and east Asian summer monsoon rainfall, *Geophysical Research Letters*, *30*(20), 2003.

Jaiprakash Company, L., Dr. Narendara Singh from Jaiprakash Company Ltd. provided hydrological data for the Sutlej and Baspa Valleys., 2002.

Ju, J. H., and J. Slingo, The Asian Summer Monsoon and Enso, *Quarterly Journal of the Royal Meteorological Society*, *121*(525), 1133–1168, 1995.

Keefer, D. K., The importance of earthquake-induced landslides to long-term slope erosion and slope-failure hazards in seismically active regions, *Geomorphology*, *10*(1-4), 265–284, 1994.

Kohl, C. P., and K. Nishiizumi, Chemical Isolation of Quartz for Measurement of Insitu-Produced Cosmogenic Nuclides, *Geochimica Et Cosmochimica Acta*, *56*(9), 3583–3587, 1992.

Koons, P. O., P. K. Zeitler, C. P. Chamberlain, D. Craw, and A. S. Meltzer, Mechanical links between erosion and metamorphism in Nanga Parbat, Pakistan Himalaya, *American Journal of Science*, *302*(9), 749–773, 2002.

Kotlia, B. S., C. Sharma, M. S. Bhalla, G. Rajagopalan, K. Subrahmanyam, A. Bhattacharyya, and K. S. Valdiya, Palaeoclimatic conditions in the late Pleistocene Wadda Lake, eastern Kumaun Himalaya (India), *Palaeogeography Palaeoclimatology Palaeoecology*, *162*(1-2), 105–118, 2000.

Krishnamurthy, V., and J. Shukla, Intraseasonal and interannual variability of rainfall over India, *Journal of Climate*, *13*(24), 4366–4377, 2000.

Kumar, K. R., G. B. Pant, B. Parthasarathy, and N. A. Sontakke, Spatial and Subseasonal Patterns of the Long-Term Trends of Indian-Summer Monsoon Rainfall, *International Journal of Climatology*, *12*(3), 257–268, 1992.

Kummerow, C., and L. Giglio, A Passive Microwave Technique for Estimating Rainfall and Vertical Structure Information from Space 1 Algorithm Description, *Journal of Applied Meteorology*, *33*(1), 3–18, 1994a.

Kummerow, C., and L. Giglio, A Passive Microwave Technique for Estimating Rainfall and Vertical Structure Information from Space 2 Applications to SSM/I Data, *Journal of Applied Meteorology*, *33*(1), 19–34, 1994b.

Kutzbach, J. E., and P. J. Guetter, The Influence of Changing Orbital Parameters and Surface Boundary-Conditions on Climate Simulations for the Past 18000 Years, *Journal of the Atmospheric Sciences*, *43*(16), 1726–1759, 1986.

Lal, D., Cosmic-Ray Labeling of Erosion Surfaces - Insitu Nuclide Production-Rates and Erosion Models, *Earth and Planetary Science Letters*, *104*(2-4), 424–439, 1991.

Lang, T. J., and A. P. Barros, An investigation of the onsets of the 1999 and 2000 monsoons in central Nepal, *Monthly Weather Review*, *130*(5), 1299–1316, 2002.

Lau, K. M., and W. Bua, Mechanisms of monsoon Southern Oscillation coupling: insights from GCM experiments, *Climate Dynamics*, *14*(11), 759–779, 1998.

Lavé, J., and D. W. Burbank, Denudation processes and rates in the Transverse Ranges, southern California: Erosional response of a transitional landscape to external and anthropogenic forcing, *Journal of Geophysical Research-Surface*, *109*(F01006), doi:10.1029/2003JF000,023, 2004.

Leuschner, D. C., and F. Sirocko, Orbital insolation forcing of the Indian Monsoon - a motor for global climate changes?, *Palaeogeography Palaeoclimatology Palaeoecology*, *197*(1-2), 83–95, 2003.

Meehl, G. A., Influence of the Land-Surface in the Asian Summer Monsoon - External Conditions Versus Internal Feedbacks, *Journal of Climate*, *7*(7), 1033–1049, 1994.

Metivier, F., and Y. Gaudemer, Mass transfer between eastern Tien Shan and adjacent basins (central Asia): Constraints on regional tectonics and topography, *Geophysical Journal International*, *128*(1), 1–21, 1997.

Metivier, F., and Y. Gaudemer, Stability of output fluxes of large rivers in South and East Asia during the last 2 million years: implications on floodplain processes, *Basin Research*, *11*(4), 293–303, 1999.

Molnar, P., The rise of the Tibetan plateau: From mantle dynamics to the Indian monsoon, *Astronomy & Geophysics*, *38*(3), 10–15, 1997.

Molnar, P., Late cenozoic increase in accumulation rates of terrestrial sediment: How might climate change have affected erosion rates?, *Annual Review of Earth and Planetary Sciences*, *32*, 67–89, 2004.

Molnar, P., and P. England, Late Cenozoic Uplift of Mountain-Ranges and Global Climate Change - Chicken or Egg, *Nature*, *346*(6279), 29–34, 1990.

Molnar, P., and P. England, Climate and Landscape Response - Reply, *Nature*, *355*(6358), 306–306, 1992.

Molnar, P., P. England, and J. Martinod, Mantle Dynamics, Uplift of the Tibetan Plateau, and the Indian Monsoon, *Reviews of Geophysics*, *31*(4), 357–396, 1993.

Montgomery, D. R., and M. T. Brandon, Topographic controls on erosion rates in tectonically active mountain ranges, *Earth and Planetary Science Letters*, *201*(3-4), 481–489, 2002.

Montgomery, D. R., and W. E. Dietrich, Channel Initiation and the Problem of Landscape Scale, *Science*, *255*(5046), 826–830, 1992.

Montgomery, D. R., and W. E. Dietrich, A Physically-Based Model for the Topographic Control on Shallow Landsliding, *Water Resources Research*, *30*(4), 1153–1171, 1994.

Montgomery, D. R., G. Balco, and S. D. Willett, Climate, tectonics, and the morphology of the Andes, *Geology*, *29*(7), 579–582, 2001.

Mulligan, M., Modelling the geomorphological impact of climatic variability and extreme events in a semi-arid environment, *Geomorphology*, *24*(1), 59–78, 1998.

Nishiizumi, K., E. L. Winterer, C. P. Kohl, J. Klein, R. Middleton, D. Lal, and J. R. Arnold, Cosmic-Ray Production-Rates of Be-10 and Al-26 in Quartz from Glacially Polished Rocks, *Journal of Geophysical Research-Solid Earth and Planets*, *94*(B12), 17,907–17,915, 1989.

Osterkamp, W. R., and J. M. Friedman, The disparity between extreme rainfall events and rare floods - with emphasis on the semi-arid American West, *Hydrological Processes*, *14*(16-17), 2817–2829, 2000.

Overpeck, J., D. Anderson, S. Trumbore, and W. Prell, The southwest Indian Monsoon over the last 18000 years, *Climate Dynamics*, *12*(3), 213–225, 1996.

Owen, L., M. Sharma, and R. Bigwood, Landscape modification and geomorphological consequences of the 20 October 1991 earthquake and the July-August 1992 monsoon in the Garhwal Himalaya, *Zeitschrift für Geomorphologie*, *103*, 359–372, 1996.

Owen, L. A., L. Gualtieri, R. C. Finkel, M. W. Caffee, D. I. Benn, and M. C. Sharma, Cosmogenic radionuclide dating of glacial landforms in the Lahul Himalaya, northern India: defining the timing of Late Quaternary glaciation, *Journal of Quaternary Science*, *16*(6), 555–563, 2001.

Owen, L. A., R. C. Finkel, M. W. Caffee, and L. Gualtieri, Timing of multiple late Quaternary glaciations in the Hunza Valley, Karakoram Mountains, northern Pakistan: Defined by cosmogenic radionuclide dating of moraines, *Geological Society of America Bulletin*, *114*(5), 593–604, 2002.

Pant, G. B., and B. Parthasarathy, Some Aspects of an Association between the Southern Oscillation and Indian-Summer Monsoon, *Archives for Meteorology Geophysics and Bioclimatology Series B-Theoretical and Applied Climatology*, *29*(3), 245–252, 1981.

Parthasarathy, B., K. R. Kumar, and D. R. Kothawale, Indian-Summer Monsoon Rainfall Indexes - 1871-1990, *Meteorological Magazine*, *121*(1441), 174–186, 1992.

Paul, S. K., S. K. Bartarya, P. Rautela, and A. K. Mahajan, Catastrophic mass movement of 1998 monsoons at Malpa in Kali Valley, Kumaun Himalaya (India), *Geomorphology*, *35*(3-4), 169–180, 2000.

Peizhen, Z., P. Molnar, and W. R. Downs, Increased sedimentation rates and grain sizes 2-4 Myr ago due to the influence of climate change on erosion rates, *Nature*, *410*(6831), 891–897, 2001.

Peterson, T. C., and R. S. Vose, An overview of the global historical climatology network temperature database, *Bulletin of the American Meteorological Society*, *78*(12), 2837–2849, 1997.

Petit, J. R., et al., Four climate cycles in Vostok ice core, *Nature*, *387*(6631), 359–360, 1997.

Petty, G. W., The Status of Satellite-Based Rainfall Estimation over Land, *Remote Sensing of Environment*, *51*(1), 125–137, 1995.

Phillips, W. M., V. F. Sloan, J. F. Shroder, P. Sharma, M. L. Clarke, and H. M. Rendell, Asynchronous glaciation at Nanga Parbat, northwestern Himalaya Mountains, Pakistan, *Geology*, *28*(5), 431–434, 2000.

Pratt, B., D. W. Burbank, A. Heimsath, and T. Ojha, Impulsive alluviation during early Holocene strengthened monsoons, central Nepal Himalaya, *Geology*, *30*(10), 911–914, 2002.

Pratt-Sitaula, B., D. W. Burbank, A. Heimsath, and T. Qjha, Landscape disequilibrium on 1000-10,000 year scales Marsyandi River, Nepal, central Himalaya, *Geomorphology*, *58*(1-4), 223–241, 2004.

Prell, W. L., and J. E. Kutzbach, Sensitivity of the Indian Monsoon to Forcing Parameters and Implications for Its Evolution, *Nature*, *360*(6405), 647–652, 1992.

Prins, M. A., and G. Postma, Effects of climate, sea level, and tectonics unraveled for last deglaciation turbidite records of the Arabian Sea, *Geology*, *28*(4), 375–378, 2000.

Rasmusson, E. M., and T. H. Carpenter, The Relationship between Eastern Equatorial Pacific Sea-Surface Temperatures and Rainfall over India and Sri-Lanka, *Monthly Weather Review*, *111*(3), 517–528, 1983.

Raymo, M. E., and W. F. Ruddiman, Tectonic Forcing of Late Cenozoic Climate, *Nature*, *359*(6391), 117–122, 1992.

Reiners, P. W., T. A. Ehlers, S. G. Mitchell, and D. R. Montgomery, Coupled spatial variations in precipitation and long-term erosion rates across the Washington Cascades, *Nature*, *426*(6967), 645–647, 2003.

Reneau, S. L., and D. P. Dethier, Late Pleistocene landslide-dammed lakes along the Rio Grande, White Rock canyon, New Mexico, *Geological Society of America Bulletin*, *108*(11), 1492–1507, 1996.

Richards, J., *Remote Sensing Digital Image Analysis: An Introduction*, Springer-Verlag, Berlin, Germany, 1994.

Riehl, *Tropical Meteorology*, McGraw Hill, New York, 1954.

Riehl, *Climate and Weather in the Tropics*, Academic Press, San Diego/New York, 1979.

Rodwell, M. J., and B. J. Hoskins, A Model of the Asian Summer Monsoon .2. Cross-Equatorial Flow and Pv Behavior, *Journal of the Atmospheric Sciences*, *52*(9), 1341–1356, 1995.

Rodwell, M. J., and B. J. Hoskins, Subtropical anticyclones and summer monsoons, *Journal of Climate*, *14*(15), 3192–3211, 2001.

Sah, M. P., and R. K. Mazari, Anthropogenically accelerated mass movement, Kulu Valley, Himachal Pradesh, India, *Geomorphology*, *26*(1-3), 123–138, 1998.

Shrestha, A. B., C. P. Wake, J. E. Dibb, and P. A. Mayewski, Precipitation fluctuations in the Nepal Himalaya and its vicinity and relationship with some large scale climatological parameters, *International Journal of Climatology*, *20*(3), 317–327, 2000.

Shrestha, M. L., Interannual variation of summer monsoon rainfall over Nepal and its relation to Southern Oscillation Index, *Meteorology and Atmospheric Physics*, *75*(1-2), 21–28, 2000.

Shukla, J., and D. A. Paolino, The Southern Oscillation and Long-Range Forecasting of the Summer Monsoon Rainfall over India, *Monthly Weather Review*, *111*(9), 1830–1837, 1983.

Sikka, D. R., and S. Gadgil, On the Maximum Cloud Zone and the Itcz over Indian Longitudes During the Southwest Monsoon, *Monthly Weather Review*, *108*(11), 1840–1853, 1980.

Sirocko, F., M. Sarnthein, H. Erlenkeuser, H. Lange, M. Arnold, and J. C. Duplessy, Century-Scale Events in Monsoonal Climate over the Past 24,000 Years, *Nature*, *364*(6435), 322–324, 1993.

Sirocko, F., D. GarbeSchonberg, A. McIntyre, and B. Molfino, Teleconnections between the subtropical monsoons and high-latitude climates during the last deglaciation, *Science*, *272*(5261), 526–529, 1996.

Sklar, L. S., and W. E. Dietrich, Sediment and rock strength controls on river incision into bedrock, *Geology*, *29*(12), 1087–1090, 2001.

Slingo, J. M., and H. Annamalai, 1997: The El Nino of the century and the response of the Indian summer monsoon, *Monthly Weather Review*, *128*(6), 1778–1797, 2000.

Smith, R., The influence of mountains on the atmosphere, *Advances in Geophysics*, *21*, 87–233, 1979a.

Smith, R. B., Some Aspects of the Quasi-Geostrophic Flow over Mountains, *Journal of the Atmospheric Sciences*, *36*(12), 2385–2393, 1979b.

Snyder, N. P., K. X. Whipple, G. E. Tucker, and D. J. Merritts, Importance of a stochastic distribution of floods and erosion thresholds in the bedrock river incision problem, *Journal of Geophysical Research-Solid Earth*, *108*(B2), art. no.–2117, 2003.

Sobel, E. R., G. E. Hilley, and M. R. Strecker, Formation of internally drained contractional basins by aridity-limited bedrock incision, *Journal of Geophysical Research-Solid Earth*, *108*(B7), 2003.

Steck, A., Geology of the NW Indian Himalaya, *Eclogae Geologicae Helvetiae*, *96*(2), 147–U13, 2003.

Stone, J. O., Air pressure and cosmogenic isotope production, *Journal of Geophysical Research-Solid Earth*, *105*(B10), 23,753–23,759, 2000.

Stuiver, M., et al., INTCAL98 radiocarbon age calibration, 24,000-0 cal BP, *Radiocarbon*, *40*(3), 1041–1083, 1998.

Tapponnier, P., Oblique stepwise growth of the Tibet Plateau, *Science*, *295*(5553), 277–277, 2002.

Thamban, M., V. P. Rao, and R. R. Schneider, Reconstruction of late Quaternary monsoon oscillations based on clay mineral proxies using sediment cores from the western margin of India, *Marine Geology*, *186*(3-4), 527–539, 2002.

Thiede, R., B. Bookhagen, J. Arrowsmith, E. Sobel, and M. R. Strecker, Climatic Control on rapid exhumation along the Southern Himalayan Front, *Earth and Planetary Science Letters*, *222*(3-4), 791–806, 2004.

Thompson, L. G., T. Yao, E. Mosley-Thompson, M. E. Davis, K. A. Henderson, and P. N. Lin, A high-resolution millennial record of the South Asian Monsoon from Himalayan ice cores, *Science*, *289*(5486), 1916–1919, 2000.

Trauth, M. H., R. A. Alonso, K. R. Haselton, R. L. Hermanns, and M. R. Strecker, Climate change and mass movements in the NW Argentine Andes, *Earth and Planetary Science Letters*, *179*(2), 243–256, 2000.

Tucker, G. E., and R. Slingerland, Drainage basin responses to climate change, *Water Resources Research*, *33*(8), 2031–2047, 1997.

Tucker, G. E., and R. L. Slingerland, Erosional Dynamics, Flexural Isostasy, and Long-Lived Escarpments - a Numerical Modeling Study, *Journal of Geophysical Research-Solid Earth*, *99*(B6), 12,229–12,243, 1994.

Vannay, J. C., and A. Steck, Tectonic Evolution of the High Himalaya in Upper Lahul (Nw Himalaya, India), *Tectonics*, *14*(2), 253–263, 1995.

Voelker, A. H. L., M. Sarnthein, P. M. Grootes, H. Erlenkeuser, C. Laj, A. Mazaud, M. J. Nadeau, and M. Schleicher, Correlation of marine C-14 ages from the Nordic Seas with the GISP2 isotope record: Implications for C-14 calibration beyond 25 ka BP, *Radiocarbon*, *40*(1), 517–+, 1998.

Walker, Correlations in seasonal variations of weather, *Memo. India Meteor. Dept.*, *VIII*(24), 75–131, 1923.

Wang, Y. J., H. Cheng, R. L. Edwards, Z. S. An, J. Y. Wu, C. C. Shen, and J. A. Dorale, A high-resolution absolute-dated Late Pleistocene monsoon record from Hulu Cave, China, *Science*, *294*(5550), 2345–2348, 2001.

Webster, P., *The Elementary Monsoon*, Wiley, New York, 1987.

Webster, P. J., and L. C. Chou, Seasonal Structure of a Simple Monsoon System, *Journal of the Atmospheric Sciences*, *37*(2), 354–367, 1980.

Webster, P. J., and S. Yang, Monsoon and Enso - Selectively Interactive Systems, *Quarterly Journal of the Royal Meteorological Society*, *118*(507), 877–926, 1992.

Webster, P. J., V. O. Magana, T. N. Palmer, J. Shukla, R. A. Tomas, M. Yanai, and T. Yasunari, Monsoons: Processes, predictability, and the prospects for prediction, *Journal of Geophysical Research-Oceans*, *103*(C7), 14,451–14,510, 1998.

Webster, P. J., A. M. Moore, J. P. Loschnigg, and R. R. Leben, Coupled ocean-atmosphere dynamics in the Indian Ocean during 1997-98, *Nature*, *401*(6751), 356–360, 1999.

Whipple, K. X., E. Kirby, and S. H. Brocklehurst, Geomorphic limits to climate-induced increases in topographic relief, *Nature*, *401*(6748), 39–43, 1999.

Wilheit, T. T., et al., Algorithms for the Retrieval of Rainfall from Passive Microwave Measurements, *Reviews of Remote Sensing*, *11*, 163–194, 1994.

Willett, S. D., Orogeny and orography: The effects of erosion on the structure of mountain belts, *Journal of Geophysical Research-Solid Earth*, *104*(B12), 28,957–28,981, 1999.

Willett, S. D., R. Slingerland, and N. Hovius, Uplift, shortening, and steady-state topography in active mountain belts, *American Journal of Science*, *301*(4-5), 455–485, 2001.

Wobus, C. W., K. V. Hodges, and K. X. Whipple, Has focused denudation sustained active thrusting at the Himalayan topographic front?, *Geology*, *31*(10), 861–864, 2003.

Wolman, M. G., and J. P. Miller, Magnitude and Frequency of Forces in Geomorphic Processes, *Journal of Geology*, *68*(1), 54–74, 1960.

Wu, G. X., and Y. S. Zhang, Tibetan Plateau forcing and the timing of the monsoon onset over South Asia and the South China Sea, *Monthly Weather Review*, *126*(4), 913–927, 1998.

Wyss, M., J. Hermann, and A. Steck, Structural and metamorphic evolution of the northern Himachal Himalaya, NW India - (Spiti-eastern Lahul-Parvati valley traverse), *Eclogae Geologicae Helvetiae*, *92*(1), 3–44, 1999.

Yalin, M., *Mechanics of Sediment Transport, 2nd ed.*, Pergamon, Tarrytown, N.Y., 1977.

Yuan, D. X., et al., Timing, duration, and transitions of the Last Interglacial Asian Monsoon, *Science*, *304*(5670), 575–578, 2004.

Zeitler, P. K., et al., Crustal reworking at Nanga Parbat, Pakistan: Metamorphic consequences of thermal-mechanical coupling facilitated by erosion, *Tectonics*, *20*(5), 712–728, 2001.

Zheng, H. B., C. M. Powell, Z. S. An, J. Zhou, and G. R. Dong, Pliocene uplift of the northern Tibetan Plateau, *Geology*, *28*(8), 715–718, 2000.

Zhisheng, A., J. E. Kutzbach, W. L. Prell, and S. C. Porter, Evolution of Asian monsoons and phased uplift of the Himalayan Tibetan plateau since Late Miocene times, *Nature*, *411*(6833), 62–66, 2001.